Downlink Resource Allocation for Orthogonal Frequency Division Multiple Access Systems

by

Kit-Ming Tommy CHEE

B.E.(Electrical & Electronic) First Hons

Thesis submitted for the degree of

Doctor of Philosophy

in

School of Electrical and Electronic Engineering,

Faculty of Engineering,

Computer and Mathematical Sciences

The University of Adelaide, Australia

April 2007

Typeset in LaTeX 2_ε
Kit-Ming Tommy CHEE

Abstract

Wireless spectral efficiency is increasingly important due to the rapid growth of demand for high data rate wideband wireless services. The design of a multi-carrier system, such as an orthogonal frequency division multiple access (OFDMA) system, enables high system capacity suited for these wideband wireless services. This system capacity can be further optimised with a resource allocation scheme by exploiting the characteristics of the wireless fading channels. The fundamental idea of a resource allocation scheme is to efficiently distribute the available wireless resources, such as the sub-carriers and transmission power, among all admitted users in the system. In this thesis, we present the findings of the investigation into the impact of several resource allocation schemes in an OFDMA environment.

We show that in an OFDMA environment without the consideration of sub-carrier assignment, the sub-optimal power allocation closed-form solution can be derived via a constrained optimisation with the duality theorem. With a perfect feedback of channel condition, the proposed low-complexity algorithm that utilises the closed-form solution can maximise the sum capacity to approach near-optimal capacity.

We derive the sub-optimal sub-carrier and power allocation closed-form solution via a similar constrained optimisation process. With an imperfect or outdated feedback of channel condition, the adaptive sub-carrier and power allocation scheme not only fails to improve but also further deteriorates the system throughput. We present and discuss the formation of the finite-state Markov channel. We show that by using the dynamics of the Markov channel, the channel quality can be reliably predicted in advance. We analyse via simulation the spectral efficiency achieved by this channel prediction scheme on an OFDMA system.

Abstract

We address the importance of fairness in resource allocation from a game-theoretic perspective. With different utility and preference functions that best describe the gain in users' throughput as more sub-carriers are allocated to the individual user, we formulate the resource allocation problem into cooperative and non-cooperative games. We study via simulation the effectiveness and fairness of the cooperative and non-cooperative resource allocation schemes on an OFDMA system.

Finally, we draw conclusions on our research work and outline the future research topics in connection with our current studies.

Statement of Originality

This work contains no material that has been accepted for the award of any other degree or diploma in any university or other tertiary institution and, to the best of my knowledge and belief, contains no material previously published or written by another person, except where due reference has been made in the text.

I give consent to this copy of the thesis, when deposited in the University Library, being available for loan and photocopying.

Signed

Date

This page is blank

Acknowledgements

I wish to express my deepest thanks and gratitude to my principal supervisor, Assoc. Prof. Cheng-Chew Lim and my external supervisor, Prof. Jinho Choi. I am indebted to them for all their invaluable guidance, support, motivation and encouragement throughout my candidature. Their outstanding expertise and zealous advice have greatly improved the technical content as well as the quality of this thesis.

I am grateful to Dr. Brian Ng who has participated in many fruitful discussions to spark the idea for the work in Chapter 4 as well as patiently helping me to improve my writing skills.

This research would not have been possible without the financial support from the University of Adelaide in the form of postgraduate scholarship and travel grants. I would like to thank Prof. Jinho Choi, Assoc. Prof. Cheng-Chew Lim and Assoc. Prof. Michael Liebelt for providing me with various opportunities to gain additional financial support. I would also like to thank IEEE South Australia section and ARC Communication Research Networks (ACoRN) for sponsoring my conference attendance in various occasions.

My sincere gratitude to the friendly staffs at the main office of the School of Electrical and Electronic Engineering for their help in regard to various matters.

I would like to thank my parents for their patience and sacrifice. Lastly, I am dedicating this to my loved one. Without your motivating encouragement and devoted companionship, I will never be able to cross the hurdle and complete my work on target.

Tommy Chee
July 2006

This page is blank

Contents

List of Figures

This page is blank

List of Tables

This page is blank

List of Abbreviations

ADC	Analog-to-Digital Converter.
ADSL	Asymmetric Digital Subscriber Line.
AWGN	Additive White Gaussian Noise.
BD	Birth-Death.
BER	Bit-error Rate.
CDMA	Code Division Multiple Access.
CPA	Constant Power Allocation.
CSI	Channel State Information.
DAB	Digital Audio Broadcasting.
DAC	Digital-to-Analog Converter.
DFT	Discrete Fourier Transform.
DVB	Digital Video Broadcasting.
DSL	Digital Subscriber Line.
FDMA	Frequency Division Multiple Access.
FPA	Fixed Power Allocation.
FSMC	Finite-state Markov Channel.
GSM	Global System for Mobile Communications.
IDFT	Inverse Discrete Fourier Transform.
ISI	Inter-symbol Interference.
KKT	Karush-Kuhn-Tucker.
MC-CDMA	Multi-carrier Code Division Multiple Access.
MC/DS-CDMA	Multi-carrier Direct Sequence Code Division Multiple Access.
MQAM	M-ary Quadrature Amplitude Modulation.
MT-CDMA	Multi-tone Code Division Multiple Access.
NBD	Non-Birth-Death.

NBS	Nash Bargaining Solution.
NE	Nash Equilibrium (Equilibria).
OFDM	Orthogonal Frequency Division Multiplexing.
OFDMA	Orthogonal Frequency Division Multiple Access.
OPA	Optimal Power Allocation.
P/S	Parallel-to-Serial.
PoA	Price of Anarchy.
QBD	Quasi-Birth-Death.
QoS	Quality of Service.
RBS	Raiffa-Kalai-Smorodinsky Bargaining Solution.
RRM	Radio resource management.
SINR	Signal-to-Interference-plus-Noise Ratio.
SNR	Signal-to-Noise Ratio.
S/P	Serial-to-Parallel.
SPA	Sub-optimal Power Allocation.
TDD	Time Division Duplex.
TDMA	Time Division Multiple Access.
UPA	User-prioritised Power Allocation.
WLAN	Wireless Local Area Network.

List of Symbols

$\mathbf{A}$	State transition matrix.
$a_{i,j}$	Transition probability of state i to j, for all $i, j \in \mathbb{Z}^+$.
$\alpha_l(t)$	Time-varying amplitude of the wireless channel response at the l^{th} path.
$\beta_{k,n}$	Sub-carrier assignment factor for user k at sub-carrier n.
b	Number of sub-carriers within one sub-band.
B	Received signal bandwidth.
C	Shannon's capacity.
χ	Decibel shadow fading component.
χ_σ	Decibel standard deviation of shadow fading component.
Δf	Sub-carrier spacing.
ΔT	Length of cyclic prefix (also known as guard interval).
d	Instantaneous distance between base station and the corresponding mobile user.
d_0	Relative distance between base station and any arbitrary mobile user.
η	Path loss exponent.
f_d	Maximum Doppler frequency.
$\mathcal{F}_k$	Fairness index for user k.
$\gamma_{k,n}$	Signal-to-noise-ratio for user k at sub-carrier n.
$h(t)$	Impulse response of the wireless fading channel.
$h_{k,n}$	Channel fading coefficient for user k at sub-carrier n.
itr	Number of iterations in an iterative algorithm.
K	Number of users.
κ	Decibel zero-mean Gaussian variable of zero decibel standard deviation.
λ	Lagrange multiplier.
$L_P(\cdot)$	Lagrangian of primal objective.
$L_D(\cdot)$	Lagrangian of dual objective.

$\mathbf{L}_q$	The q^{th} partition of lumpable states.
μ	Lagrange multiplier.
N	Number of sub-carriers.
$n_{k,n}$	Additive white Gaussian noise for user k at sub-carrier n.
ν	Lagrange multiplier.
$O(\cdot)$	Computational complexity of an iterative algorithm.
$\boldsymbol{\pi}$	Steady-state probability vector.
π_i	Steady-state probability for state i, for all $i \in \mathbb{Z}$.
$P^{\max}$	Total power budget for one transmission cycle.
$P_{k,n}$	Instantaneous transmit power for user k at sub-carrier n.
$PL(\cdot)$	Decibel path loss.
R	Transmission rate.
$\sigma^2_{k,n}$	Noise variance for user k at sub-carrier n.
s_i	State i, for all $i \in \mathbb{Z}$.
S_t	Markov process at time t.
$\tau_{\max}$	Maximum delay spread.
τ_l	Time delay of the wireless channel response at the l^{th} path.
T	OFDMA symbol duration.
u_k	Utility function for user k.
w_k	Weighting factor for user k.
$x_{k,n}$	Transmitted signals for user k at sub-carrier n.
$y_{k,n}$	Received signals for user k at sub-carrier n.

List of Publications

1. **T. K. Chee**, C.-C. Lim, J. Choi, "Sub-optimal Power Allocation for Downlink OFDMA Systems", *in Proceedings of the IEEE 60th Vehicular Technology Conference - Fall*, vol. 3, pp. 2105-2109, September 2004.

2. **T. K. Chee**, C.-C. Lim, J. Choi, "Adaptive Power Allocation with User Prioritization for Downlink OFDMA Systems", *in Proceedings of the IEEE 9th International Conference on Communications System*, pp. 210-214, September 2004.

3. **T. K. Chee**, C.-C. Lim, J. Choi, "A Lumpable Finite-State Markov Model for Channel Prediction and Resource Allocation in OFDMA Systems", *in Proceedings of the IEEE 1st International Conference on Wireless Broadband and Ultra Wideband Communications*, March 2006.

4. **T. K. Chee**, C.-C. Lim, J. Choi, "Channel Prediction using Lumpable Finite-State Markov Channels in OFDMA Systems", *in Proceedings of the IEEE 63rd Vehicular Technology Conference - Spring*, May 2006.

5. **T. K. Chee**, C.-C. Lim, J. Choi, "A Cooperative Game Theoretic Framework for Resource Allocation in OFDMA Systems", *in Proceedings of the IEEE 10th International Conference on Communications System*, October 2006.

6. **T. K. Chee**, C.-C. Lim, J. Choi, "Sub-channel and Power Allocation with Channel Prediction Using Lumpable Finite-State Markov Model", *submitted for journal publication.*

7. **T. K. Chee**, C.-C. Lim, J. Choi, "A Cross-Layer Resource Allocation for OFDMA Systems Using Cooperative and Non-Cooperative Game Theory", *submitted for journal publication.*

This page is blank

Chapter 1

Introduction

The growth in cellular wireless communications in the last two decades has made it possible for people to communicate with anyone, from anywhere, at any time. The appreciation of the mobile radio communication industry in commercial interest has become a great driving force to push the technologies in achieving better link quality and higher system capacity. Unlike a single-user communication environment, a cellular wireless system is more complicated since it is often subjected to mutual interference among users. Furthermore, a wireless communication system also faces more challenges than its wired counterpart due to a volatile propagation environment with limited radio resources.

A basic mobile communication system consists of a base station, a mobile telephone switching office and multiple mobile units. The two communication links between a base station and multiple mobile units are known as the *downlink* and *uplink*. A *downlink* (or forward link) is a communication link from a base station to a mobile unit whereas an *uplink* (or reverse link) is a communication link from a mobile unit to a base station. The communication between the mobile unit and the base station via an air interface can utilise various multiple access schemes such as Time Division Multiple Access (TDMA) in a Global System for Mobile communications (GSM) system, Frequency Division Multiple Access (FDMA) in IS-136 or Code Division Multiple Access (CDMA) in IS-95. Hara and Prasad in [40] suggested that CDMA could combat the hostile channel frequency selectivity and provide higher capacity over conventional access techniques such as TDMA and FDMA. This suggestion was verified by numerical analysis and simulation.

Apart from these multiple access schemes, the multi-carrier modulation scheme, which is based on Orthogonal Frequency Division Multiplexing (OFDM), has become attractive, especially in high data rate wireless communications, due to its robustness and flexibility in resource allocation. The advantages of multi-carrier modulation and CDMA technique have motivated researchers to investigate the suitability of the new hybrid scheme, which combines the multi-carrier modulation and multiple access technique. This was proposed in recent years, namely OFDM-CDMA [99]. In general, there are three types of hybrid scheme, i.e. Multi-carrier Direct Sequence CDMA (MC/DS-CDMA), Multi-carrier CDMA (MC-CDMA) and Multitone CDMA (MT-CDMA) [40,70]. Not limited to these hybrid schemes, Orthogonal Frequency and Code Division Multiplexing (OFCDM), which was originally based on the MC-CDMA scheme, has been extensively studied in [2,3,65–68]. OFCDM has been shown to exhibit better performance than the conventional DS-CDMA approach in a broadband channel. On the other hand, some researchers placed their attention on the less complex multiple access OFDM, which is also known as Orthogonal Frequency Division Multiple Acess (OFDMA) [27,37,54]. It is an extension of OFDM which has the advantage of flexible resource allocation where the controllable radio resources are sub-carriers and transmission power. This thesis is mainly focusing on the downlink of an Orthogonal Frequency Division Multiple Acess (OFDMA) system.

1.1 Multi-carrier Systems

OFDM is a modulation technique that first appeared in the mid-1950s mainly for military communication systems. Chang [10] was one of the pioneers in exploring the concept of OFDM systems for dispersive fading channels during the 1960s. However, a lack of practicability in this initial concept of OFDM had slowed down its development. In the 1980s, Cimini introduced the use of OFDM for mobile communications in [21] due to its ability to support high-speed transmission in highly dispersive fading environments. Since then, this work has received much attention and has been the incentive for implementing the OFDM system as the standard for the Digital Audio Broadcasting (DAB) and the Digital Video Broadcasting (DVB) systems in Europe. Furthermore, OFDM has also been an active topic of research, especially for Asymmetric Digital Subscriber Line (ADSL) and Wireless Local Area Network (WLAN).

OFDM is a multi-carrier modulation scheme. It divides the frequency-selective wideband channel into multiple parallel frequency-flat narrowband sub-channels. An OFDM system with a fixed number of orthogonal sub-carriers can split a high data rate signal into the some parallel low data rate signals and transmit them simultaneously over all the sub-carriers. By extending the concept of a multi-carrier modulation scheme like OFDM to accommodate multiple access, researchers have become more attentive to the concept of an OFDMA system. An OFDMA system exploits the benefit of flexible resource allocation where the controllable radio resources are sub-carriers and transmission power. The scarce radio resources can be used more efficiently with the two-dimensional (i.e. sub-carriers and transmission power) resource control. Furthermore, the flexibility in sub-carrier allocation also helps to minimise multiple access interference, from which most CDMA related systems are suffering, by assigning a disjoint set of sub-carriers to individual users. Hence, OFDMA is one of the promising candidates to replace the existing multiple access schemes for the next generation of mobile communication systems [79].

1.2 Literature Reviews

The problem of assigning sub-carriers and transmission power to different users in an optimal manner has been an area of active research for OFDMA systems [27, 37, 54, 84, 86, 87, 106]. This section reviews the different types of adaptive sub-carrier and power allocation schemes, discusses the issues of performance degradation with these schemes when the OFDMA system experiences imperfect feedback information, and expatiates the works on resource allocation with cooperative and non-cooperative game theoretic frameworks.

1.2.1 Sub-carrier and Power Allocation

In the next generation of wireless communication systems, adaptive techniques will play an important role. Non-adaptive systems are constrained to use a single setting which is often designed to maintain acceptable performance when the channel quality is poor. In other words, these systems only work effectively in worst-case scenarios. As the OFDMA system is one of the prominent candidates of future high data rate wireless communication systems, an efficient resource allocation is necessary to improve system performance. The

scarce wireless radio resources can be used more efficiently with the two-dimensional resource control of an OFDMA system than with traditional one-dimensional control where the radio resource is either a frequency bin, a time slot or transmission power. The one-dimensional power allocation problem for a single user case was examined as a form of the *water-filling* problem in [23]. The graphical illustration of the water-filling concept is shown in Figure 1.1 where the polynomial curve, horizontal line and vertical arrows are defined as the water-filling condition, water level and amplitude of control variables, respectively. In a typical power allocation problem, the polynomial curve is derived from the inverse of the time-domain or frequency-domain channel gain and the horizontal line is determined as the amplitude level where the system throughput is optimised. By assigning different power levels at different time slots or frequency bins according to the various heights of the vertical arrows, the system achieves the optimum throughput.

There are many existing works that implement the concept of water-filling [16,18,19, 96,100,114,116,117]. For Gaussian multiple access channels with inter-symbol interference (ISI), Cheng and Verdú [16] studied the capacity regions of a two-user scenario and also obtained a non-trivial generalisation of the single-user water-filling theorem. By utilising the fact that the capacity region for an arbitrary number of users has a polymatriod structure, it is shown in [96] that the optimal power and rate allocation can be obtained in a greedy manner. This problem was extended to consider multiple users by Viswanath *et al.* in [100], where the behaviour of the asymptotically optimal water-filling policy in various regimes of number of users per unit degree of freedom and signal-to-noise ratio (SNR) were studied. The practicality of the water-filling concept was investigated when a group of researchers, who were actively involved in digital subscriber line (DSL) research, were implementing an iterative water-filling algorithm in power allocation to optimise

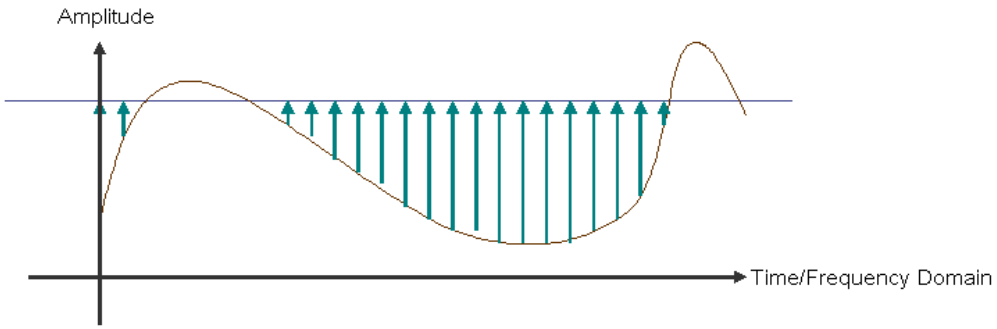

Figure 1.1. Water-filling.

the achievable capacity of frequency-selective Gaussian interference channels under the condition of strong interference [18, 19, 59, 114, 116, 117]. If the channel information is assumed to be perfectly known in advance, they showed that an iterative water-filling algorithm should be considered as a practical option since near-optimum performance is guaranteed for certain channel scenarios. However, one main drawback of an iterative water-filling algorithm is its complexity. Most existing literature propose to implement a heuristic approach in the iterative water-filling algorithm which leads to an increasingly high computational complexity as the dimension of the control variable increases. This issue may be insignificant in DSL systems because DSL systems allow implementation of a sophisticated power allocation algorithm due to the slowly varying channel. On the contrary, the fading channels of wireless systems are much more volatile than those in DSL systems. Therefore the computational complexity of an iterative water-filling algorithm has to be reduced, otherwise it may not be suitable for power allocation in wireless systems.

1.2.2 Adaptive Transmission Schemes with Imperfect Feedback

Research on adaptive transmission schemes, e.g. power allocation [20,33], modulation and coding [9,11,32,34,35], has reached a state of maturity. Ideally, in an adaptive transmission scheme, the channel state information (CSI) is assumed to be perfectly known to both the transmitter and the receiver. This assumption only holds if the receiver has accurate channel estimation and the feedback of this channel estimation to the transmitter has insignificant delay as compared to the symbol duration. For very slowly fading channels, imperfect or outdated CSI may be sufficient for reliable adaptive system design. When the fading environment becomes moderately to fast fading, imperfect CSI can cause severe degradation in performance, especially for adaptive transmission schemes that depend on accurate CSI [17, 31, 45, 88, 89, 111].

To enlarge the utilisable bandwidth to cater for the increasing applications of wireless devices, the future wireless systems are moving to a higher carrier frequency. However, this high carrier frequency results in very large Doppler shifts as the vehicular speed of the mobile user increases. A high Doppler shift indicates significant variations in the fading channel over a short period of time. Thus the feedback of imperfect or outdated CSI to the transmitter not only becomes less useful but could be a disruption to an adaptive scheme.

To realise the potential of adaptive transmission schemes, fading channel variations have to be reliably predicted at least several symbol durations ahead. While some researchers have addressed a related problem of estimation of current channel conditions [60–63, 97], the prediction of future channel conditions has not been addressed by many until recently. In [90], the outcome of channel prediction was obtained using a combined pilot-aided and decision-directed approach based on Kalman filtering. In [83], a short-range channel prediction method using polynomial approximation was proposed where only a few previous channel samples are required to estimate the next CSI. Nevertheless, one of the more attentive approaches is an auto-regressive approach which is known as the adaptive long-range prediction algorithm proposed by Duel-Hallen *et al.* in [24, 28, 46]. In [109,110], the long-range prediction algorithm was extended into the frequency domain. By observing the feedback CSI at carrier frequency f_1, the prediction of CSI at the adjacent carrier frequency f_2 can be obtained without additional feedback information. However, one main drawback of this prediction is that the predicted samples must be sufficiently correlated with the observations in both time and frequency, such that these correlation functions are known a priori.

The involvement of Markov theory in various telecommunication issues has led to the use of Markov chains in channel modelling and estimation [57]. Gilbert [30] and Elliott [25] were the first to model the communication channel with Markov processes during 1960s. The Gilbert-Elliott channel belongs to a binary-state Markov process. Although Markov modelling of a communication channel is a simple and effective approach for channel description, the oversimplification of binary-state Markov channel is inadequate to describe the channel quality that varies dramatically. Wang and Moayeri [102] utilised the idea of the finite-state Markov model to partition the range of received SNR into a finite number of intervals, where each interval forms the state of the Markov chain. Wang and Chang [101] extended this model by using analytical first-order statistics to obtain model parameters. The first-order Markovian assumption for Rayleigh fading channel is verified to be adequately accurate compared to the higher order Markov models of much higher complexity. A similar conclusion on the usefulness of the first-order finite-state Markov model in representing flat-fading channel was drawn by Tan and Beaulieu in [93]. Other existing literature [4, 15, 42, 118] also suggested that the first-order Markov models are reliable for approximating a quantised Rayleigh fading channel. With the availability of state transition probabilities and steady-state probabilities of a finite-state Markov

process, it would be interesting to see if the Markov model could reliably predict the channel information for slow, moderate and fast Rayleigh fading channels.

1.2.3 Cooperative and Non-cooperative Resource Allocation

After the successful implementation of the concept of utility from economics into radio resource management, the utility-based game theoretic framework in the context of telecommunications has been studied by many. Game theory studies the behavior of rational economic agents in mathematically well-defined competitive situations called games, which can be branched to cooperative and non-cooperative forms. A game theoretic framework for resource allocation problem has been considered in many studies [36–38, 44, 71, 81, 91, 107, 108].

Due to the difficulty in implementing centralised algorithms for resource allocation, most researchers emphasised distributed algorithms which belong to the domain of non-cooperative game theory [36,38,81,91,107]. In a non-cooperative game, each user is selfish and only interested in achieving their own goals. An ideal outcome of a non-cooperative game is to achieve a Nash equilibrium, which is perceived as a set of strategies where no user has anything to gain by changing only his/her own strategy unilaterally. However, some have shown that the Nash equilibria are inefficient from the point of overall system utility [7,48,49]. The authors in [48,49] have quantised the efficiency loss suffered at Nash equilibria as compared to the optimal aggregate surplus. This loss in efficiency is known as the price of anarchy [75].

On the other hand, the work in [37,44,108] belong to the domain of cooperative game theory. Since all users will be competing for the use of the available wireless resources, one of the most important criteria is the notion of fairness. Dealing with fairness while satisfying different requirements from users might be challenging. A more well known approach that provides a satisfactory outcome in resource allocation is to use the fairness criteria from the Nash bargaining framework [72, 73]. The sole reason that cooperative game theory is more favourable than its non-cooperative counterpart is because the solution of the Nash bargaining model is Pareto optimal. The idea of using the Nash bargaining model in the context of packet-switched networks was first proposed in [69]. Yaïche *et al.* in [108] extended this study to the context of elastic services in broadband networks.

They proposed to decentralise a centralised problem so that a greedy distributed algorithm can yield an optimal and fair bandwidth allocation. Although the Nash bargaining model gives us precise mathematical characterisation of the resource allocation problem, the main difficulty in solving the problem is that it cannot be formulated as a convex optimisation problem. Thus, neither the Karush-Kuhn-Tucker (KKT) conditions nor the duality theorems are able to provide the sufficient and necessary condition for optimality. This problem becomes more severe and non-linear if we consider resource allocation in an OFDMA system due to the involvement of multi-carrier transmission. To face this challenge, Han *et al.* in [37] formulated a cooperative game theoretic sub-channel allocation problem for an OFDMA system. The authors did not derive a closed-form Nash bargaining solution (NBS), instead they approximated the optimality condition of the two-user case with constraint relaxation. By grouping all users into pairs, an iterative algorithm was proposed to check the two-user optimality condition for all possible combinations until convergence occurred. However, this algorithm might not converge towards the NBS due to the non-linear nature of the formulated problem. Therefore, the existence of closed-form NBS for resource allocation still remains unanswered.

1.3 Motivation

Most, if not all, existing works on adaptive sub-carrier and power allocation schemes for an OFDMA system strongly depend on the optimisation of the system spectral efficiency, often known as Shannon's capacity [82]. Even though the research on power allocation with water-filling has reached a state of maturity, most existing literature did not derive the closed-form solution of the power allocation problem but relied on some computationally complex algorithms [18, 114, 115, 117]. Very few existing works actually provide a cost-effective and delay-sensitive algorithm which approximates closely to the result of optimal water-filling. The work in [84] proposed a low-complexity algorithm to allocate transmission power under the condition that an independent sub-channel allocation is pre-determined. It was shown that their power allocation algorithm can achieve about 95% of the optimal capacity in a two-user system. In a rational circumstance, we expect their power allocation algorithm to achieve much less than 95% of the optimal capacity as the number of users increases. This motivates us to consider another approach to further improve the achievable capacity to a near-optimum level such that the relative loss in

optimal capacity is minimal as the number of users increases. This work forms the basis of this research. We shall extend this work to consider more practical issues, such as the imperfect feedback CSI, huge feedback overheads and unfairness in rate distribution.

The perfect feedback of CSI has been an essential assumption for most resource allocation. In reality, perfect channel information is not always available since the wireless communication channel is much more volatile than its wired counterpart. Moreover, the impact of outdated CSI can be quite severe in performance degradation, especially for an adaptive transmission scheme that strongly relies on accurate CSI. Most common channel prediction schemes in wireless communication are strongly dependent on adaptive filter theory. One example is the long range prediction scheme based on an auto-regressive model to reliably predict channel conditions several symbol durations ahead [24, 28, 46, 110]. This approach relies strictly on one condition, i.e. the time and frequency correlation functions must be known a priori. In a multi-user single-carrier system, the computational complexity of a long range prediction scheme may still be acceptable. However, its complexity increases exponentially in a multi-user multi-carrier system. Therefore, a reduced-complexity and simple-to-implement alternative is desirable for a multi-user multi-carrier system such as OFDMA. We use the concept of a finite-state Markov channel, which is conventionally used in a single-carrier environment, to model the vibrant wireless communication channel. Since the dynamics of the Markov process has been proven to reliably estimate CSI in a slow fading environment, we extend the channel estimation models in [102, 118] to solve a channel prediction problem for an OFDMA system in a moderately fast fading environment.

A conventional feedback communication system requires the receiver to feed back all detailed channel information to the transmitter [43]. As the communication technology advances from a wired to a wireless environment, and as the characteristic of the feedback information changes from a point-to-point to a multi-user multi-carrier communication system, a full feedback of detailed channel information may not be practical anymore, especially for large number of users and carriers. One way to reduce the overheads for CSI feedback was proposed in [113]. An aggregated sub-channel structure is formed using a similar concept as the clustered OFDM [62], where each sub-channel consists of a set of adjacent sub-carriers. By obtaining the first- and second-order statistical moments of the channel gain at each set of the adjacent sub-carriers, Yoon *et al.* in [113] proposed

to feedback the statistical measurements to the transmitter instead of the detailed sub-channel information. This approach indeed reduces the feedback overheads significantly, however it sacrifices the detail of CSI for each sub-channel. This motivates us to develop a limited feedback scheme that is low in overheads but maintains partial detail on channel quality.

In the multi-access wireless networks, adaptive transmission schemes such as sub-carrier and power allocation often involve greedy algorithms that maximise the system throughout. These algorithms usually allocate maximal resources to those users whose channel conditions are above a certain threshold and restrain those whose channel conditions are below that threshold. Therefore users with better channel quality often enjoy the privilege of exceptionally good quality of service (QoS) while other users suffer with poor QoS. To counter this unfair scenario, a game theoretic framework is adopted to solve the resource allocation problem. Due to the extremely high complexity of a centralised resource allocation algorithm, most existing works have chosen to implement the non-cooperative game theory [36, 38, 91, 107]. To the best of our knowledge, very limited work has been done on modelling a non-cooperative resource allocation game for an OFDMA system. Some researchers have investigated the Pareto-efficiency of a non-cooperative game theoretic framework and quantified the efficiency loss of such a framework in [48, 49, 81]. This motivates us to model a non-cooperative resource allocation game for an OFDMA system. There is another branch of game theory, namely the cooperative game, which emphasises collective rationality, maintains stricter fairness criteria and attains Pareto optimality. According to Cao *et al.* in [7], there are three forms of bargaining models in cooperative game theory, namely the Nash bargaining model, the Raiffa-Kalai-Smorodinsky bargaining model and the Modified Thomson bargaining model. The work in [37] is the only work which outlined a cooperative resource allocation game for an OFDMA system using the Nash bargaining model. However, they did not derive a closed-form NBS, instead they approximated the optimality condition of the two-user case with constraint relaxation, which led to an inefficient algorithm with high computational complexity. This motivates us to model a cooperative resource allocation game for an OFDMA system to attain a fair distribution of wireless resources with the Nash and Raiffa-Kalai-Smorodinsky bargaining models. Note that we do not consider the Modified Thomson bargaining model due to its complexity. By deriving the corresponding closed-form solutions for the bargaining models, we can generate a simple

and reduced-complexity algorithm to attain the outcome of the resource allocation. By reviewing the existing literature in cooperative and non-cooperative games, we found that none of them had compared the performance of cooperative and non-cooperative games but they claimed that one is better than the other. Since we have modelled the resource allocation problem for an OFDMA system in both cooperative and non-cooperative games, this motivates us to compare the fairness, achievable rates and efficiency losses of the cooperative and non-cooperative resource allocation schemes under the same system with the same wireless resources for sharing. Our aim is to provide a quantitative proof that a cooperative scheme is better than a non-cooperative scheme.

1.4 Contributions and Organisation of Thesis

The main focus of this research is to optimise the system achievable spectral efficiency of the downlink OFDMA system with resource allocation. The basic idea behind dynamic resource allocation is to utilise the wireless channel more efficiently by sharing the available wireless resources. We exploit the characteristics of the fading channel to adaptively allocate sub-carriers and transmission power to individual users in order to achieve optimal transmission rates. The main objective of this thesis is to provide answers to the issues involving computational complexity, outdated channel information and the fairness constraint in downlink resource allocation for OFDMA systems. A brief description of each chapter in this thesis and its contribution are given as follows:

Chapter 2:
Background

In Chapter 2, we outline the characteristics of the basic channel and system models of a downlink OFDMA system and provide sufficient and concise mathematical background on the constrained optimisation with duality, the finite-state Markov model and game theory.

Chapter 3:
Adaptive Power Allocation with Sub-carrier Sharing

In Chapter 3, we develop a multi-user power allocation algorithm in an OFDMA system to achieve near-optimal capacity. For the purpose of simplicity, we will not consider sub-channel allocation because we want to compare the complexity of the existing water-filling algorithm to the proposed power allocation algorithm. This work may be perceived to be idealistic but shall form the basis of our research and help us to model more practical problems in later chapters. We summarise the original contribution of this chapter as follows:

- **Sub-optimal closed-form power allocation solution**
  We obtain the sub-optimal closed-form solution of the power allocation problem by the duality theorem and propose two algorithms with this sub-optimal solution. Simulation results show that the method is capable of achieving 99% of the optimal capacity.

- **Reduced complexity algorithm**
  Most existing water-filling algorithms in power allocation schemes are heuristic algorithms where their complexity may be exponentially proportional to the number of users, K, or carriers N. By utilising our sub-optimal power allocation closed-form solution, the proposed algorithm only requires computational complexity of $O(KN)$.

- **User-prioritisation**
  It has been widely accepted in the link layer that a power control scheme can allow an uneven power budget among users in order to meet different quality of service (QoS). However, this is a rare practice in the physical layer. We formulate the power allocation problem with two control variables, namely the transmission power and a weighting factor that determines the proportional power budget for individual user based on the different priorities among requested services.

Chapter 4:
Sub-channel and Power Allocation with Limited Feedback

In Chapter 4, we extend the concept of a finite-state Markov channel to model the fading channel of an OFDMA system. Most existing works on channel quantisation are modelled with a uni-chain finite-state Markov channel, which is only realisable if the channel is perceived as a single stream. For a multi-carrier environment, an expanded Markov channel is required to model the channel dynamics of the multi-carrier transmission. One main challenge for the expanded Markov channel is its extremely high complexity due to the extremely large number of states. We propose a two-step approach to reduce the expanded Markov channel into a feasible size. A channel predictor is developed to reliably predict CSI at least one symbol duration in advance. We summarise the original contribution of this chapter as follows:

- **Closed-form sub-carrier and power allocation solutions**
  We decompose the capacity optimisation problem to two, viz. sub-carrier and power allocation problems. Using the concept of constrained optimisation with duality, we obtain the sub-optimal and optimal closed-form solutions to the sub-carrier and power allocation problems, respectively.

- **Lumpable finite-state Markov channels**
  In the second step of the two-step approach, we propose to use the concept of lumpability, where an aggregated state is formed from multiple atomic states of the finite-state Markov channel. This process reduces the expanded Markov channel to multiple parallel uni-chain Markov channels. The lumpable finite-state Markov model forms the core of the limited feedback prediction.

- **Channel prediction with limited and full feedback CSI**
  The expanded Markov channel represents the fading channel as a whole, thus the corresponding feedback CSI is perceived as a form of full feedback. The lumpable Markov channels, on the other hand, requires much less feedback bits than the expanded model, thus it implies that this is a limited feedback.

Chapter 5:
A Game Theoretic Framework for Resource Allocation

In Chapter 5, we incorporate the concept of utility function into an OFDMA resource allocation problem. With different preference and utility functions, the resource allocation problem can be classified into cooperative and non-cooperative games. We summarise the original contribution of this chapter as follows:

- **Non-cooperative resource allocation game**
  We formulate a sigmoid-like utility function such that it describes the gain in throughput of an individual user as more sub-carriers are allocated to the corresponding user. The non-cooperative game is a form of a dynamic game where the system will pre-specify the order of users to choose a set of sub-carriers from the available sub-carriers that maximise their own utilities.

- **Cooperative resource allocation game**
  Based on the preference function concept proposed in [7] and [44], we derive the closed-form Nash bargaining solution (NBS) and the closed-form Raiffa-Kalai-Smorodinsky bargaining solution (RBS). Both solutions are shown to be fair and Pareto optimal according to the users' maximum and minimum rate requirements.

- **Performance comparison between cooperative and non-cooperative resource allocation games**
  We provide a comprehensive comparison between the cooperative and non-cooperative resource allocation schemes under the same multi-carrier system with the same wireless resources for sharing. The substances of the performance comparison include fairness, achievable transmission rates and efficiency losses. To our best knowledge, we are the first to do such work.

Chapter 6: Conclusion and Future Research

This chapter summarises the research performed and suggests some future research directions in connection with our current research work.

Chapter 2

Background

In this chapter, we discuss the technical background of this research by outlining the characteristics of the wireless channel and system model of a downlink OFDMA system. We provide sufficient and concise mathematical background on the three main mathematical tools which are used in this research. These are constrained optimisation with duality, the Markov model and game theory.

2.1 Downlink OFDMA System

2.1.1 Channel Model

Consider a mobile radio channel consisting of a number of paths, or moving scatters. Its impulse response can be described by [47]

$$h(t,\tau) = \sum_l \alpha_l(t)\delta(\tau - \tau_l), \tag{2.1}$$

where $\alpha_l(t)$ is the time-varying amplitude of the channel response at the l^{th} path, $\delta(\cdot)$ is an impulse function and τ_l is the time delay of the l^{th} path.

As the number of paths grows infinitely large, the $\alpha_l(t)$ terms are assumed to be wide-sense stationary narrowband complex Gaussian processes where all paths are independent among each other, i.e. $E[\alpha_i(t)\alpha_j(t)] = 0$ for all $i \neq j$. The Fourier transform of $h(t,\tau)$ with $\tau \to f$ is the time-varying frequency response, which is defined as

$$H(t,f) = \int_{-\infty}^{\infty} h(t,\tau)e^{-j2\pi f\tau}d\tau = \sum_l \alpha_l(t)e^{-j2\pi f\tau_l}. \tag{2.2}$$

The auto-correlation function of the frequency response for time difference Δt and frequency separation Δf is given by

$$\begin{aligned} r(\Delta t, \Delta f) &= E[H(t+\Delta t, f+\Delta f)\cdot H^*(t,f)] \\ &= E\left[\sum_l \alpha_l(t+\Delta t)e^{-j2\pi(f+\Delta f)\tau_l}\cdot\sum_k \alpha_k(t)e^{-j2\pi f\tau_k}\right] \\ &= \sum_l E\left[\alpha_l(t+\Delta t)\cdot\alpha_l(t)\right]e^{-j2\pi\Delta f\tau_l}. \end{aligned} \tag{2.3}$$

If the time-varying amplitude $\alpha_l(t)$ has the same normalised auto-correlation function $r_t(\Delta t)$ for all l-path [61], the ensemble-average term in (2.3) can be written as

$$E\left[\alpha_l(t+\Delta t)\cdot\alpha_l(t)\right] = \sigma_l^2 r_t(\Delta t), \tag{2.4}$$

where σ_l^2 is the variance of the channel amplitude at l^{th} path.

Using (2.4), the auto-correlation function in (2.3) can be simplified to

$$\begin{aligned} r(\Delta t, \Delta f) &= r_t(\Delta t)\sum_l \sigma_l^2 e^{-j2\pi\Delta f\tau_l} \\ &\approx r_t(\Delta t)e^{-j2\pi\Delta f\sigma}\sum_l \sigma_l^2 \\ &= r_t(\Delta t)r_f(\Delta f), \end{aligned} \tag{2.5}$$

where σ is denoted as the rms delay spread. Note that the term $\sum_l \sigma_l^2$ in (2.5) is normalised to unity and thus $r_f(\Delta f)$ takes the form of $e^{-j2\pi\Delta f\sigma}$. Hence, the correlation function of the frequency response for time difference Δt and frequency separation Δf is separated into a time-domain correlation $r_t(\Delta t)$ and a frequency-domain correlation $r_f(\Delta f)$. The classical Jakes model [47] shows that the time-domain correlation is given by

$$r_t(\Delta t) = J_0(2\pi f_d \Delta t), \tag{2.6}$$

where $J_0(\cdot)$ is the zeroth order Bessel function, $f_d = vf_c/c$ is the maximum Doppler frequency, which is related to the moving speed of mobile user v, carrier frequency f_c and speed of light c. On the other hand, the frequency-domain correlation can be written as

$$r_f(\Delta f) = e^{-j2\pi\Delta f\sigma} = \cos(2\pi\Delta f\sigma) - j\sin(2\pi\Delta f\sigma). \tag{2.7}$$

2.1.2 OFDM System

Consider an OFDM system with N orthogonal sub-carriers, each spaced by Δf Hz. A high data rate signal is split into N parallel low data rate signals and these are transmitted simultaneously over the N sub-carriers. The transmitter and receiver configurations of an OFDM system are illustrated in Figure 2.1.

The binary data stream is first encoded and modulated with an arbitrary modulation and coding scheme. The resulting data stream with a symbol duration of $\frac{N}{\Delta f}$ is serial-to-parallel (S/P) converted into N parallel streams of reduced data rate narrowband signals. Each parallel stream is transmitted on a separate sub-carrier. The Inverse Discrete Fourier Transform (IDFT) and Discrete Fourier Transform (DFT) are used for modulation and demodulation, respectively, to reduce computational complexities on transmitter and receiver. At the transmitter, a cyclic prefix (also known as guard interval) of length $\Delta T = \frac{d}{\Delta f}$ is appended in between successive OFDM symbols, in order to suppress the effect of inter-symbol interference (ISI), which is caused by the multi-path environments, while preserving the orthogonality of the sub-carriers. Therefore, the new OFDM symbol duration is $T = T' + \Delta T$, where $T' = \frac{N}{\Delta f}$. Let τ_{max} be denoted as the maximum delay spread, and f_d be the maximum Doppler frequency, $\Delta T > \tau_{max}$ can result in mitigation of ISI and $T > \frac{1}{f_d}$ ensures that each sub-channel is observed as a frequency-flat fading channel. After parallel-to-serial (P/S) and digital-to-analog conversion (DAC), the signal is sent through a frequency-selective channel.

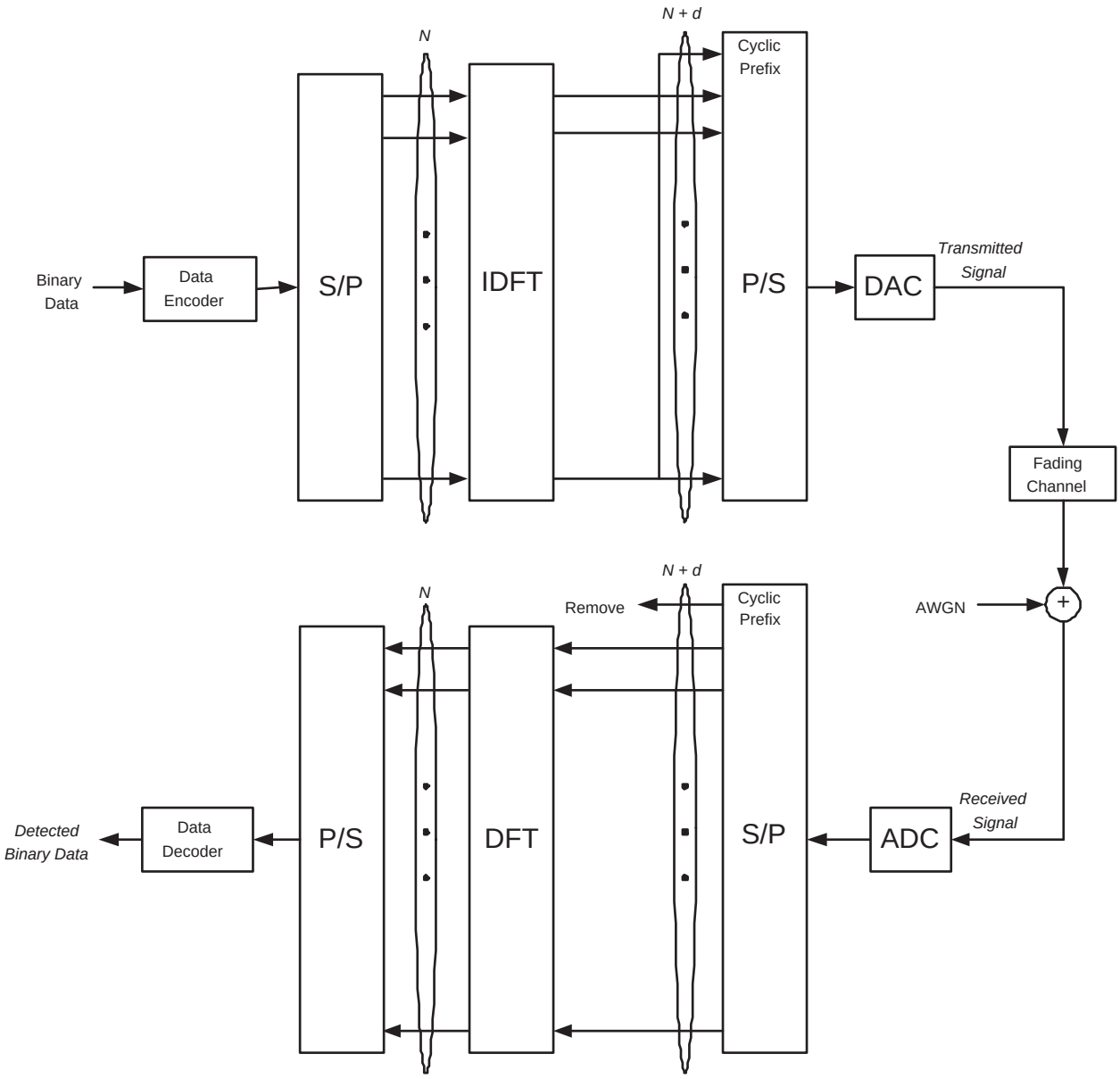

Figure 2.1. OFDM system configuration.

2.1.3 OFDMA System Model

An OFDMA system has the same configuration as the OFDM system, except that the total signal bandwidth is shared by multiple users. Consider the downlink of a single-cell OFDMA system of N sub-carriers with a frequency-selective fading channel. There are K users randomly located within this cell. The entire bandwidth B is shared among N sub-carriers and this allows all users to transmit simultaneously. Assuming that the

sub-carrier separation is smaller than the coherent bandwidth, each sub-carrier can be considered as a flat fading sub-channel.

Assuming unity average transmission power, a general downlink received signal for an arbitrary k^{th} user at its n^{th} sub-carrier is modelled as

$$y_{k,n} = x_{k,n}h_{k,n} + n_{k,n}, \tag{2.8}$$

where $x_{k,n}$ and $y_{k,n}$ are the transmitted and received signals, respectively, $n_{k,n}$ is the additive white Gaussian noise (AWGN) and $h_{k,n}$ is extracted from the channel vector $\mathbf{h}_k = [h_{k,1}, \ldots, h_{k,N}]$. The corresponding signal-to-noise ratio (SNR) for the k^{th} user's n^{th} sub-channel is expressed as $\gamma_{k,n} = |h_{k,n}|^2/\sigma_{k,n}^2$, where $\sigma_{k,n}^2$ is the noise variance of AWGN.

As the overall bandwidth, B, is evenly allocated to each sub-channel, the noise variance of any arbitrary user k at all sub-channels are identical, i.e. $\sigma_{k,n}^2 = \sigma_k^2/N$. Assuming unit power for each sub-channel, the Shannon's capacity [82] is defined as

$$C = \sum_{k=1}^{K}\sum_{n=1}^{N} \frac{B}{N} \log_2\left(1 + \gamma_{k,n}\right). \tag{2.9}$$

2.2 Mathematical Background

2.2.1 Constrained Optimisation with Duality

The concept of constrained optimisation is used in this research. A convex optimisation problem with primal variable x can be written in the form of:

$$\begin{aligned} \min_{x} \quad & f_0(x) \\ \text{s.t.} \quad & f_i(x) \leq 0 \quad \forall i \in \{1, \ldots, L\}, \end{aligned} \tag{2.10}$$

where $f_0(x)$ is the primal objective and $f_i(x)$, for all i, denote a set of constraints. One or more optimal solutions exist if and only if the primal objective and all its constraints are convex. To solve the optimisation problem, we need to construct a Lagrangian, which is given by

$$L_P(x, \lambda_i) = f_0(x) + \sum_{i=1}^{L} \lambda_i f_i(x), \tag{2.11}$$

where λ_i, for all i, are denoted as the Lagrangian multipliers, of which each λ_i corresponds to the constraint of $f_i(x) \leq 0$.

By setting the first derivative of $L_p(x, \lambda_i)$ with respect to x to zero, we obtain

$$\frac{\partial f_o(x)}{\partial x} + \sum_{i=1}^{L} \lambda_i \frac{\partial f_i(x)}{\partial x} = 0. \tag{2.12}$$

We can express x explicitly in terms of λ_i, such that $x = g(\lambda_i)$. By substituting the expression of $x = g(\lambda_i)$ to (2.11), the primal variable x vanishes and we obtain

$$L_D(\lambda_i) = f_0\big(g(\lambda_i)\big) + \sum_{i=1}^{L} \lambda_i f_i\big(g(\lambda_i)\big), \tag{2.13}$$

where $f_0\big(g(\lambda_i)\big)$ is the dual objective and $f_i\big(g(\lambda_i)\big)$, for all i, denote a set of dual constraints.

The minimisation of primal objective over the original constraint set is called the *primal problem* whereas the maximisation of dual objective over the dual constraints is called the *dual problem*. According to [6], we can relate the primal and dual problems in this form:

$$\min_x f_0(x) \geq \max_{\lambda_i} f_0\big(g(\lambda_i)\big), \tag{2.14}$$

where the difference between these two optimal solutions is defined as the duality-gap $\Gamma = f_0(x) - f_0\big(g(\lambda_i)\big)$.

By setting the first partial derivative of $L_D(\lambda_i)$ with respect to λ_i to zero, we obtain

$$\frac{\partial f_0\big(g(\lambda_i)\big)}{\partial \lambda_i} + f_0\big(g(\lambda_i)\big) + \lambda_i \frac{\partial f_0\big(g(\lambda_i)\big)}{\partial \lambda_i} = 0. \tag{2.15}$$

We can derive the optimal solution of dual variable, λ_i^*, explicitly by rearranging (2.15). The optimal solution of primal variable can be determined subsequently as $x^* = g(\lambda_i^*)$. If an optimum pair of (x^*, λ_i^*) exists, where x^* and λ_i^* are the primal and dual variables at their optimum, respectively, the duality gap reduces to zero, while the following Karush-Kuhn-Tucker (KKT) conditions, which are necessary and sufficient for optimality, shall be satisfied:

$$f_i(x^*) \leq 0; \tag{2.16}$$

$$\lambda_i^* \geq 0; \tag{2.17}$$

$$\frac{\partial}{\partial x} L_P(x^*, \lambda_i^*) = 0; \tag{2.18}$$

$$\lambda_i^* f_i(x^*) = 0. \tag{2.19}$$

2.2.2 Finite-state Markov Model

A Markov process is a stochastic process where only the current state is necessary for predicting a subsequent state or multiple states. The Markovian assumption states that all states prior to the current state are not needed if the current state is known. Let $\mathcal{S} = \{s_1, s_2, \ldots, s_i, s_j, \ldots\}$ denote a set of states and $\{S_t\}$, where the discrete time index is given as $t \in \{0, 1, \ldots\}$, be a constant Markov process, which has stationary transitions [102]. The Markov property for a first order Markov process states that

$$\Pr\big(S_t = s_i \mid S_{t-n} = s_k, \ldots, S_{t-1} = s_j\big) \;=\; \Pr\big(S_t = s_i \mid S_{t-1} = s_j\big). \tag{2.20}$$

In a discrete state space with M finite states, where $\mathcal{S} = \{s_1, s_2, \ldots, s_M\}$, the Markov process can be realised as a state transition process. The transition probability distribution can be represented as a square matrix of size M, which is called the state transition matrix, $\mathbf{A}$, with its (i, j) element given in the form of

$$a_{i,j} \;=\; \Pr\big(S_{t+1} = s_j \mid S_t = s_i\big). \tag{2.21}$$

Since $a_{i,j}$ is a probability term, it must satisfy two requirements, such that $0 < a_{i,j} < 1$ and $\sum_{j=1}^{M} a_{ij} = 1$, for all $i \in [1, M]$.

By raising the state transition matrix $\mathbf{A}$ to a very high power, we obtain

$$\mathbf{\Phi} = \mathbf{A}^{\infty}, \tag{2.22}$$

where each row indicates the probability assignment over the states of the Markov process that must exist for each starting state when the number of transitions are allowed to increase to be infinitely large. Since it is proven by many that all rows in $\mathbf{\Phi}$ are identical, one can intuitively conclude that the probability assignment does not depend on the initial state of the process. To characterise the behaviour of an M-state Markov process, we define a row vector of steady-state probabilities, $\boldsymbol{\pi}$, whose i^{th} element is given by

$$\pi_i \;=\; \Pr\big(S_t = s_i\big), \tag{2.23}$$

where $\pi_i \in \boldsymbol{\pi}$ and $\boldsymbol{\pi}$ is denoted as one of the M identical rows in $\mathbf{\Phi}$. Note that the condition of $\sum_{i=1}^{M} \pi_i = 1$ must always be satisfied. Given that we know the current state is state s_i, we can define the probability of being in state s_j at the next time frame as

$$\Pr\big(S_{t+1} = s_j\big) \;=\; \Pr\big(S_{t+1} = s_j \mid S_t = s_i\big) \cdot \Pr\big(S_t = s_i\big) \;=\; a_{i,j}\pi_i. \tag{2.24}$$

A typical M-state Markov process can be classified into three different categories: birth-death (BD), quasi-birth-death (QBD) [55] and non-birth-death (NBD) processes, which are shown in Figures 2.2, 2.3 and 2.4, respectively. From the illustrations, we can observe that the BD process involves a uni-chain transition that only allows state transition of not more than one adjacent state. The QBD process involves a multi-chain transition whereby grouping necessary states into a block can help to resemble the structure of a uni-chain transition. For any other Markov processes that do not resemble the transition structures of the BD and QBD processes, they are generally classified as NBD processes. To clarify the differences between these processes, let us consider the following examples with $M = 4$:

Assume the transition probabilities are piecewise uniform, such that the probability of state transition from state i to state j, for all $i \neq j$, is given by

$$a_{i,j} = \begin{cases} p, & \text{for all } i > j; \\ q, & \text{for all } i < j. \end{cases} \tag{2.25}$$

The state transition matrices for the three processes are defined as:

1. BD Process,

$$\mathbf{A}^{\text{BD}} = \begin{bmatrix} 1-p & p & 0 & 0 \\ q & 1-p-q & p & 0 \\ 0 & q & 1-p-q & p \\ 0 & 0 & q & 1-q \end{bmatrix}. \tag{2.26}$$

2. QBD Process,

$$\mathbf{A}^{\text{QBD}} = \begin{bmatrix} 1-2p & p & p & 0 \\ q & 1-p-q & 0 & p \\ q & 0 & 1-p-q & p \\ 0 & q & q & 1-2q \end{bmatrix} \tag{2.27}$$

$$= \begin{bmatrix} 1-2p & P & 0 \\ Q^T & R & P^T \\ 0 & Q & 1-2q \end{bmatrix}, \tag{2.28}$$

where $P = [p \quad p]$, $Q = [q \quad q]$ and $R = \text{diag}(1-p-q, 1-p-q)$.

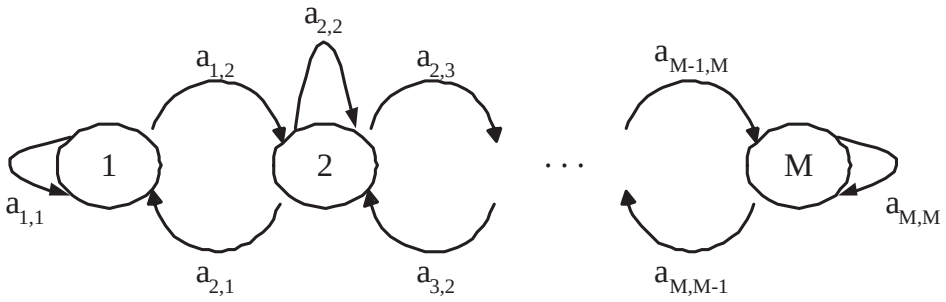

Figure 2.2. Illustration of a birth-death M-state Markov chain.

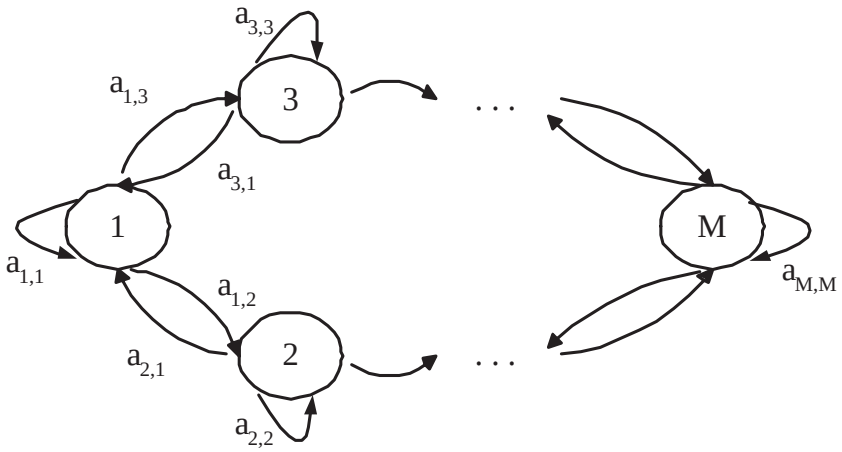

Figure 2.3. Illustration of a quasi-birth-death M-state Markov chain.

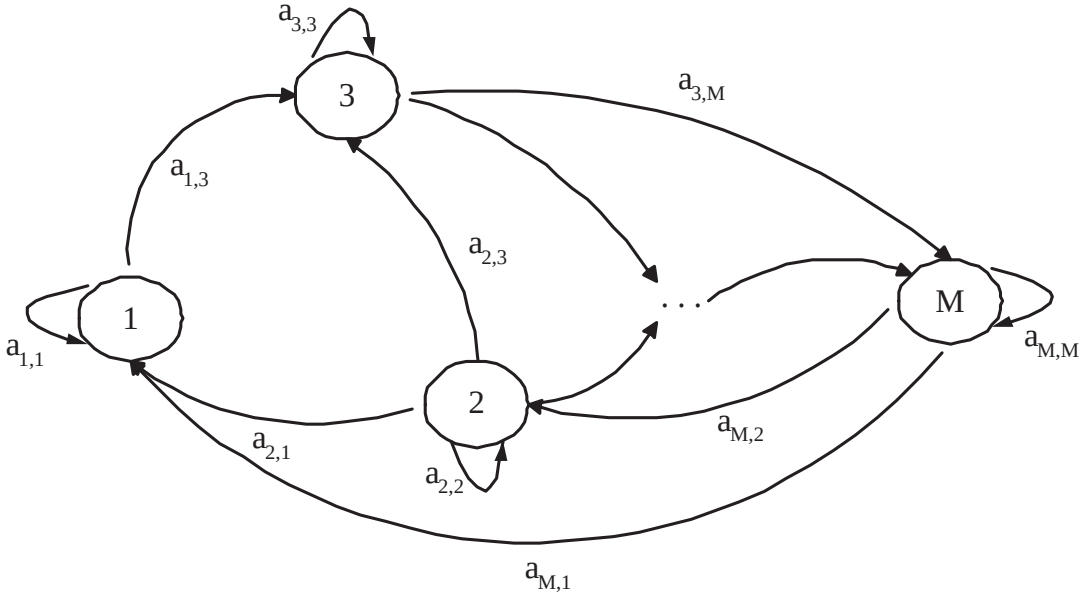

Figure 2.4. Illustration of a non-birth-death M-state Markov chain.

3. NBD Process,

$$\mathbf{A}^{\mathrm{NBD}} = \begin{bmatrix} 1-p & 0 & p & 0 \\ q & 1-2p-q & p & p \\ 0 & 0 & 1-p & p \\ q & q & 0 & 1-2q \end{bmatrix}. \tag{2.29}$$

The state transition matrix $\mathbf{A}^{\mathrm{BD}}$ in (2.26) attains the diagonal pattern which is commonly used to recognise one as a uni-chain Markov process. By grouping entries of states 2 and 3 in the original state transition matrix $\mathbf{A}^{\mathrm{QBD}}$ in (2.27), we can perceive $\mathbf{A}^{\mathrm{QBD}}$ in (2.28) to closely resemble this diagonal pattern. The similarity of state transition matrix $\mathbf{A}^{\mathrm{QBD}}$ in (2.28) with the state transition matrix $\mathbf{A}^{\mathrm{BD}}$ in (2.26) gives this process the name of quasi-birth-death. Since each state in the NBD process is allowed to transit randomly to any other states, its state transition matrix does not form any regular pattern. For simplicity sake, when the wireless communication channels are modelled as Markov processes, these models are often fitted with BD or QBD processes.

2.2.3 Game Theory

Modern game theory is generally attributed to *John von Neumann* due to his papers of 1928 and 1937, although it may be said that the work of *Ernest Zermelo* (1913) and *Emile Borel* (1921) laid the foundation of game theory. The formal conception of game theory was organised in *Theory of Games and Economic Behavior* [74], which von Neumann wrote in collaboration with *Oskar Morgenstern*. In 1950, *John Nash* earned his Ph.D. with his 27-page dissertation on non-cooperative games. He demonstrated that finite games always have an equilibrium point, which is known as the *Nash Equilibrium*, where all players choose to make choices that are best for them given their counterparts' choices. This forms the first branch of game theory, namely *non-cooperative games*. In the same year, Nash published a paper on bargaining models [73] which has driven a revolution in game theory. It forms the second branch of game theory, namely *cooperative games*.

Game theory is the formal study of conflict and cooperation. The object of study in game theory is the *game*, which is a formal model of an interactive situation that involves several *players*. Its concepts apply whenever the actions of these players are interdependent. Thus game theory provides a language to formulate, structure, analyse and understand strategic scenarios. A central assumption in game theory is that all players

are rational and always chooses an action which gives the outcome one most prefers, given what one expects his opponents to do. This common knowledge of rationality is the key to achieve an equilibrium point.

A non-cooperative game models the process of players making choices out of their own interest to achieve a Nash equilibrium. A Nash equilibrium, also called a strategic equilibrium, is a set of strategies (one for each player) where no player has anything to gain by changing only his own strategy unilaterally. Non-cooperative games can be divided into two categories: static and dynamic games. In a static game, players make decisions simultaneously without knowing the decisions of other players. This is known as the strategic form of a game. Players in a dynamic game are governed by a strict order of play such that each player takes turn to make their decisions with the knowledge of the decisions of all previous players. This type of game is often referred as the extensive form [98]. In general, a non-cooperative game may attain multiple Nash equilibria with a different set of strategies. Even though there exists one or more Nash equilibria in one game, it is possible that none of these Nash equilibria belongs to the true optimum.

A cooperative game which derived from the bargaining problem is a high-level description, specifying what payoffs each potential group can obtain by the cooperation of its players. Nash bargaining model fits within the cooperative framework in that the solution does not define a specific timeline of offers and counteroffers, but rather focuses solely on the outcome of the bargaining process. Therefore a Nash bargaining solution is a Pareto optimal solution to the cooperative game [7]. A set of solutions is considered as Pareto optimal if and only if there is no wasted utility such that no player can be better off without making any other worse off.

This page is blank

Chapter 3

Adaptive Power Allocation with Sub-carrier Sharing

This chapter investigates the problem of minimising overall transmission power while maximising the spectral efficiency in an orthogonal frequency division multiple access (OFDMA) system. We assume all K users share the N sub-carriers without the effect of multi-user interference. Two adaptive power allocation schemes are presented to allocate transmission power to individual sub-carriers of each user in the downlink path. These algorithms offer significant computational advantage over the conventional water-filling algorithm. With the aid of these computationally efficient schemes, the problem of maximising capacity with prioritisation of user-services is investigated. An iterative algorithm is proposed to determine the capacity of an individual user from a limited and varying power budget. Simulation shows that the proposed algorithm can not only obtain achievable capacity of the users' requested services but also conserve excess transmit power if less power budget is adequate to achieve the desired capacity.

3.1 Introduction

Generally, in order to increase the spectral efficiency while reducing the total required transmission power, the transmission power of each user is assigned based on the channel state information (CSI) which is known to both transmitter and receiver. One method to obtain this outcome is commonly through the *water-filling* approach [23]. As the water-filling algorithms have reached a state of maturity, several implementations have been proposed in [16, 18, 19, 100, 114, 116, 117]. For Gaussian multiple access channels with inter-symbol interference (ISI), Cheng and Verdú [16] studied the capacity regions of a two-user scenario and also obtained a non-trivial generalisation of the single-user water-filling theorem. This problem was extended to consider multi-user by Viswanath *et al.* in [100], where the behaviour of the asymptotically optimal water-filling policy in various regimes of number of users per unit degree of freedom and signal-to-noise ratio (SNR) were studied. Moreover, the allocation of wireless resources, such as power, bandwidth and bit rates, in the context of OFDM systems were studied in [104–106, 112, 119]. These works studied the minimisation of overall transmission power by optimally assigning a number of sub-carriers to each user and a number of bits to be sent via each sub-carrier. In order to mitigate the multi-user interference without implementing an extra coding scheme, no more than one user can occupy the same sub-carrier in their proposed OFDM system. We illustrate the similar problem in power and sub-carrier allocation in Chapter 4.

The evolution of mobile communication has brought up the importance of spectral efficiency due to the demand of higher data rate services. The conventional wireless communication physical layer standards are implemented with little consideration of a multi-user scenario, yet the multi-user case is always of more practical interest. The problems in multi-user rate and power control, with an individual power constraint for each user rather than an aggregate power constraint over all users, were particularly investigated in [18, 59]. However, the issues on user prioritisation and weighting factor that determines the individual power constraint were not evaluated in their work. Furthermore, the potential of multi-carrier code division multiple access (MC-CDMA) with an adaptive frequency allocation was implemented in [22]. The proposed system advantageously exploit the channel frequency-selectivity while taking into account different user-service demand, such that the user-groups with highly demanding services may be favoured in the assignment of the less faded sub-channels.

In the context of information-theoretic power control for multi-user systems, existing literature mainly relied on complex iterative power allocation algorithms [117]. Therefore, two reduced complexity power allocation algorithms which apply the water-filling theorem to an orthogonal frequency division multiple access (OFDMA) system are proposed in this chapter. This part of the work focuses on downlink slowly time-varying frequency-selective fading channels. Due to the effects of channel fading, shadowing and propagation path loss, the strength of the channel can fluctuate enormously. A general strategy to combat these detrimental effects is through the dynamic allocation of resources based on the accurate CSI. Optimal resource allocation, which focuses on fundamental multiple access fading channels, from an information-theoretic point of view was proposed in a two-part paper by Tse and Hanly [39, 96]. Motivated by this work, the problem of capacity optimisation in the downlink OFDMA system is re-formulated with user prioritisation in this chapter. We propose an iterative algorithm to distribute an individual user's transmission rate by taking into account prioritisation among user-services based on a limited and varying power budget.

In this chapter, a brief introduction on the system model is outlined in Section 3.2. The problem formulation of power allocation with even power budget among users are introduced in Sections 3.3.1 and 3.3.2. In Section 3.3.3, two reduced complexity power allocation algorithms are presented. Furthermore, the implementation of user prioritisation in power control is illustrated in Section 3.4. An outline of another problem formulation of power allocation with uneven power budget among users can be found in Section 3.4.1, followed by the proposed algorithm on power control with user prioritisation in Section 3.4.2. The performance comparison between the optimal, proposed sub-optimal and conventional schemes is given in Section 3.5. The conclusion of this chapter is presented in Section 3.6.

3.2 System Model

The configuration of the downlink OFDMA system is shown in Figure 3.1. Consider a single-cell K-user OFDMA system of N sub-carriers with a frequency-selective fading channel. Each user is allowed to occupy up to N sub-carriers, and to transmit up to N symbols in parallel. If the parallel stream of each user has its own distinctive code,

it is possible for more than one data symbol of the same user to be transmitted on the same sub-carrier. In this chapter, we assume that the multi-user interference is perfectly eliminated by implementing a set of Walsh-Hadamard orthogonal codes.

Path loss in a macrocellular environment often shows an increasing trend with distance between the base station and mobile users. It is a common practice to represent path loss as some power of $2 \leq \eta \leq 4$, which is known as the path loss exponent, together with a random variation about this power law due to shadowing fading [26]. Hence, the decibel path loss at a distance of d metres apart is expressed as

$$PL(d) = \overline{PL}(d_0) + 10\eta \log_{10}\left(\frac{d}{d_0}\right) + \chi, \qquad \text{(in dB)} \tag{3.1}$$

where $\overline{PL}(d_0)$ is the decibel relative path loss at distance d_0 metres away from base station (note that $d_0 \leq d$), η is the path loss exponent and χ is the decibel shadow fading component. The decibel relative path loss at distance d_0 can be observed as a fixed quantity given by the free-space path loss formula [26],

$$\overline{PL}(d_0) = 20 \log_{10}\left(\frac{4\pi d_0}{\lambda}\right), \tag{3.2}$$

where the free-space wavelength in metres is defined as $\lambda = c/f_c$, for c/f_c is the ratio of speed of light to the carrier frequency. The decibel variable χ, which varies randomly from one terminal location to another within any given macrocell, is a decibel zero-mean Gaussian variable [78] and it can be expressed as $\chi = \kappa + \chi_\sigma$ where κ is a decibel zero-mean Gaussian variable of zero decibel standard deviation and χ_σ is the decibel standard deviation of χ.

Assuming that the sub-carrier separation is smaller than the coherent bandwidth, each sub-carrier can be considered as a flat fading sub-channel. Assuming unity average transmission power, a general downlink received signal for an arbitrary k^{th} user at its n^{th} sub-carrier is modelled as

$$y_{k,n} = x_{k,n} h_{k,n} + n_{k,n}, \tag{3.3}$$

where $x_{k,n}$ and $y_{k,n}$ are the transmitted and received signals, respectively, $n_{k,n}$ is the additive white Gaussian noise (AWGN) and $h_{k,n}$ is extracted from the channel vector $\mathbf{h}_k = [h_{k,1}, \ldots, h_{k,N}]$.

With the consideration of propagation path loss in the channel model, the channel coefficient of user k at sub-carrier n is modelled as

$$h_{k,n} = 10^{-PL(d)/10}. \tag{3.4}$$

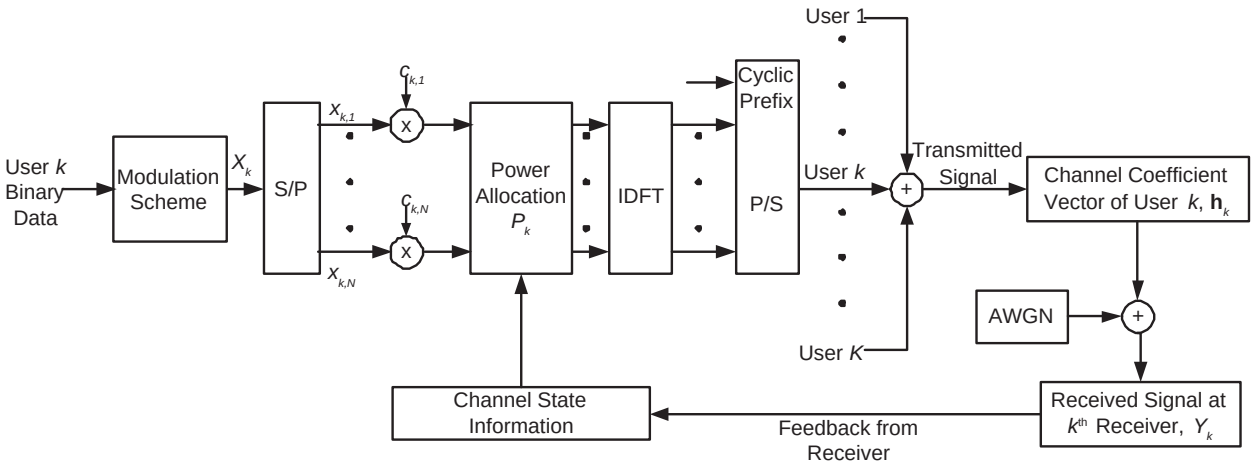

Figure 3.1. The downlink OFDMA.

The corresponding signal-to-noise ratio (SNR) for user k at sub-channel n is expressed as $\gamma_{k,n} = |h_{k,n}|^2/\sigma_{k,n}^2$, where $\sigma_{k,n}^2$ is the noise variance of AWGN. As the overall bandwidth, B, is evenly divided among all sub-channels, the noise variance of any arbitrary user k at all sub-channels are identical, i.e. $\sigma_{k,n}^2 = \sigma_k^2/N$. Assuming that unit power for each sub-channel, the Shannon's capacity for user k is defined as

$$C_k = \sum_{n=1}^{N} \frac{B}{N} \log_2 (1 + \gamma_{k,n}) . \tag{3.5}$$

To model an adaptive power allocation problem, we define the instantaneous transmission power and sub-carrier assignment vector of user k as $\mathbf{P}_k = [P_{k,1}, \ldots, P_{k,N}]$ where $P_{k,n} \geq 0$ and the sum of all transmission power is bounded by a total power budget, i.e. $\sum_{k=1}^{K} \sum_{n=1}^{N} P_{k,n} \leq P^{\max}$. Consider the k^{th} user as shown in Figure 3.1. Assume that a set of orthogonal code, $\mathbf{c}_k = [c_{k,1}, \ldots, c_{k,N}]$, is implemented such that the multi-user interference can be perfectly eliminated. The downlink received signal of user k at sub-carrier n can be rewritten as:

$$y_{k,n} = \sqrt{P_{k,n}} h_{k,n} x_{k,n} + n_{k,n}. \tag{3.6}$$

Hence, the Shannon's capacity for user k can be rewritten as a function of transmission power, which is given by

$$C_k(P_{k,n}) = \sum_{n=1}^{N} \frac{B}{N} \log_2 (1 + P_{k,n}\gamma_{k,n}) . \tag{3.7}$$

3.3 Power Control without User Prioritisation

3.3.1 Power Control with Even Power Budget

We consider a slowly time-varying or time invariant broadcast channel. The CSI is assumed accurately known at the transmitter and K receivers. Given a set of users and their corresponding CSI, we aim to maximise the capacity for each user and maintain the power distribution under a limited total power budget. We model this problem as a constrained optimisation problem

$$\begin{aligned} \max_{P_{k,n}} \quad & \sum_{k=1}^{K} C_k(P_{k,n}) \\ \text{subject to} \quad & \sum_{n=1}^{N} P_{k,n} \leq P_k^{\max}, \\ & P_{k,n} \geq 0, \end{aligned} \tag{3.8}$$

where $P_k^{\max}$ is the power budget for user k, such that $\sum_{k=1}^{K} P_k^{\max} \leq P^{\max}$.

In this section, all users are assumed to have an even portion of the total power budget, $P^{\max}$. The issue of different priority assignment among users will be discussed in Section 3.4. Hence, the total power budget is evenly assigned to each user such that $P_k^{\max} = P^{\max}/K$. The solution to this optimisation problem required the use of the water-filling and duality theorems.

3.3.2 Optimisation Techniques

The optimisation problem in (3.8) belongs to the class of the convex programming problems, where a convex objective function is to be minimised, subject to a convex constraint set. Note that the maximisation of achievable capacity is equivalent to the minimisation of its negative counterpart. Thus, the primal objective of this problem can be written as a general form of a convex problem:

$$\begin{aligned} \min_{P_{k,n}} \quad & \sum_{k=1}^{K} \sum_{n=1}^{N} -\frac{B}{N} \log_2 \left(1 + P_{k,n}\gamma_{k,n}\right) \\ \text{subject to} \quad & \sum_{n=1}^{N} P_{k,n} - P_k^{\max} \leq 0, \\ & -P_{k,n} \leq 0. \end{aligned} \tag{3.9}$$

The Lagrangian of the optimisation problem is formulated as

$$L_P(P_{k,n},\lambda_k,\mu_{k,n}) = \sum_{k=1}^{K}\sum_{n=1}^{N} -\frac{B}{N}\log_2\left(1+P_{k,n}\gamma_{k,n}\right) + \sum_{k=1}^{K}\lambda_k\left[\left(\sum_{n=1}^{N}P_{k,n}\right) - P_k^{\max}\right] + \sum_{k=1}^{K}\sum_{n=1}^{N}\mu_{k,n}\left(-P_{k,n}\right), \tag{3.10}$$

where λ_k and $\mu_{k,n}$ are Lagrangian multipliers.

Since (3.10) is partial differentiable with respect to $P_{k,n}$ for all possible k and n combinations, a K-parallel single-user water-filling condition [114] can be derived by solving these partial derivatives.

$$P_{k,n} + \frac{1}{\gamma_{k,n}} = \frac{B}{N(\lambda_k-\mu_{k,n})\ln 2}, \tag{3.11}$$

where the terms $P_{k,n}$ and $1/\gamma_{k,n}$ are denoted as the *control variable* and *water-filling condition*, respectively, while the constant term on the right hand side is denoted as the *water-level*.

Substituting (3.11) into (3.10) vanishes the primal variable $P_{k,n}$ in the primal Lagrangian, which eventually produces the dual Lagrangian:

$$L_D(\lambda_k,\mu_{k,n}) = \sum_{k=1}^{K}\sum_{n=1}^{N}\left[-\frac{B}{N}\log_2\left(\frac{B\gamma_{k,n}}{N(\lambda_k-\mu_{k,n})\ln 2}\right) + \frac{B}{N\ln 2} + \frac{(\mu_{k,n}-\lambda_k)}{\gamma_{k,n}}\right] + \sum_{k=1}^{K}\lambda_k P_k^{\max}. \tag{3.12}$$

The dual problem in (3.12) is differentiated with respect to λ_k, for $k = 1, 2, \ldots K$, and set to zero as

$$\sum_{n=1}^{N}\frac{-B}{N(\lambda_k-\mu_{k,n})\ln 2} + \sum_{n=1}^{N}\frac{1}{\gamma_{k,n}} + P_k^{\max} = 0. \tag{3.13}$$

However, an explicit expression of λ_k in terms of $\mu_{k,n}$ from (3.13) cannot be readily obtained unless a slack assumption is introduced. Assume that $\mu_{k,n}$ remains constant for all n sub-carriers, i.e. $\mu_{k,n} \simeq \widetilde{\mu}_k, \forall n$, thus the critical points of λ_k can be expressed as

$$\lambda_k^* = \frac{B}{\left(P_k^{\max} + \sum_{n=1}^{N}\frac{1}{\gamma_{k,n}}\right)\ln 2} + \widetilde{\mu}_k. \tag{3.14}$$

Hence, substituting (3.14) into (3.11) gives the solution to the primal problem, which is written as

$$P_{k,n}^* = \frac{P_k^{\max} + \sum_{i=1}^{N}\frac{1}{\gamma_{k,i}}}{N} - \frac{1}{\gamma_{k,n}}, \tag{3.15}$$

where the following Karush-Kuhn-Tucker (KKT) conditions can be satisfied:

$$\left(\sum_{n=1}^{N} P_{k,n}^{*}\right) - P_{k}^{\max} \leq 0; \tag{3.16}$$

$$\lambda_{k}^{*} \geq 0; \tag{3.17}$$

$$\frac{\partial}{\partial P_{k,n}} L_{P}\left(P_{k,n}^{*}, \lambda_{k}^{*}\right) = 0; \tag{3.18}$$

$$\lambda_{k}^{*}\left[\left(\sum_{n=1}^{N} P_{k,n}^{*}\right) - P_{k}^{\max}\right] = 0. \tag{3.19}$$

The graphical illustration of the water-filling solution is shown in Figure 3.2 where the polynomial curve and vertical arrows indicate $1/\gamma_{k,n}$ and $P_{k,n}^{*}$, respectively. Note that the vertical arrows that point upwards indicate positive power and those that point downwards indicate negative power. The horizontal line in Figure 3.2 denotes the water-filling condition, also known as the water-level, where its magnitude is derived from the constant term on the right hand side of (3.11). To obtain this water-filling solution, a slack assumption was introduced on the Lagrangian multiplier, $\mu_{k,n}$, which causes the positivity constraint to be violated. This is evidenced in Figure 3.2. Some sub-carriers are allocated with negative power, which does not exist in reality. Therefore, one way to ensure the satisfaction of the positivity constraint is by suppressing the negative power terms to zero while proportionally scaling down the remaining positive power terms to meet the individual user's power budget. This implies that the solution presented in (3.15) is a sub-optimal solution to the primal problem in (3.9). In the process of generating the sub-optimal solution, we expect the achievable capacity to be slightly degraded. This is illustrated in Figure 3.3, where the solid horizontal line indicates the original water-level and the dashed horizontal line denotes the degraded water-level after readjustment.

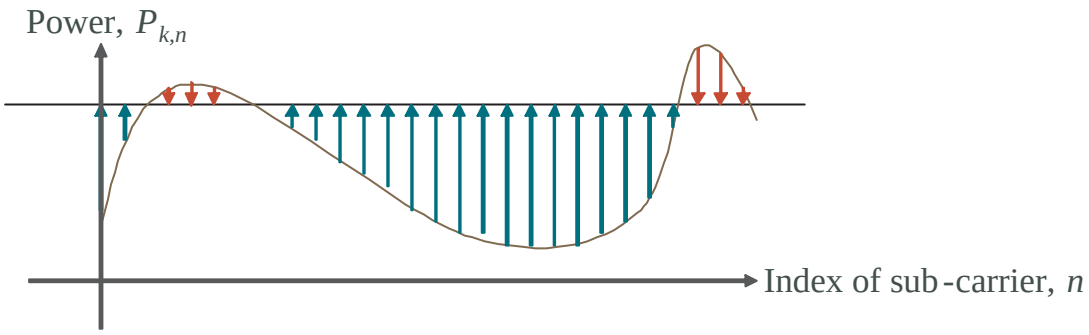

Figure 3.2. Illustration of $P_{k,n}^{*}$ for an arbitrary user k.

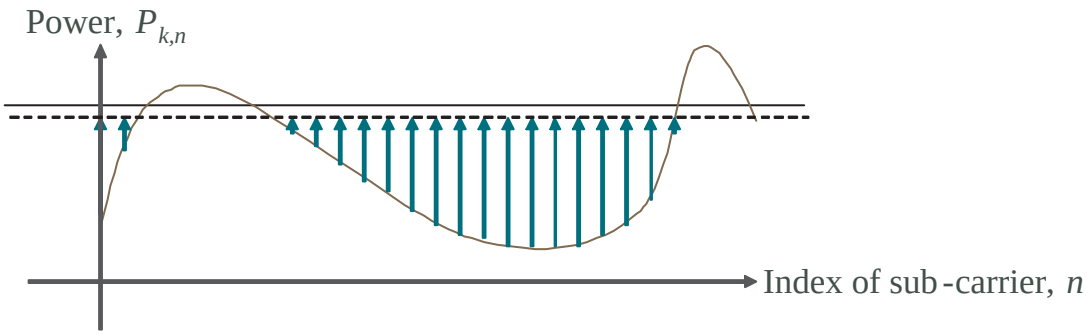

Figure 3.3. Illustration of $P^*_{k,n}$ for an arbitrary user k after readjustment.

3.3.3 Sub-optimal Power Allocation Schemes

In this section, we introduce two sub-optimal allocation schemes, namely the sub-optimal power allocation (SPA) and constant power allocation (CPA) schemes. The main reason for implementing these schemes is to provide a reduced complexity algorithm to achieve an efficient power control outcome as compared to the conventional algorithm which is more computationally expensive. For effectiveness, power allocation must be done sufficiently quickly in a wireless communication channel with fading. However, the optimal power allocation (OPA) schemes in most conventional power controls were obtained via slow convergence due to the computational complexity of the heuristic and iterative algorithms. We want to show in this chapter that the proposed SPA and CPA schemes can achieve similar performance as the OPA scheme but with much lower computational complexity.

The optimisation problem in (3.8) is generally decomposed into multiple simultaneous single-user water-filling problems. The sub-optimal solution in (3.15) is used to assign an instantaneous transmit power to the sub-channels of each user whose channel gain is sufficiently high for the corresponding transmission. To achieve the adjusted water-filling solution as shown in Figure 3.3, we propose to implement SPA scheme, which is given by

$$P^{\text{SPA}}_{k,n} = \begin{cases} P^*_{k,n} + \epsilon_k, & \text{if } P^*_{k,n} > |\epsilon_k|, \text{ for all } k \text{ and } n; \\ 0, & \text{otherwise;} \end{cases} \tag{3.20}$$

where $\epsilon_k \leq 0$ and it denotes the adjustment in transmission power for the corresponding k^{th} user. The algorithm for the SPA scheme is given as follows:

Algorithm 3.1. *Consider a K-user system with N sub-carriers. With the transmit power $P^*_{k,n}$ given by (3.15), the outcome of this algorithm is determined in the form of $P^{\text{SPA}}_{k,n}$:*

1. *For k^{th} user, if $P^*_{k,n} \geq 0$ for all N sub-carriers, repeat for next user; else set $\epsilon_k = 0$ and initialise redo list,* R*, and violated list,* V*.*

2. *Generate* R *list of size M for any n sub-carrier that has $P^*_{k,n} \geq 0$ and generate* V *list of size $(N - M)$ for the remaining sub-carriers that satisfy $P^*_{k,n} < 0$.*

- ***2a.*** *Accumulate all negative powers in* V *to compute $\epsilon_k = \sum_{v \in V} P^*_{k,v}/M$ and set $P^{\text{SPA}}_{k,v} = 0$, for all $v \in V$.*
- ***2b.*** *Identify the minimum transmission power, $P_{k,i} = \min\{P^*_{k,r}\}$, for all $r \in R$.*
- ***2c.*** *If $|\epsilon_k| \geq P_{k,i}$, recalculate $\epsilon_k = (M \cdot \epsilon_k + P_{k,i})/(M-1)$, set $P^{\text{SPA}}_{k,i} = 0$, remove i^{th} sub-carrier from* R *list and repeat step **2b**; else compute $P^{\text{SPA}}_{k,r} = P^*_{k,r} + \epsilon_k$, for all $r \in R$. Repeat step **1** for next user.*

Remark 3.1. *For each user, Algorithm 3.1 requires N iterations to execute (3.15) and M iterations to adjust the power distribution if the positivity constraint is violated, where M is always less than N. This algorithm has a reduced complexity of $O(KN + KM) \approx O(KN)$ since $M < N$. In comparison, the conventional water-filling algorithm [117] has a complexity of $O(itr \cdot KN \log_2 N)$ where K, N and itr are the number of users, number of sub-carriers and maximum number of iterations, respectively. The latter is always a factor of $(itr \cdot \log_2 N)$ higher than the former one. As the number of sub-carriers N increases, the complexity of the conventional algorithm becomes even higher than Algorithm 3.1.*

Motivated by the work in [114], the proposed SPA scheme can be further simplified by replacing the individually assigned power at each sub-carrier with an average power. Note that each user may subject to a different average power due to the difference in the number of occupied sub-carriers[1]. Thus, the proposed CPA scheme is given by:

$$P^{\text{CPA}}_{k,n} = \begin{cases} P^{\max}_k / c_k, & \text{if } P^*_{k,n} > 0, \text{ for all } k \text{ and } n; \\ 0, & \text{otherwise;} \end{cases} \tag{3.21}$$

where c_k is denoted as the number of occupied sub-carriers for k^{th} user. The procedure to implement the CPA scheme is given in the algorithm as follow:

[1]Occupied sub-carrier is defined as the sub-carrier which carries positive transmission power.

Algorithm 3.2. *Consider a K-user system with N sub-carriers. With the transmit power $P^*_{k,n}$ given by (3.15), the outcome of this algorithm is determined in the form of $P^{\text{CPA}}_{k,n}$:*

1. *For k^{th} user, if $P^*_{k,n} \geq 0$ for all N sub-carriers, repeat for next user; else initialise redo list,* R*, and violated list,* V*.*

2. *Generate* R *list of size M for any n sub-carrier that has $P^*_{k,n} \geq 0$ and generate* V *list of size $(N - M)$ for the remaining sub-carriers that satisfy $P^*_{k,n} < 0$.*

3. *Set $P^{\text{CPA}}_{k,v} = 0$, for all $v \in V$ and assign constant power to all elements in* R *list, such that $P^{\text{CPA}}_{k,r} = P^{\max}_k/M$, for all $r \in R$. Repeat step **1** for next user.*

Remark 3.2. *For each user, Algorithm 3.2 requires N iterations to determine the number of occupied sub-carriers such that an average power would be assigned to each of these sub-carriers. This algorithm has a complexity of $O(KN)$. However, the use of average power may compromise the overall achievable capacity.*

As discussed in *Remarks 3.1* and *3.2*, the complexity of the SPA scheme is determined as $O(KN + KM)$ and for the CPA scheme is $O(KN)$. When $K = 10$ and $N = 256$, the computational complexities become $KN + KM < 2KN = 5120$ and $KN = 2560$, respectively. An optimal water-filling algorithm was proposed in [117] with a complexity of $O(itr \cdot KN \log_2 N)$ where itr is the number of iterations before convergence is observed. Assume that their algorithm converges within 5 iterations, its complexity reaches $itr \cdot KN \log_2 N = 102400$. It appears that the SPA and CPA schemes are more efficient than the conventional water-filling algorithm.

3.4 Power Control with User Prioritisation

3.4.1 Power Control with Uneven Power Budget

Consider a slowly time-varying or time invariant broadcast channel. The CSI is assumed accurately known at the transmitter and K receivers. For a set of users and their corresponding CSI, we aim to maximise the capacity for a set of users in different priority groups located at some distance away from the base station, and maintain the power distribution under a limited total power budget. We formulate this power allocation problem

as a constrained optimisation problem

$$\begin{aligned} \max_{P_{k,n},w_k} \quad & \sum_{k=1}^{K} C_k(P_{k,n}) \\ \text{subject to} \quad & \sum_{n=1}^{N} P_{k,n} \leq \frac{w_k P^{\max}}{K}, \\ & P_{k,n} \geq 0, \\ & \sum_{k=1}^{K} w_k \leq K, \\ & 0 \leq w_k \leq K, \end{aligned} \tag{3.22}$$

where $P^{\max}$ is the total power budget of a base station for a single transmission and w_k is the weighting factor of user k, which is used to gauge the individual user's power budget based on the difference in priority among users. Since optimisation problem consists of two control variables, its analytical solution is rather complex. Thus an iterative algorithm is proposed to obtain the outcome of this optimisation problem.

3.4.2 Proposed Algorithm

One approach to solving similar optimisation problem with priority among users was to run an inner and an outer iterative algorithms [18]. The inner algorithm is to obtain the power allocation and the outer is for the capacity. This approach becomes less practical as the numbers of users and sub-carriers increase due to its heuristic nature. We propose an user-prioritised power allocation (UPA) scheme to reduce the complexity of the power allocation problem. The inner iterative algorithm of the UPA scheme is replaced with the reduced complexity algorithms in Section 3.3.3.

The iterative algorithm initially determine the power allocation among users based on the CSI and total power budget. It calculates the corresponding achievable capacity for each user. Based on different requested user services, a set of desired capacities, C_k^{desired} for all k, is generated. By implementing the sub-optimal power allocation schemes in Section 3.3.3, the UPA scheme iteratively adjusts the weighting factor (and hence adjust the individual user's power budget) in order to attain a set of achievable capacities that approaches the pre-determined desired capacities, C_k^{desired}. The algorithm ends when the stopping criteria are met. The procedure to perform these tasks is given in the algorithm below.

Algorithm 3.3. *Consider a K-user system with N sub-carriers. Assume all users are allowed to request different services which each user-service may subject to a different desired capacity, C_k^{desired}. With the outcomes of the sub-optimal power allocation are given by (3.20) and (3.21), a set of achievable capacities is determined in the form of $C_k(itr)$, where itr denotes the number of iterations before the convergence is established.*

1. *Initialise desired capacity, $C_k^{\text{desired}} = 0$, the gap between achievable and desired capacity, $C_k^{\text{gap}} = 0$, weighting factor, $w_k = 1$, $\forall k$, and iteration counter, $itr = 1$.*

2. *Compute the power budget for each user, $P_k^{\max} = w_k P^{\max}/K$, and run Algorithm 3.1 for SPA scheme or Algorithm 3.2 for CPA scheme.*

3. *Obtain $C_k(itr)$ for each user based on the outcome of power allocation and compute $C_k^{\text{gap}} = C_k^{\text{desired}} - C_k(itr)$.*

3a. *Update weighting factor, $w_k = K2^{C_k^{\text{gap}}} / \sum_{j=1}^{K} 2^{C_j^{\text{gap}}}$, compute new power budget for each user, $P_k^{\max} = w_k P^{\max}/K$, and run Algorithm 3.1 for SPA scheme or Algorithm 3.2 for CPA scheme.*

3b. *Perform counter increment on itr and calculate achievable capacity for each user, $C_k(itr)$. If $|C_k^{(Itr)} - C_k^{(Itr-1)}| >$ stopping criteria, repeat step **3**; else convergence is established.*

Remark 3.3. *Algorithm 3.3 benefits from its versatility to adaptively adjust the individual user's power budget while maintaining the total power budget, in order to support different services based on users' demand. A set of desired capacities is determined based on the users' requested service prior to running this algorithm. Since C_k^{gap} is a 2-base logarithmic function, the weighting factor is updated based on the term of $2^{C_k^{\text{gap}}}$. This allows the power budget of each user to be linearly adjusted instead of logarithmically according to the gap assesses between the desired capacity and the corresponding achievable capacity.*

Remark 3.4. *When the current achievable capacity approaches at least 95% of its previous value, the algorithm is exited. This algorithm ensures that all transmission power terms satisfy the positivity constraint (which is governed by the SPA or CPA schemes) while the weighting factor satisfies the final two constraints in (3.22).*

3.5 Simulation Results and Discussions

3.5.1 Power Allocation Schemes

The main objective of the simulations is to investigate and compare the performance of four schemes. The four power allocation schemes are given by

1. *OPA scheme* - it is derived from (3.8);
2. *SPA scheme* - it is supported by *Algorithm 3.1*;
3. *CPA scheme* - it is supported by *Algorithm 3.2*;
4. *FPA scheme* - a conventional scheme that assigns the same transmission power to all sub-carriers, such that $P_{k,n}^{fixed} = P_k^{\max}/\text{number of sub-carriers}, \forall n$.

In the first simulation, we generate the realisation of the frequency-selective fading channel, as shown in Figure 3.4, for 2 users 16 sub-carriers with path loss exponent of 3, log-shadowing of 0 dB mean (standard deviation of 7 dB) and both users at fixed

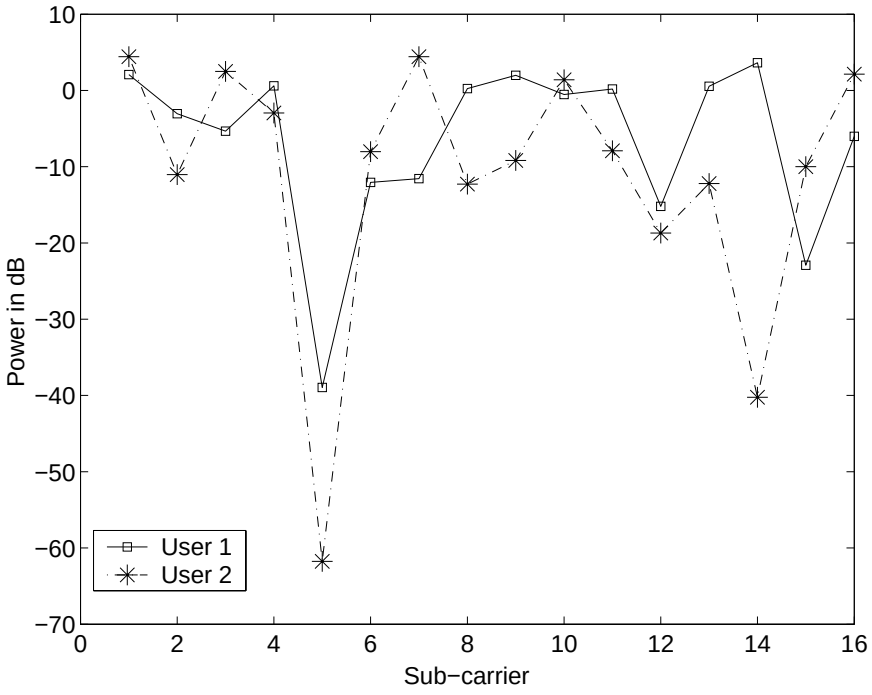

Figure 3.4. Frequency-selective fading channel realisation for one transmission cycle.

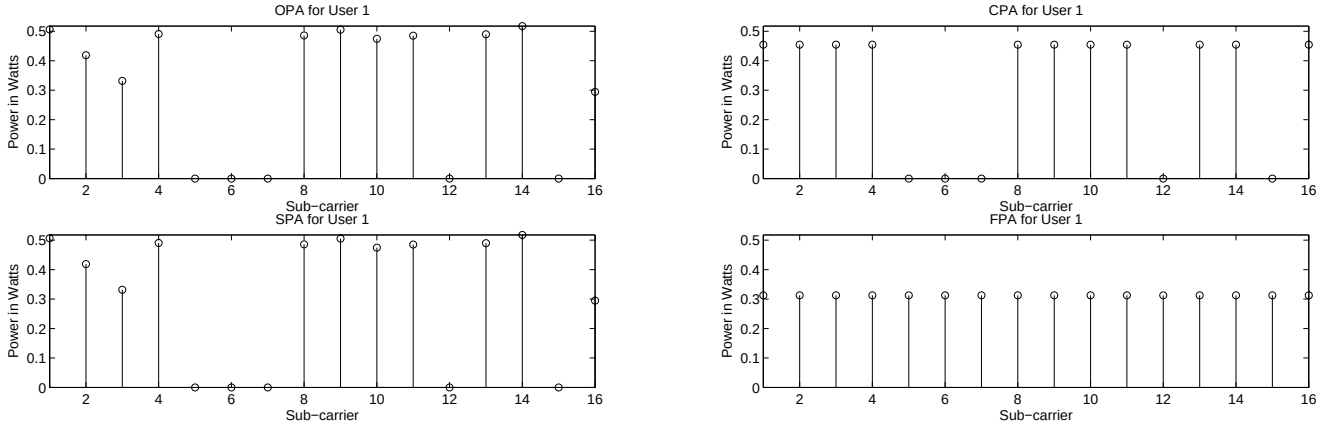

(a) User 1

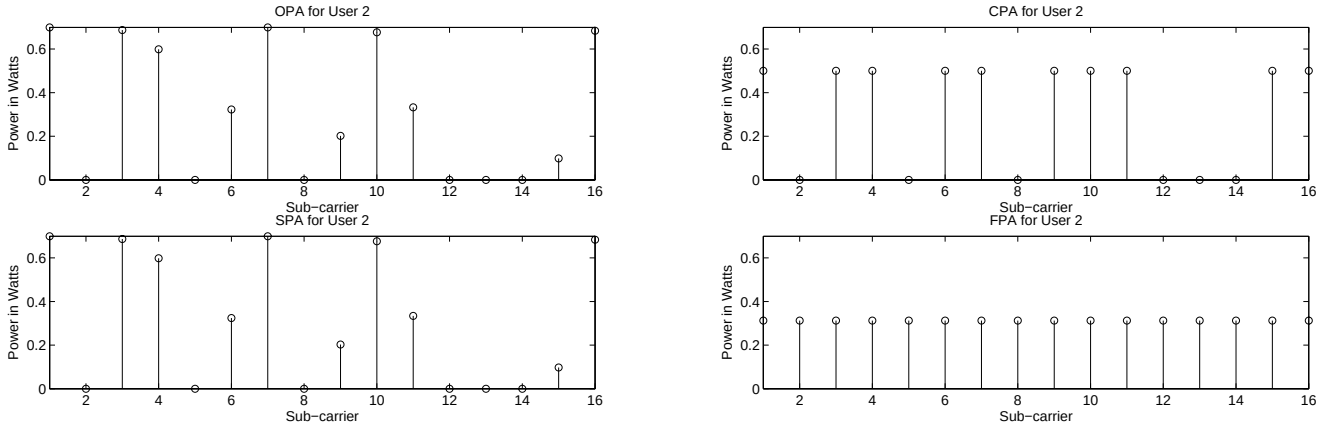

(b) User 2

Figure 3.5. Power allocation of users 1 and 2 corresponded to fading channel in Figure 3.4.

Table 3.1. Achievable spectral efficiency (bit/s/Hz) for users 1 and 2, which perceived the wireless fading channel as given in Figure 3.4

	User 1		*User 2*	
Schemes	*Capacity,* C_1	*Percentage of OPA*	*Capacity,* C_2	*Percentage of OPA*
OPA	2.0301	100%	1.7236	100%
SPA	2.0300	99.99%	1.7232	99.97%
CPA	2.0224	99.62%	1.6831	97.65%
FPA	1.7832	87.83%	1.4608	84.75%

distance of 100 metres from base station. The total power budget at the base station is set at 10 dB (10 watts) and the power budget for each user is thus approximately 7 dB (5

watts). Figures 3.5(a) and (b) illustrate the four power allocation schemes for users 1 and 2, respectively. A set of achievable spectral efficiencies for the two-user case is tabulated in Table 3.1. It is shown that the proposed power allocation strategies are able to achieve up to 99% of the optimum spectral efficiency.

In the second simulation, we vary the total power budget within a feasible range of values and randomly generate 10^4 sets of frequency-selective fading channels. For each set of the frequency-selective fading channels, we compute the corresponding achievable spectral efficiencies for all four power allocation schemes. The comparison of the average achievable spectral efficiencies between these schemes is shown in Figure 3.6. To investigate the performance of these schemes for different number of users and sub-carriers, we have repeated the simulation with 2 users 256 sub-carriers, 10 users 16 sub-carriers and 10 users 256 sub-carriers. Figures 3.7, 3.8 and 3.9 show their achievable spectral efficiencies. The comparison of the achievable spectral efficiencies between the optimal, SPA, CPA and conventional schemes indicated that both the SPA and CPA schemes outperformed the conventional FPA scheme. The SPA scheme, in particular, has consistent performance and its achievable spectral efficiency is proven to approach the optimum spectral efficiency for all cases. Besides, as we fixed the number of users and increased the number of sub-carriers, the comparisons between Figures 3.6 and 3.7, and between Figures 3.8 and 3.9, indicated that the increase in the number of sub-carriers only produce very marginal improvement. Since all sub-carriers are shared between users and the received bandwidth is fixed at B, the increase in the number of sub-carriers only decreases the size of sub-carrier spacing. This approach may improve the overall spectral efficiency if the sub-channels are highly uncorrelated; however, for most practical scenario, all sub-channels are usually correlated. On the other hand, as we fixed the number of sub-carriers and increase the number of users, the comparison between Figures 3.6 and 3.8 indicated that the gap between the conventional FPA scheme and the proposed schemes is increasing as the numbers of users and sub-carriers increase. A similar outcome can be observed between Figures 3.7 and 3.9.

3.5.2 User Prioritisation

In this section, the performance of *Algorithm 3.3* is investigated with different power allocation schemes. The priority order among users is decided based on their requested

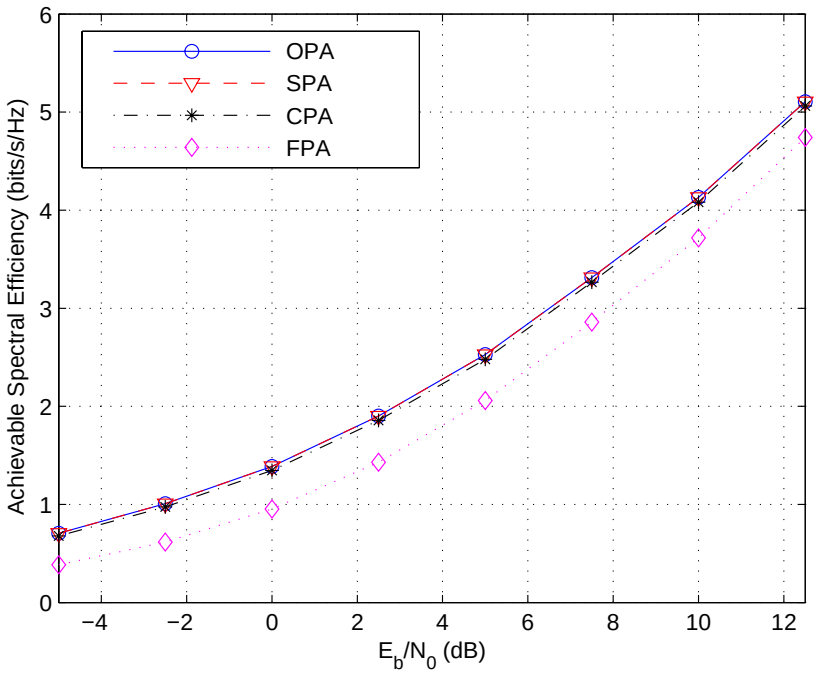

Figure 3.6. Achievable spectral efficiency for 2 users 16 sub-carriers.

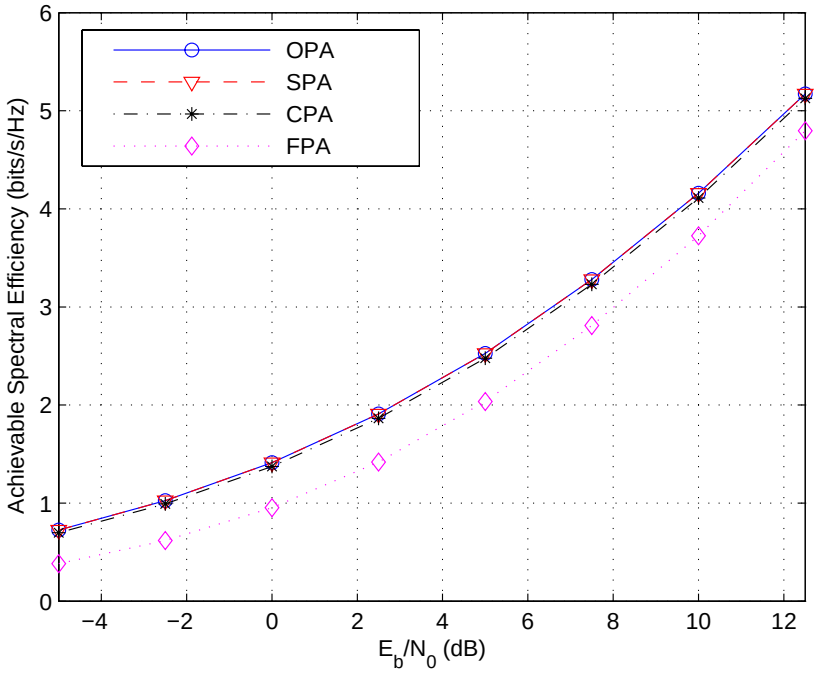

Figure 3.7. Achievable spectral efficiency for 2 users 256 sub-carriers.

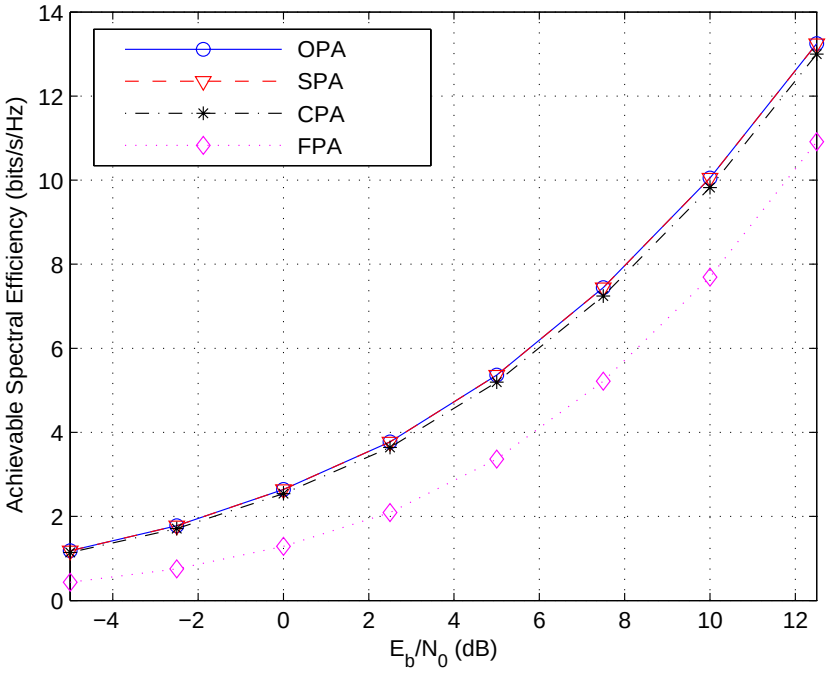

Figure 3.8. Achievable spectral efficiency for 10 users 16 sub-carriers.

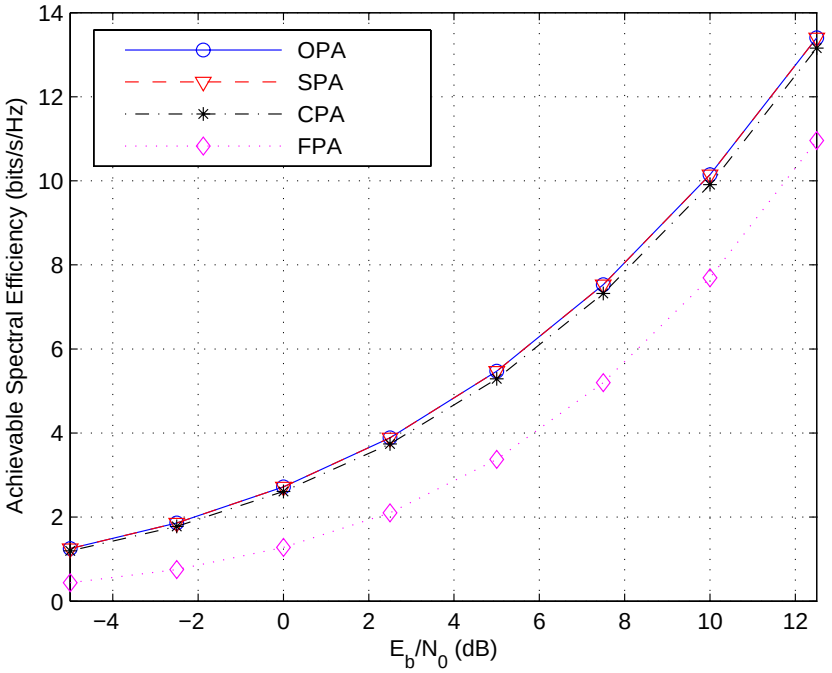

Figure 3.9. Achievable spectral efficiency for 10 users 256 sub-carriers.

Table 3.2. Priority group assignment

	Voice	*Video*	*Data 1*	*Data 2*	*Data 3*
Rate (kbit/s)	9.6	64	384	2000	5000
Priority group	1	2	3	4	5

Table 3.3. Simulation parametres

Parametres	*Values/Descriptions*
Number of users, K	8
Number of carriers, N	32
Overall bandwidth, B	5 MHz
Spreading code	Walsh-Hadamard Code
Channel model	Rayleigh (frequency selective)
Path loss model	Log-shadowing (mean 0 dB, standard deviation 7 dB)
Path loss exponent	3 (urban area)
Propagation model	Figure 3.10
Cell radius	800 m

services, which can be found in Table 3.2. The fundamental service is known as the voice communication service which requires the minimum resources, whereas the essential service for 3G or beyond is the video conference service which requires 64 kbit/s. The remaining services belong to the wireless broadband data transmission which provide transmission rates of up to 384 kbit/s, 2 Mbit/s and 5 Mbit/s. The priority order of each service is decided by its delay requirement. Thus, services such as voice calls and video conference are assigned to higher priorities than other data transmission services, which are less sensitive to real-time delay. To evaluate the performance of *Algorithm 3.3*, we have generated 10^4 sets of frequency selective Rayleigh fading channels of which each consists of K independent channels (one for each channel). An OFDMA system with K users and N sub-carriers over a B MHz bandwidth is used in the simulation. The detailed simulation parametres are tabulated in Table 3.3.

In the third simulation, we assume that the total power budget is 10 dB and the noise density is -50 dBm. For comparison, three multi-user power allocation schemes are considered along with and without the UPA scheme. For all users having the same amount of power budget, each scheme has the following characteristics:

- *SPA scheme* - the transmit power is adaptively distributed based on the instantaneous sub-channel condition, such that optimal transmit power is assigned to sub-channel with good channel quality while zero power to any sub-channel with bad channel quality.
- *CPA scheme* - An average power is assigned to all sub-channels with good channel quality while zero power is assigned to any sub-channel with bad channel quality.
- *FPA scheme* - regardless of the sub-channel condition, the transmit power is fixed for all users at all sub-channels.

For any of these methods to be implemented with *Algorithm 3.3*, their features remain the same except that each user may be allocated different power budget due to the effect of the pre-assigned priority order.

The mobile users are placed such that each user is ranging from 100 metres to 800 metres away from the base station in one cell. The sample distribution of the mobile users is shown in Figure 3.10. Assume that all users are either stationary or moving at a relatively slow speed within a radial distance, which is modelled as a zero mean gaussian random variable with standard deviation of 25 metres. Note that doppler shift effect is not considered in this section. The performance of the power allocation policy without the consideration of user prioritisation is shown in Figure 3.11. It indicates that the achievable spectral efficiency is monotonically decreasing as the mobile user is getting further away from the base station due to the dominant effect of the propagation path

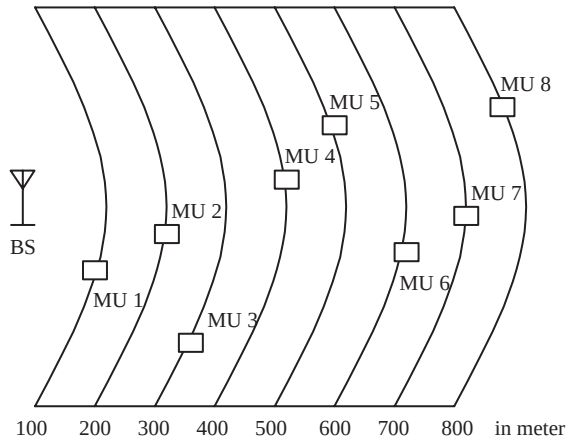

Figure 3.10. Sample distribution of the mobile users in a cell, where BS is the base station and MU is the mobile user.

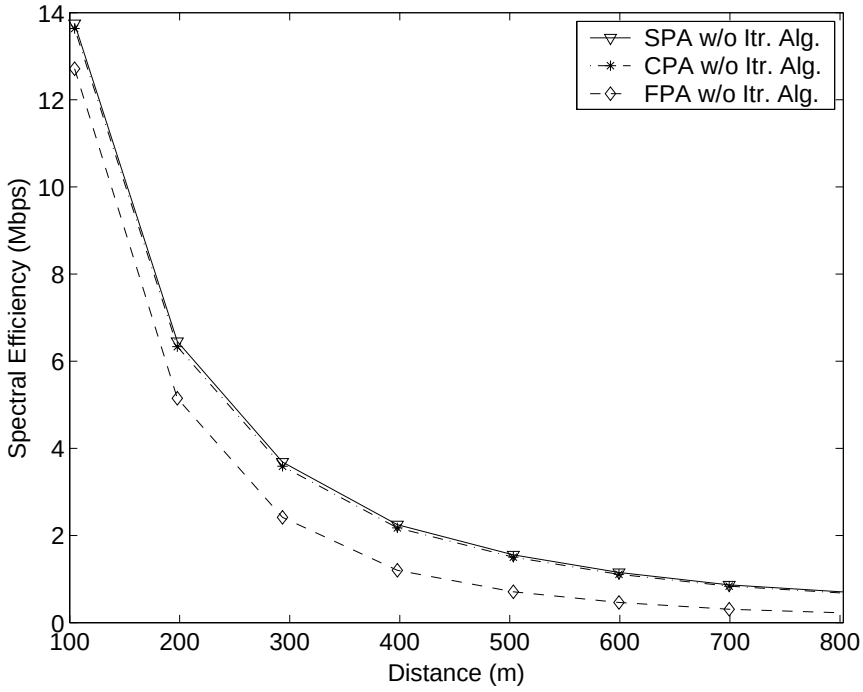

Figure 3.11. Achievable spectral efficiency without user prioritisation.

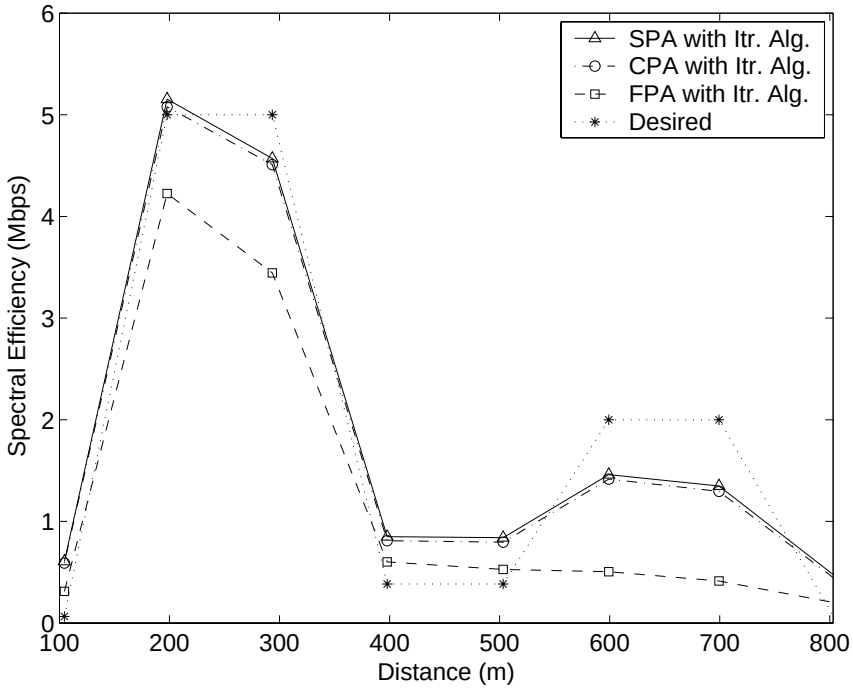

Figure 3.12. Achievable spectral efficiency with the users' priority order given as {2 5 5 3 3 4 4 2} for mobile users 1 to 8, respectively.

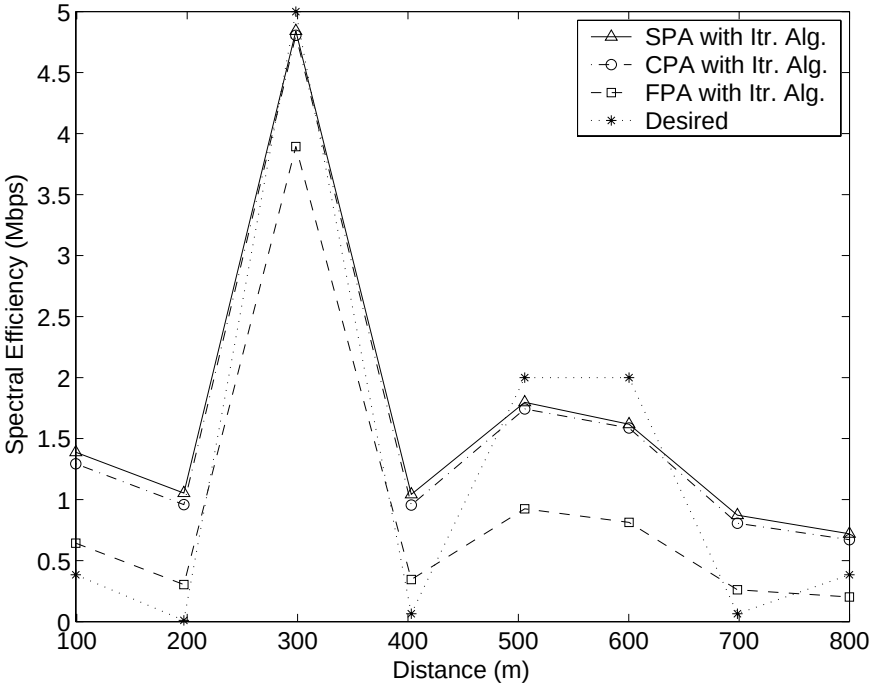

Figure 3.13. Achievable spectral efficiency with the users' priority order given as {3 1 5 2 4 4 2 3} for mobile users 1 to 8, respectively.

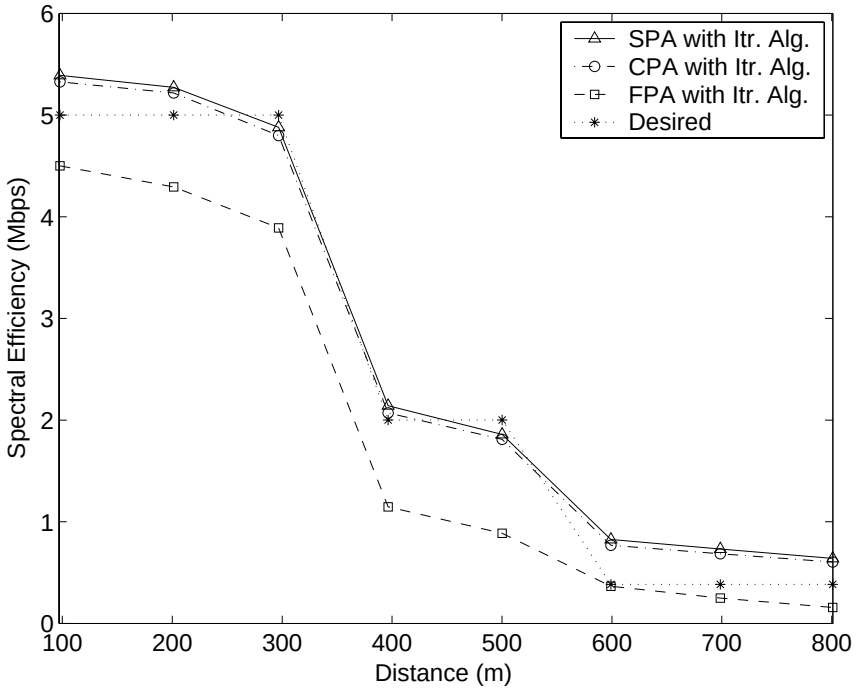

Figure 3.14. Achievable spectral efficiency with the users' priority order given as {5 5 5 4 4 3 3 3} for mobile users 1 to 8, respectively.

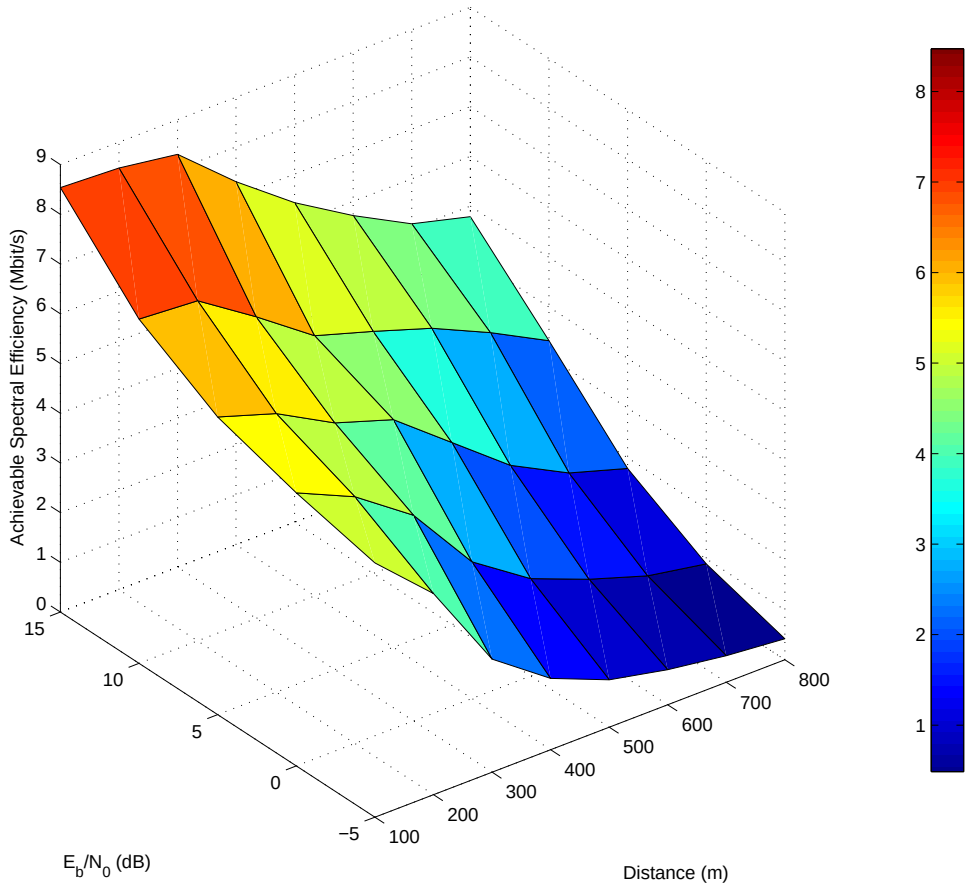

Figure 3.15. Upper bound of achievable spectral efficiency for SPA scheme.

loss. This poses a huge disadvantage to any mobile user who is not located near the base station. This situation can be improved if user prioritisation is considered because each user will be distinguished by their requested services. It can be seen from Figures 3.12 and 3.13 that based on a randomly requested service, the base station would adjust the power allocation policies while maintaining the same total power in order to achieve a capacity as close as possible to the desired capacity. Nevertheless, in certain situations, the proposed algorithm would try to conserve total power by reducing excess power budget. Comparison of Figures 3.11 and 3.14 shows that the system without the UPA scheme uses up the total power budget whereas the system implemented with the UPA scheme conserves the excess power budget of individual user as long as the achievable capacity is sufficiently close to the desired value.

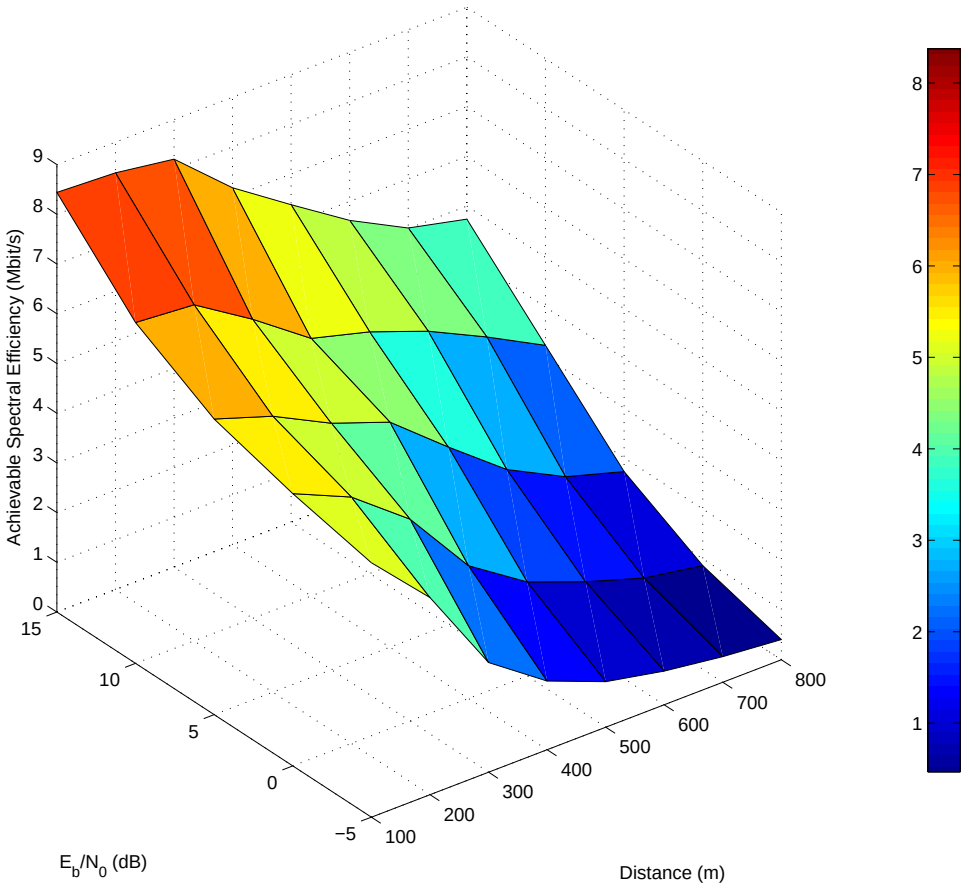

Figure 3.16. Upper bound of achievable spectral efficiency for CPA scheme.

Due to the dominant effect of the propagation path loss, those users who are positioned at some distance far away from the base station may not always satisfy the high data rate services. After a number of trials, it was observed that there exist a limitation on users' request of services based on their position in a cell and other users' requests. This is examined in the fourth simulation. The upper bound of the achievable spectral efficiency can be defined by allowing one arbitrary user to request for the highest data rate service whereas the remaining users are restricted to only fundamental voice call services. Hence, the upper bound of the achievable spectral efficiency for each scheme is plotted in Figures 3.15, 3.16 and 3.17, for SPA, CPA and FPA schemes, respectively. It is shown that the upper bound of the achievable spectral efficiency is a monotonically increasing function as the total power budget increases. With an increasing total power budget, the power budget for each user is also increasing, thus there is more potential for each

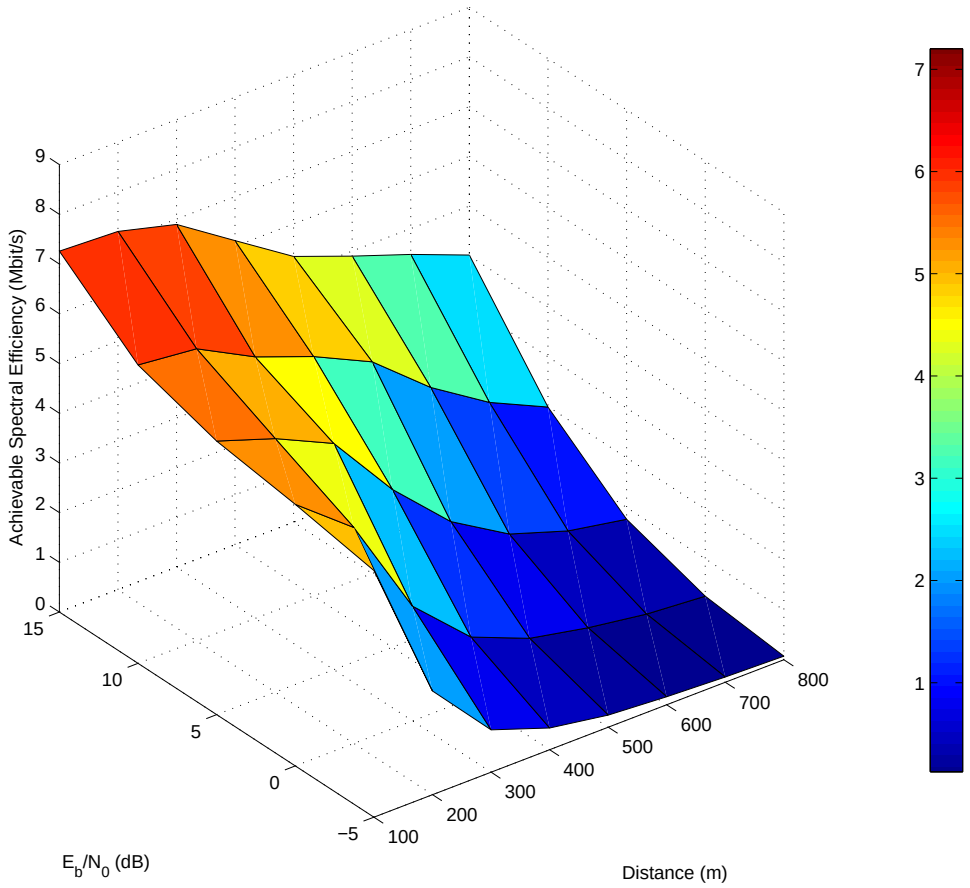

Figure 3.17. Upper bound of achievable spectral efficiency for FPA scheme.

user to achieve a higher spectral efficiency. On the contrary, the upper bound becomes a monotonically decreasing function as the distances between the base station and mobile users increase due to the effect of the propagation path loss. Besides, the comparison of these upper bounds also shows that the conventional FPA scheme is always outperformed by the reduced complexity SPA and CPA schemes.

3.6 Conclusion

The key idea of the power allocation scheme is to minimise the transmission power while improving the achievable spectral efficiency. In fast time-varying fading channels, the

power allocation algorithm must not be computationally complex. The proposed sub-optimal and constant power allocation algorithms offer a significant computational advantage over the conventional water-filling algorithm. Simulation results demonstrated that the sub-optimal and constant power allocation schemes are able to obtain up to 99 % of the optimal capacity.

A novel iterative algorithm for capacity optimisation with user prioritisation is further proposed in this chapter. The algorithm applies the reduced complexity power allocation schemes and optimises the capacity of each user, who is allowed to request different data rate services. The proposed algorithm has shown its versatility to adjust users' power budget. This algorithm ensures that the power distribution meets the total power constraint while satisfying users' demand on different types of services. Furthermore, the proposed iterative algorithm would also conserve the excess power budget if a smaller power budget is adequate to achieve the desired capacity.

Chapter 4

Sub-channel and Power Allocation with Limited Feedback

This chapter addresses two important issues concerning adaptive transmission schemes: (i) feedback delay of channel state information (CSI), and (ii) limited feedback of CSI for multiple sub-carriers. Novel closed-form solutions to the sub-channel and power allocation problems of an orthogonal frequency division multiple access (OFDMA) system are presented. We model the Rayleigh fading channel as a finite-state Markov channel (FSMC) by partitioning the received signal-to-noise ratio (SNR) into several intervals. We reduce the size of the feedback CSI with the aid of sub-band formation and lumpability. This approach involves reducing a Markov channel with a fixed number of states to multiple smaller Markov channels with lumpable states. By reliably predicting CSI with the corresponding state transition and steady-state probabilities at least one symbol duration ahead, the prediction can mitigate the effect of feedback delay that often deteriorates performance of an adaptive transmission scheme. Simulation results show that the limited feedback scheme due to lumpable FSMC is not only experiencing less prediction error than the full feedback scheme but also capable of achieving near-optimum capacity.

4.1 Introduction

Orthogonal frequency division multiple access (OFDMA) is a multi-user OFDM in which each user is assigned a subset of sub-carriers for use, and each sub-carrier is assigned exclusively to one user. The entire bandwidth is shared by multiple users and this allows them to transmit simultaneously. As spectral efficiency is becoming more important, the OFDMA system is undoubtedly one prominent candidate for the fourth generation wireless network [79]. Adaptive modulation and resource allocation are the common techniques for improving spectral efficiency in an OFDMA system. Ideally, multi-user adaptive transmission schemes require channel state information (CSI) to be known perfectly at both the transmitter and receiver [54, 105]. With this knowledge, the Shannon's capacity of a fading channel can be achieved using optimal adaptation of control variables such as transmit power, data rate, coding rate or sub-carrier sharing factor [33, 94]. A dynamic sub-carrier, bit and power allocation scheme for an OFDM system with the objective of minimising the total transmit power is proposed in [105]. Although the Lagrangian relaxation method in [105] can achieve good performance over fixed assignment strategies, the algorithm is computationally intensive and difficult to implement due to computational delay. Kivanc *et al.* [54] presented several low complexity algorithms which offer comparable performance to the iterative algorithms in [105]. Another approach to deriving a multi-user convex optimisation problem to find the optimal allocation of sub-channels was proposed in [80]. This work was extended by Shen *et al.* in [84] to consider a set of proportional fairness constraints, which was imposed to ensure that each user can achieve a required data rate.

However, the assumption of knowing perfect CSI only holds if the receiver has accurate channel estimation and the feedback of this channel estimation to the transmitter has insignificant delay compared to the symbol duration. Otherwise, imperfect CSI may cause severe degradation in the performance of adaptive transmission schemes [33, 54, 94, 105]. The impact of the performance degradation due to the imperfect CSI is illustrated in [17, 111]. To realise the potential of adaptive transmission schemes over time-varying channels, CSI has to be reliably predicted in advance [29]. Although the feedback of CSI helps to achieve higher spectral efficiency, a lot of resources are needed to convey the exact CSI of each sub-carrier from receiver to transmitter. In this chapter, we propose to model the time-varying Rayleigh fading channel in an OFDMA system as a finite-state

Markov channel (FSMC). By partitioning the received signal-to-noise ratio (SNR) into several intervals, the required feedback to the transmitter can be reduced to a quantised vector that carries the instantaneous states of the current channel. The corresponding state transition and steady-state probabilities are used to predict CSI in multiple symbol durations ahead.

The study of FSMC was initiated by Gilbert [30] and Elliott [25]. They started with a two-state Markov channel known as Gilbert-Elliott channel. It consists of a good state and a bad state, where the good state indicates the instantaneous channel SNR is above certain threshold and otherwise for the bad state. This approach provides an efficient way for the system to identify the channel quality. However, it is inadequate to describe the channel quality that varies drastically. Wang and Moayeri [102] utilised the idea of a finite-state Markov model to partition the range of received SNR into a finite number of intervals, where each interval forms the state of the Markov chain. Wang and Chang [101] extended the model by using analytical first-order statistics to obtain model parameters. The first-order Markovian assumption for Rayleigh fading channel is verified to be adequately accurate compared to the higher order Markov models of much higher complexity. Therefore we will only use first-order Markovian assumption throughout this chapter. Zhang and Kassam [118] adopted the view of [102] and developed a methodology to partition the received SNR into a number of states based on the time duration of each state.

By modelling the fading channel of an OFDMA system as FSMC, its state transition matrix size grows exponentially as the number of sub-carriers increases. Thus, a novel approach is proposed to reduce the size of the feedback information. It is outlined as a two-step method which involves the formation of sub-band and lumpable FSMC. Firstly, a fixed number of adjacent sub-carriers are grouped as a sub-band. This helps to reduce the size of the feedback CSI because only an average channel condition of a sub-band is required, rather than the CSI of each sub-carrier. The size of the feedback CSI can be further reduced using the concept of lumpability. This approach reduces the expanded Markov channel to multiple smaller Markov channels while maintaining similar behaviour. By integrating the lumpable FSMC with a channel prediction scheme, we can predict the states of sub-bands at least one symbol duration ahead. Hence, the main contributions of our work are to address two important issues in the OFDMA system, i.e. to reduce full feedback to limited feedback for multiple sub-carriers and to reduce the effect of feedback

delay for each transmission cycle. Unlike most existing work [33, 54, 94, 105] that assumes exact CSI to be available without any feedback delay, we relax this assumption in the study of optimal resource allocation strategies for multi-user system. We then formulate the capacity optimisation problem on the basis of sub-channel and power allocation, and present the sub-optimal closed-form expressions. With these expressions, we investigate the reliability of the proposed channel prediction scheme with limited feedback based on the lumpable FSMC.

This chapter is organised as follows. We formulate the optimal resource allocation problem in the OFDMA system in Section 4.2. The Markov model is outlined in Section 4.3.1 and the expanded Markov model is discussed in Section 4.3.2. In Section 4.4, the lumpability approach is presented, followed by the implementation of FSMC in capacity optimisation problems with channel prediction in Section 4.5. Simulation results and conclusions are then presented in Sections 4.6 and 4.7 respectively.

4.2 Sub-optimal Resource Allocation in OFDMA

The configuration of the downlink OFDMA system is shown in Figure 4.1. Consider a single-cell K-user OFDMA system of N sub-carriers operating on a frequency-selective fading channel. Each user is assigned a subset of sub-carriers for use, and each sub-carrier is assigned exclusively to one user. The entire bandwidth B is shared among N sub-carriers and this allows all users to transmit simultaneously. Assuming that the sub-carrier separation is smaller than the coherent bandwidth, each sub-carrier can be considered as a flat fading sub-channel. Assuming unity average transmission power, a general downlink received signal for an arbitrary k^{th} user at its n^{th} sub-carrier is modelled as

$$y_{k,n} = x_{k,n}h_{k,n} + n_{k,n}, \tag{4.1}$$

where $x_{k,n}$ and $y_{k,n}$ are the transmitted and received signals, respectively, $n_{k,n}$ is the additive white Gaussian noise (AWGN) and $h_{k,n}$ is the channel coefficient of user k at sub-carrier n, which is extracted from the channel vector $\mathbf{h}_k = [h_{k,1}, \ldots, h_{k,N}]$.

The corresponding SNR for the k^{th} user's n^{th} sub-channel is expressed as $\gamma_{k,n} = |h_{k,n}|^2/\sigma_{k,n}^2$, where $\sigma_{k,n}^2$ is the noise variance of the AWGN. As the overall bandwidth, B, is evenly divided among all sub-channels, the noise variance of any arbitrary

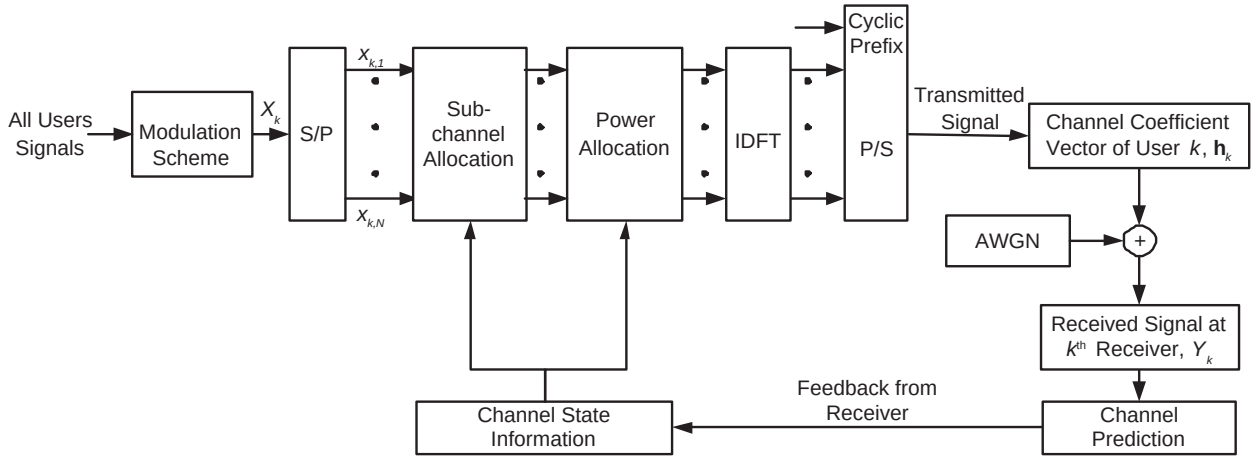

Figure 4.1. System configuration of downlink OFDMA.

user k at all sub-channels are identical, i.e. $\sigma_{k,n}^2 = \sigma_k^2/N$. Assuming that user k occupies all sub-channels and unit power for each sub-channel, the Shannon's capacity for user k is defined as

$$C_k = \sum_{n=1}^{N} \frac{B}{N} \log_2 (1 + \gamma_{k,n}) . \tag{4.2}$$

To realise the potential of utilising sub-carrier and power allocation to improve spectral efficiency, the feedback of accurate CSI is necessary. As we are addressing power allocation problem, we are only interested in the channel amplitude, not its phase. We define the instantaneous transmission power and sub-carrier assignment vector of user k as $\mathbf{P}_k = [P_{k,1}, \ldots, P_{k,N}]$ and $\boldsymbol{\beta}_k = [\beta_{k,1}, \ldots, \beta_{k,N}]$ where $P_{k,n} \geq 0$ and $\beta_{k,n}$ indicates the assignment of sub-carrier n to user k, such that

$$\beta_{k,n} = \begin{cases} 1, & \text{if sub-carrier } n \text{ is assigned to user } k, \\ 0, & \text{otherwise.} \end{cases} \tag{4.3}$$

There are two criteria that must always be met. Firstly, the sum of all transmission power is bounded by a total power budget, i.e. $\sum_{k=1}^{K} \sum_{n=1}^{N} \beta_{k,n} P_{k,n} \leq P^{\max}$. Secondly, not more than one user is permissible for transmission in any n^{th} sub-carrier, i.e. $\sum_{k=1}^{K} \beta_{k,n} \leq 1$. Assuming that the feedback channel condition is given as $\gamma_{k,n}$ for all k and n, the achievable transmission rate for user k is denoted as

$$R_k = \sum_{n=1}^{N} \frac{B}{N} \log_2 (1 + \beta_{k,n} P_{k,n} \gamma_{k,n}) . \tag{4.4}$$

4.2.1 Sub-channel Allocation

An optimal sub-channel allocation can be obtained by allowing transmission of an arbitrary user at one or more of his sub-channels which are experiencing the least fading. This approach is similar to the concept of water-filling. A sub-channel allocation problem was solved in [105] of which the goal of the optimisation is to minimise the transmission power for a given transmission rate. However, no optimal closed-form solution was obtained. In order to find the sub-optimal assignment, we modify the goal to maximise the achievable transmission rate. Note that we have not considered power allocation. The primal objective of this problem is written as

Problem (P1)

$$\begin{aligned} \max_{\beta_{k,n}} \quad & \sum_{k=1}^{K}\sum_{n=1}^{N} \frac{B}{N}\log_2\left(1+\beta_{k,n}\gamma_{k,n}\right) \\ \text{subject to} \quad & \sum_{k=1}^{K}\beta_{k,n} \leq 1, \\ & \beta_{k,n} \geq 0. \end{aligned} \tag{4.5}$$

The Lagrangian is formulated as:

$$\begin{aligned} L_P(\beta_{k,n},\lambda_n,\mu_{k,n}) &= \sum_{k=1}^{K}\sum_{n=1}^{N}\frac{B}{N}\log_2\left(1+\beta_{k,n}\gamma_{k,n}\right) - \sum_{n=1}^{N}\lambda_n\left[\sum_{k=1}^{K}\left(\beta_{k,n}\right)-1\right] \\ &\quad + \sum_{k=1}^{K}\sum_{n=1}^{N}\mu_{k,n}\beta_{k,n}, \end{aligned} \tag{4.6}$$

where λ_n and μ are the Lagrangian multipliers.

By differentiating (4.6) with respect to $\beta_{k,n}$ for all possible k and n combinations and equating it to zero, we have

$$\beta_{k,n} = \frac{B}{N(\lambda_n-\mu_{k,n})\ln 2} - \frac{1}{\gamma_{k,n}}\,. \tag{4.7}$$

Substituting (4.7) into (4.6) eliminates the primal variable $\beta_{k,n}$ in the Lagrangian resulting in the dual objective function,

$$\begin{aligned} L_D(\lambda_n,\mu_{k,n}) &= \sum_{k=1}^{K}\sum_{n=1}^{N}\left[\frac{B}{N}\log_2\left(\frac{B\gamma_{k,n}}{N\ln 2(\lambda_n-\mu_{k,n})}\right) - \frac{B}{N\ln 2} + \frac{\lambda_n-\mu_{k,n}}{\gamma_{k,n}}\right] \\ &\quad + \sum_{n=1}^{N}\lambda_n. \end{aligned} \tag{4.8}$$

The dual objective function in (4.8) is differentiated with respect to λ_n, for $n = 1, 2, \ldots, N$, and set to zero as

$$\sum_{k=1}^{K} \frac{-B}{N(\lambda_n - \mu_{k,n}) \ln 2} + \sum_{k=1}^{K} \frac{1}{\gamma_{k,n}} + 1 = 0. \tag{4.9}$$

However, an explicit expression of λ_n in terms of $\mu_{k,n}$ from (4.9) cannot be readily obtained. To proceed, we assume that the positivity constraint can be relaxed such that the Lagrangian multipliers $\mu_{k,n} \approx 0, \forall k, n$. The critical points of λ_n^* is expressed as

$$\lambda_n^* = \frac{KB}{N\left(1 + \sum_{k=1}^{K} \frac{1}{\gamma_{k,n}}\right) \ln 2}. \tag{4.10}$$

Substituting (4.10) into (4.7) gives the sub-optimal solution to problem (P1) as

$$\beta_{k,n}^* = \frac{\sum_{i=1}^{K} \frac{1}{\gamma_{i,n}} + 1}{K} - \frac{1}{\gamma_{k,n}}, \tag{4.11}$$

in which the following Karush-Kuhn-Tucker (KKT) conditions can be satisfied:

$$\sum_{k=1}^{K} \left(\beta_{k,n}^*\right) - 1 \leq 0; \tag{4.12}$$

$$\sum_{k=1}^{K} \sum_{n=1}^{N} \left(\beta_{k,n}^*\right) - N \leq 0; \tag{4.13}$$

$$\frac{\partial}{\partial \beta_{k,n}} L_P\left(\beta_{k,n}^*, \lambda_n^*, \right) = 0; \tag{4.14}$$

$$\lambda_n^* \left[\sum_{k=1}^{K} \left(\beta_{k,n}^*\right) - 1\right] = 0. \tag{4.15}$$

Due to the relaxation on the positivity constraint, the sub-optimal solution of $\beta_{k,n}^*$ in (4.11) may violate the positivity constraint. In other words, to optimise the transmission rate, $\beta_{k,n}^*$ takes values between the interval of $\left[-(1 - \frac{2}{K}), 1 - \frac{2}{K}\right]$ for normalised $\gamma_{k,n}$. Since a sub-carrier assignment should strictly take either 0 or 1 to indicate that the sub-carrier is not in used or in used, respectively, the sub-optimal solution in (4.11) is conflicting with the definition of sub-carrier assignment vector in (4.3). To attain a feasible sub-optimal sub-carrier allocation based on (4.11), we impose a rule for the sub-carrier assignment vector, $\tilde{\beta}_{k,n} \in \{0, 1\}$ to follow.

Proposition 4.1. *For an arbitrary sub-carrier n, only one user is allowed for transmission at that sub-carrier. If more than one user is assigned to use sub-carrier n, any user*

which enters the system earlier (user with lower notation value) will be favourable. It can be expressed as:

$$\tilde{\beta}_{k,n} = \begin{cases} 1, & \text{if } \beta^*_{k,n} > \beta^*_{i,n}, \forall i \neq k \text{ and } \beta^*_{k,n} = \beta^*_{j,n}, \forall j > k; \\ 0, & \text{otherwise.} \end{cases} \tag{4.16}$$

Proposition 4.1 restricts $\tilde{\beta}_{k,n}$ to take either 0 or 1, it also deals with scenarios where some sub-channels are experiencing equally high SNR for multiple users at one time instant. *Proposition 4.1* applies a similar concept as the well-known maximum SNR scheduling [56] but for a multi-user multi-carrier system. The maximum SNR scheduling concept indicates that transmission is only allowed at the sub-channel of one user that experiences the largest SNR at that time instant. Our goal here is to allocate any particular sub-channel to only one user among all the contending users. Since the issues of user prioritisation or fairness are not the main emphasis of this chapter, we will not deal with these topics further in this chapter.

4.2.2 Power Allocation

In problem (P1), we address a sub-optimal sub-carrier allocation problem. We extend this problem to maximise the sum-capacity while maintaining the power distribution under a limited power budget. A similar problem with power budget of individual user is considered in Chapter 3. Due to the implementation of sub-channel allocation scheme, we consider that the sum of all transmission powers must not exceed the total power budget of the system. Assuming that the outcome of the sub-optimal sub-carrier allocation is known, the power allocation problem is posed as a constrained optimisation problem.

Problem (P2)

$$\begin{aligned} \max_{P_{k,n}} \quad & \sum_{k=1}^{K}\sum_{n=1}^{N} \frac{B}{N} \log_2\left(1 + P_{k,n}\tilde{\beta}_{k,n}\gamma_{k,n}\right) \\ \text{subject to} \quad & \sum_{k=1}^{K}\sum_{n=1}^{N} \tilde{\beta}_{k,n}P_{k,n} \leq P^{\max}, \\ & P_{k,n} \geq 0, \end{aligned} \tag{4.17}$$

where $P^{\max}$ is the total power budget and $\tilde{\beta}_{k,n}$ is the sub-optimal solution of the sub-carrier allocation which only takes the value of 0 or 1.

By ignoring the positivity constraint, $P_{k,n} \geq 0$, we have the following Lagrangian:

$$L_P(P_{k,n}, \lambda) \;=\; \sum_{k=1}^{K}\sum_{n=1}^{N}\left[\frac{B}{N}\log_2\left(1 + P_{k,n}\tilde{\beta}_{k,n}\gamma_{k,n}\right) - \lambda\tilde{\beta}_{k,n}P_{k,n}\right] + \lambda P^{\max}, \quad (4.18)$$

where λ is the Lagrangian multiplier.

By partial differentiating (4.18) with respect to $P_{k,n}$ for $\tilde{\beta}_{k,n} = 1$ and equating them to zero, we can obtain

$$\lambda = \frac{B\gamma_{k,n}}{N(1 + P_{k,n}\gamma_{k,n})\ln 2}\,. \quad (4.19)$$

Note that for $\tilde{\beta}_{k,n} = 0$, we already have a solution of $P_{k,n} = 0$. Then, the expression in (4.19) can deduce a water-filling solution for $\tilde{\beta}_{k,n} = 1$, which is given by

$$P^*_{k,n} = \left[\frac{B}{N\lambda^* \ln 2} - \frac{1}{\gamma_{k,n}}\right]^+, \quad (4.20)$$

where $[x]^+ = \max(0, x)$ and λ^* is the solution of

$$P^{\max} = \sum_{k=1}^{K}\sum_{n=1}^{N}\tilde{\beta}_{k,n}\left[\frac{B}{N\lambda^* \ln 2} - \frac{1}{\gamma_{k,n}}\right]^+. \quad (4.21)$$

Thus we can obtain the expression of λ^* by rearranging (4.21), which is given by

$$\lambda^* = \frac{B\sum_{k=1}^{K}\sum_{n=1}^{N}\tilde{\beta}_{k,n}}{N\left(P^{\max} + \sum_{k=1}^{K}\sum_{n=1}^{N}\frac{\tilde{\beta}_{k,n}}{\gamma_{k,n}}\right)\ln 2}. \quad (4.22)$$

Substituting (4.22) into (4.20) gives the solution to problem (P2) as

$$P^*_{k,n}|_{\tilde{\beta}_{k,n}=1} = \left[\frac{P^{\max} + \sum_{i=1}^{K}\sum_{j=1}^{N}\frac{\tilde{\beta}_{i,j}}{\gamma_{i,j}}}{\sum_{i=1}^{K}\sum_{j=1}^{N}\tilde{\beta}_{i,j}} - \frac{1}{\gamma_{k,n}}\right]^+, \quad (4.23)$$

in which the following KKT conditions can be satisfied:

$$\sum_{k=1}^{K}\sum_{n=1}^{N}\left(\tilde{\beta}_{k,n}P^*_{k,n}\right) - P^{\max} \leq 0\,; \quad (4.24)$$

$$\lambda^* \geq 0\,; \quad (4.25)$$

$$\frac{\partial}{\partial P_{k,n}}L_P\left(P^*_{k,n}, \lambda^*\right) = 0\,; \quad (4.26)$$

$$\lambda^*\left[\sum_{k=1}^{K}\sum_{n=1}^{N}\left(\tilde{\beta}_{k,n}P^*_{k,n}\right) - P^{\max}\right] = 0. \quad (4.27)$$

In Chapter 3, the OFDMA power allocation problem was solved by suppressing all negative power terms to zero and adjusting the remaining positive power terms to meet the total power budget. It is shown that the sub-optimal scheme is able to achieve 99% of the optimal achievable rate. Unlike Chapter 3, the solution presented in (4.23) is an optimal solution to problem (P2) since the $[x]^+ = \max(0, x)$ operation takes into the consideration of positivity constraint. For any circumstance where $\sum_{k=1}^{K}\sum_{n=1}^{N} P_{k,n}^* < P^{\max}$, we impose a rule for the transmission power $\tilde{P}_{k,n}$ to follow.

Proposition 4.2. *For an arbitrary sub-carrier n, the corresponding transmission power for user k can be expressed as:*

$$\tilde{P}_{k,n} = \begin{cases} \dfrac{P^{\max} P_{k,n}^*}{\sum_{i=1}^{K}\sum_{j=1}^{N} P_{i,j}^*}, & \text{for } \tilde{\beta}_{k,n} = 1; \\ 0, & \text{otherwise.} \end{cases} \tag{4.28}$$

Given a known outcome of the sub-optimal sub-carrier allocation scheme, *Proposition 4.2* presents the outcome of the optimal power allocation scheme, which satisfies KKT conditions whilst not violating the positivity constraint.

Both the capacity optimisation problems of (P1) and (P2) assume perfect knowledge of feedback CSI. However, there are two main issues when implementing the sub-carrier and power allocation schemes that we have derived. Firstly, the feedback of CSI for a time-varying channel may experience delay that leads to detrimental performance on adaptive transmission schemes. The second issue is that the implementation of feedback in an OFDMA system consumes more resources than a conventional single carrier system because the feedback information of an N-carrier system is always N times larger. In the next sections, we provide solutions to answer these two problems. We will first model the fading channel as an FSMC, where the instantaneous received envelope is partitioned into different levels. Instead of having to transmit the exact CSI, FSMC helps to reduce the required feedback bits of each sub-carrier. Further reduction can be achieved by grouping the sub-carriers into sub-bands and using lumpability to reduce the number of states in the FSMC. Then, we propose to predict CSI at least one symbol duration ahead in order to mitigate the negative effect caused by feedback delay.

4.3 Finite-state Markov Channel

4.3.1 Markov Model

Let $\mathcal{S} = \{s_1, s_2, \ldots, s_M\}$ denote a set of M states and $\{S_t\}$, $t = 0, 1, \ldots$, be a constant Markov process, which has stationary transitions [102]. The illustration of the M-state Markov chain is shown in Figure 4.2. The probability that the Markov process remains at an arbitrary state s_i after an infinitely long time is defined as the steady-state probability, which can be written as

$$\pi_i \quad = \quad \Pr(S_t = s_i), \tag{4.29}$$

for all $i \in \{0, 1, \ldots, M-1\}$. On the other hand, the probability that the Markov process transits from state s_i to state s_j is defined as the state transition probability[2], which can be written as

$$a_{i,j} \quad = \quad \begin{cases} \Pr(S_{t+1} = s_j \mid S_t = s_i), & \text{for } |i-j| \leq 1; \\ 0, & \text{otherwise.} \end{cases} \tag{4.30}$$

for all $i, j \in \{0, 1, \ldots, M-1\}$.

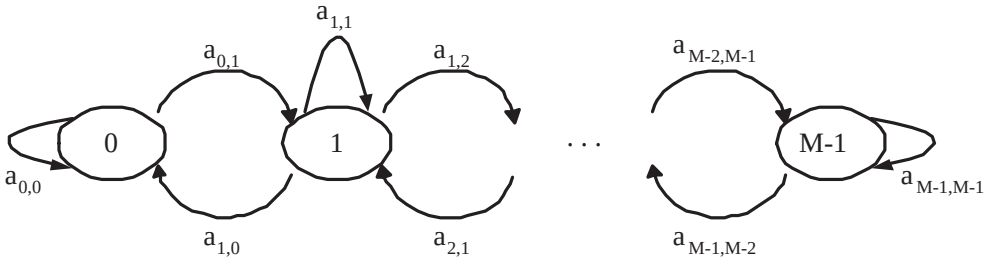

Figure 4.2. Illustration of M-state Markov chain.

With (4.29) and (4.30), we can define an $(M \times 1)$ steady-state probability vector, $\boldsymbol{\pi}$ and an $(M \times M)$ transition matrix, $\mathbf{A}$, with the properties that the sum of all the elements in $\boldsymbol{\pi}$ equals 1, i.e. $\sum_{i=0}^{M-1} \pi_i = 1$, and the sum of the elements on each row of $\mathbf{A}$ equals to 1, i.e. $\sum_{j=0}^{M-1} a_{i,j} = 1$.

[2]For a Markov process, only the last state occupied by the process is relevant in determining its future behaviour. We can neglect any other information we have about the past in predicting the future. Thus, the probability of making a transition to each state of the process depends only on the state presently occupied [53].

In a typical multipath propagation channel, the received signal envelope can be modelled using a Rayleigh distribution. Let γ denote the received SNR which is proportional to the square of the signal envelope. One can show that γ is exponentially distributed [76] with its probability density function as

$$p(\gamma) = \frac{1}{\bar{\gamma}} \exp\left(-\frac{\gamma}{\bar{\gamma}}\right), \tag{4.31}$$

where $\bar{\gamma}$ is both the mean and standard deviation of γ.

Given that the Jakes model [47] is assumed for the time-domain correlation, the expected number of times per second the received SNR γ passes downward across a quantised level γ_m is given by

$$N_m = \sqrt{\frac{2\pi\gamma_m}{\bar{\gamma}}} f_d \exp\left(-\frac{\gamma_m}{\bar{\gamma}}\right), \tag{4.32}$$

where f_d is the maximum Doppler frequency, which is defined as $f_d = v f_c/c$, for v/c is the ratio of moving speed of mobile terminal to speed of light and f_c is the carrier frequency. In other literatures, N_m is also known as *level crossing rate* [1].

With the thresholds of the quantised SNR levels defined as $0 = \gamma_0 < \ldots < \gamma_{M-1} = \infty$, the Rayleigh fading channel is said to be in state s_m if the received SNR is within the interval of $[\gamma_m, \gamma_{m+1})$. With the exponentially distributed SNR, the steady-state probability for each state is given as

$$\begin{aligned} \pi_m &= \int_{\gamma_m}^{\gamma_{m+1}} \frac{1}{\bar{\gamma}} \exp\left(-\frac{u}{\bar{\gamma}}\right) du \\ &= \exp\left(-\frac{\gamma_m}{\bar{\gamma}}\right) - \exp\left(-\frac{\gamma_{m+1}}{\bar{\gamma}}\right). \end{aligned} \tag{4.33}$$

The transition probabilities $a_{m,m+1}$ and $a_{m,m-1}$ can be approximated by

$$a_{m,m+1} \approx \frac{N_{m+1}}{R_t \pi_m}, \quad \text{for } m = 0, 1, \ldots, M-2; \tag{4.34}$$

$$a_{m,m-1} \approx \frac{N_m}{R_t \pi_m}, \quad \text{for } m = 1, 2, \ldots, M-1; \tag{4.35}$$

where R_t represents the transmission rate and π_m is the steady-state probability during which the channel is at state m. Thus, the transition probability can be rewritten as

$$a_{m,m+1} \approx \frac{N_{m+1} T}{\pi_m}, \quad \text{for } m = 0, 1, \ldots, M-2; \tag{4.36}$$

$$a_{m,m-1} \approx \frac{N_m T}{\pi_m}, \quad \text{for } m = 1, 2, \ldots, M-1; \tag{4.37}$$

where T represents the time interval for each transmission over the channel, i.e. symbol duration. Other transition probabilities are given by

$$a_{m,m} = \begin{cases} 1 - a_{m,m+1}, & \text{for } m = 0\,; \\ 1 - a_{m,m-1}, & \text{for } m = M-1; \\ 1 - a_{m,m-1} - a_{m,m+1}, & \text{otherwise.} \end{cases} \tag{4.38}$$

4.3.2 Expanded Markov Channel

For an arbitrary user k of an OFDMA system, $\gamma_{k.n}$, the SNR at sub-channel n, is modelled as an M-state Markov chain such that $\gamma_{k,n} \in \{0, 1, \ldots, M-1\}$ is given to indicate the quantised SNR level. Then, we briefly describe the effect of time-domain correlation of the fading channel in the modelling of the expanded Markov channel. In a *slow fading* environment, we assume that at most one sub-channel shall vary only one quantised level at either direction.

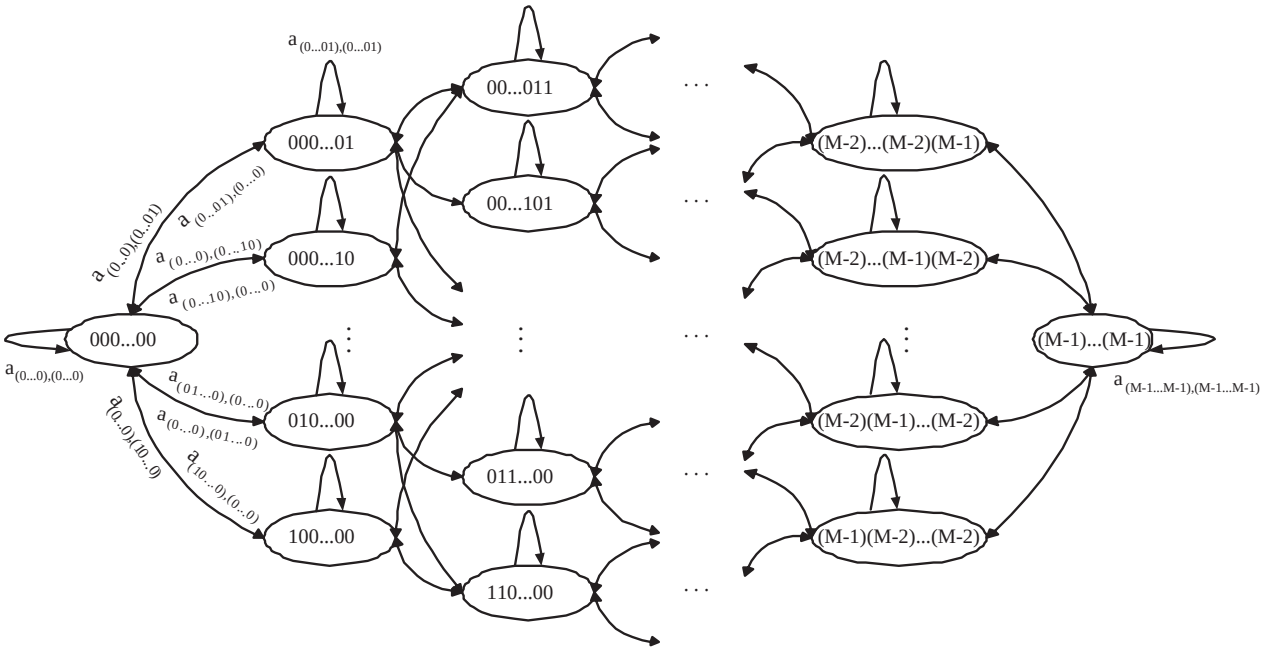

Figure 4.3. Illustration of M^N-state Markov chain where each state comprises N sub-states.

By an expanded process, each state is formed with all N consecutive conditions in the channel matrix. An M^N-state Markov channel is formed and shown in Figure 4.3. Now considering the Markov chain with M^N states, such as

$$\mathbf{s}_0 = (00\ldots0), \quad \mathbf{s}_1 = (0\ldots01), \quad \ldots \quad , \quad \mathbf{s}_{M^N-1} = (M-1\ldots M-1),$$

the steady-state probability vector, $\boldsymbol{\pi}_c = \{\pi_{\mathbf{s}_i}\}$, is defined as

$$\pi_{\mathbf{s}_i} = \Pr(S_t = \mathbf{s}_i). \tag{4.39}$$

The state transition probability matrix, $\mathbf{A}_c = \{a_{\mathbf{s}_i,\mathbf{s}_j}\}$, can be defined as

$$a_{\mathbf{s}_i,\mathbf{s}_j} = \begin{cases} \Pr(S_{t+1} = \mathbf{s}_j \,|\, S_t = \mathbf{s}_i), & \text{for } |\mathbf{s}_i - \mathbf{s}_j| \leq 1; \\ 0, & \text{otherwise.} \end{cases} \tag{4.40}$$

The transition from state $\mathbf{s}_i$ to state $\mathbf{s}_j$, which originally occurs in N successive steps with the original chain, is restricted to one step transition such that only one sub-channel is susceptible to a state transition. For all transition probability $a_{\mathbf{s}_i,\mathbf{s}_j} \neq 0$ in the state transition probability matrix $\mathbf{A}_c$, we define

$$a_{\mathbf{s}_i,\mathbf{s}_j} = \begin{cases} \dfrac{a_{x,y}}{N}, & \text{for transition from sub-state } x \text{ to sub-state } y; \\ 1 - \sum_{k \neq i} a_{\mathbf{s}_i,\mathbf{s}_k}, & \text{for all } \mathbf{s}_i = \mathbf{s}_j; \end{cases} \tag{4.41}$$

where the transition probability $a_{x,y}$ belongs to the M-state Markov chain which is shown in Figure 4.2.

To explain the reason for dividing the fundamental transition probability by the number of sub-carriers in (4.41), we consider the following example with $M = 2$ and $N = 2$:

$$\mathbf{A} = \begin{bmatrix} 0.6 & 0.4 \\ 0.2 & 0.8 \end{bmatrix}, \quad \mathbf{A}_c = \begin{bmatrix} 0.6 & 0.2 & 0.2 & 0 \\ 0.1 & 0.7 & 0 & 0.2 \\ 0.1 & 0 & 0.7 & 0.2 \\ 0 & 0.1 & 0.1 & 0.8 \end{bmatrix}, \tag{4.42}$$

where $\mathbf{A}$ and $\mathbf{A}_c$ are the state transition probability matrices for 2-state Markov channel and 2^2-state Markov channel, respectively. Given $a_{0,1} = 0.4$ and $a_{1,0} = 0.2$ which are retrieved from $\mathbf{A}$, we can generate $\mathbf{A}_c$ based on (4.41). Consider the first row of $\mathbf{A}_c$ with the state transition probabilities of $\mathbf{s}_0 = (00)$ to $\mathbf{s}_1 = (01)$, to $\mathbf{s}_2 = (10)$ and to $\mathbf{s}_3 = (11)$ are determined as 0.2, 0.2 and 0, respectively. Since the transitions of (00) to (01) and to (10) is observed as the true sub-state transition of 0 to 1, we show that $a_{\mathbf{s}_0,\mathbf{s}_1} + a_{\mathbf{s}_0,\mathbf{s}_2} = a_{0,1} = 0.4$ and hence $a_{\mathbf{s}_0,\mathbf{s}_0} = a_{0,0} = 0.6$. A similar approach can be applied to show that $a_{\mathbf{s}_3,\mathbf{s}_1} + a_{\mathbf{s}_3,\mathbf{s}_2} = a_{1,0} = 0.2$ and $a_{\mathbf{s}_3,\mathbf{s}_3} = a_{1,1} = 0.8$.

The steady-state probabilities, $\boldsymbol{\pi}_c = [\pi_{\mathbf{s}_i}]$, for $i = 0, 1, \ldots, M^N - 1$, of the M^N-state Markov chain can be computed by

$$\pi_{\mathbf{s}_0} = \prod_{i=1}^{N} \pi_0^{(i)}, \tag{4.43}$$

$$\pi_{\mathbf{s}_1} = \pi_1^{(1)} \prod_{i=2}^{N} \pi_0^{(i)}, \tag{4.44}$$

$$\pi_{\mathbf{s}_2} = \pi_0^{(1)} \pi_1^{(2)} \prod_{i=3}^{N} \pi_0^{(i)}, \tag{4.45}$$

$$\vdots$$

$$\pi_{\mathbf{s}_{M^N-1}} = \prod_{i=1}^{N} \pi_{M-1}^{(i)}\ , \tag{4.46}$$

where $\pi_0^{(n)}$, $\pi_1^{(n)}$, ..., $\pi_{M-1}^{(n)}$ are the n^{th} sub-channel's steady-state probabilities for state 0, state 1, ..., and state $(M-1)$ of the original M-state Markov chain, respectively. To meet one property of the probability theory, the sum of all steady-state probabilities, $\pi_{\mathbf{s}_i}$, should be 1. *Theorem 4.1* verifies this property.

Theorem 4.1. *Given that the sum of all steady-state probabilities for an arbitrary n^{th} sub-channel, $\pi_i^{(n)}$, of an M-state Markov chain is 1, the sum of all the steady-state probabilities, $\pi_{\mathbf{s}_i}$, of the expanded M^N-state Markov chain is also 1, i.e.*

$$\sum_{i=0}^{M^N-1} \pi_{\mathbf{s}_i} = 1^N = 1. \tag{4.47}$$

Proof. For proof, please refer to Appendix A. □

If the variation of all N sub-channels is subjected to have the same distribution characteristics, such as identical mean SNR, then all sub-channels can be modelled as an identical M-state Markov channel, such that $\pi_m^{(1)} = \pi_m^{(2)} = \cdots = \pi_m^{(N)}$, for $m = 0, 1, \ldots, M-1$. Thus, the steady-state probabilities in (4.43)-(4.46) are redefined as $\tilde{\pi}_{\mathbf{s}_i}$, such that

$$\tilde{\pi}_{\mathbf{s}_0} = (\pi_0)^N, \tag{4.48}$$

$$\tilde{\pi}_{\mathbf{s}_1} = (\pi_0)^{N-1} \pi_1, \tag{4.49}$$

$$\tilde{\pi}_{\mathbf{s}_2} = (\pi_0)^{N-1} \pi_1, \tag{4.50}$$

$$\vdots$$

$$\tilde{\pi}_{\mathbf{s}_{M^N-1}} = (\pi_{M-1})^N. \tag{4.51}$$

Theorem 4.2 verifies the property that the sum of all steady-state probabilities, $\tilde{\pi}_{\mathbf{s}_i}$, should be 1.

Theorem 4.2. *Given that the steady-state probabilities of all sub-channels are identical, and the sum of these steady-state probabilities for any arbitrary sub-channel, π_i, of an M-state Markov chain is 1, the sum of all the steady-state probabilities, $\pi_{\mathbf{s}_i}$, of the expanded M^N-state Markov chain is also 1, i.e.*

$$\sum_{i=0}^{M^N-1} \tilde{\pi}_{\mathbf{s}_i} = 1^N = 1. \tag{4.52}$$

Proof. For proof, please refer to Appendix B. □

Apart from the *slow fading* environment, there are also *moderate* and *fast fading* environments that lead to different expanded Markov models. In a *moderate fading* environment, we assume that one or more sub-channels shall vary only one quantised level at either direction; whereas in a *fast fading* environment, we assume that one or more sub-channels shall vary to any quantised levels at any direction. However, to model the expanded Markov channel for the *moderate* and *fast fading* cases will result in extremely complex non-birth-death Markov processes. To ensure that the expanded model remains as a quasi-birth-death Markov process, we can only model for a *slow fading* environment. Therefore, the expanded Markov model in Figure 4.3 may not cover all true events and may be susceptible to performance degradation in *moderate* and *fast fading* environments. In later section, we will introduce a lumpable approach such that the Markov channel can be modelled to describe the channel variation of *slow* and *moderate fading* environments. The simulation results in Section 4.6 shall verify this phenomenon.

Throughout this chapter, we consider only the case where all N sub-channels are subjected to variation. In any practical system, the SNR level can be quantised to at least 2 levels whereas the number of sub-channels of an OFDM system can go to 512 or higher. Simply relating these figures to M and N, the matrix dimension can approach to $2^{512} \approx 1.34 \times 10^{154}$, which is too big to be practical. We need to define a way to reduce the size of the matrix in order to realise the channel prediction at transmitter.

4.4 Lumpability

In this section, we reduce the size of the M^N-state Markov channel based on two steps:

1. For an OFDMA system with N sub-channels, a small fixed number of, say b, sub-channels are gathered into a sub-band in order to reduce the M^N-state Markov chain to N/b parallel M^b-state Markov chains, where $N/b \in \mathbb{Z}^+$ and $b \leq N$;

2. For each of the N/b subsystems, the M^b-state Markov chain is reduced to a much smaller size by lumping some states among the M^b-state to form a new $[(M-1)b+1]$-state Markov chain.

4.4.1 Formation of Sub-bands

For an OFDMA system with N correlated sub-channels, we propose to gather a small fixed number of, say b, sub-channels into one sub-band. The approach of forming sub-bands is similar to the concept of *clustered OFDM* [63, 92] where multiple tones (sub-channel) are gathered to become a cluster (sub-band). Unlike *clustered OFDM*, the formation of sub-bands is virtually done in the mathematical model but the OFDMA system remains unchanged. The choice of b is decided by the frequency correlation between sub-channels. Assume that B_c is the coherent bandwidth and B is the signal bandwidth.

1. For $B_c \ll B$, we observe a severe frequency-selective fading environment. We expect $b = 1$ because each sub-channel can be treated as an independent channel, which means the severe frequency-selective fading channel can be modelled as N independent M-state Markov channels.

2. For $B_c < B$, we observe a typical frequency-selective fading environment. The choice of b falls within the range of $1 < b < N$, where $N/b \in \mathbb{Z}^+$, such that the frequency-selective fading channel is modelled as N/b independent M^b-state Markov channels.

3. For $B_c \geq B$, we observe a flat fading environment as all sub-channels are fully-correlated. The choice of b is restricted to only $b = N$ because all sub-channels are identical and can be considered as one whole channel. In other words, the flat fading channel is modelled as an M-state Markov channel.

At this stage, we only consider the second case because it is the only realistic scenario among all three cases. The original N sub-channels modelled with M^N-state Markov channel can now be transformed into N/b parallel sub-bands, each modelled as an M^b-state Markov channel with $(M^b \times M^b)$ transition matrices, $\mathbf{A}_s^{(z)}$, where $z \in \{1, 2, \ldots, N/b\}$. Since it becomes a parallel problem, the notation of $\mathbf{A}_s$ will be used throughout this chapter for the purposes of simplicity.

The M^b-state Markov chain can be illustrated in a way similar to Figure 4.3 except that each state comprises b sub-states. Referring to *Theorem 4.1*, by replacing N with b, the sum of all steady-state probabilities in $\boldsymbol{\pi}_s$ is obtained as $\sum_{i=0}^{M^b-1} \hat{\pi}_{\mathbf{s}_i} = 1^b = 1$. For all state transition probabilities $a_{\mathbf{s}_i,\mathbf{s}_j} \neq 0$ in $\mathbf{A}_s$, we define

$$\hat{a}_{\mathbf{s}_i,\mathbf{s}_j} = \begin{cases} \dfrac{a_{x,y}}{b}, & \text{for transition from sub-state } x \text{ to sub-state } y; \\ 1 - \sum_{k \neq i} a_{\mathbf{s}_i,\mathbf{s}_k}, & \text{for all } \mathbf{s}_i = \mathbf{s}_j; \end{cases} \tag{4.53}$$

where the transition probability $a_{x,y}$ belongs to the original M-state Markov chain as shown in Figure 4.2.

In practice, if the quality of channel is quantised into 2 levels and the system has 512 sub-channels where every 4 sub-channels are gathered into a sub-band, then it is possible to reduce the original $(2^{512} \times 2^{512})$ transition matrix to $512/4 = 128$ matrices each of size (16×16). However, the handling of all 128 matrices is not an easy task because these matrices is equivalent to a matrix of size (2048×2048). Therefore, a second step is required to minimise the resultant feedback information.

4.4.2 Lumpable States

The concept of the lumpability of a Markov chain has been previously discussed in [53,103]. In essence, the property of lumpability means that there is a partition of aggregated states of a Markov chain and yet the behaviour of the Markov chain remains in a similar manner as far as the state dynamics and observation statistics are concerned. We first observe the pattern of an M^b-state Markov chain.

Definition 4.1. *Consider an M^b-state Markov chain with states $\mathbf{s}_i = (s_{i1}s_{i2}\cdots s_{ib})$ where each of the sub-states, $s_{ik} \in \{0, 1, \ldots, M-1\}$ for all $i = 0, 1, \ldots, M^b - 1$ and $k = 1, 2, \ldots, b$. All M^b states can then be divided into $Q = (M-1)b + 1$ lumpable*

partitions, of which the q^{th} partition is defined as

$$\mathbf{L}_q = \left\{ \mathbf{s}_i \left| \sum_{k=1}^{b} s_{ik} = q, \forall i = 0, 1, \ldots, M^b - 1 \right. \right\}, \tag{4.54}$$

where $q = 0, 1, \ldots, Q-1$.

Definition 4.2. *Let q be the index of the lumpable partitions, such that $q \in [0, (M-1)b]$. It can be written in the form of*

$$q = 0 \cdot n_0 + 1 \cdot n_1 + \ldots + (M-1) \cdot n_{M-1} = \sum_{i=0}^{M-1} i \cdot n_i \ , \tag{4.55}$$

where n_i is the number of occurrence of sub-state i in a given state for $i = 0, 1, \ldots, M-1$, which is subjected to a constraint of

$$\sum_{i=0}^{M-1} n_i = b. \tag{4.56}$$

Hence, the number of aggregated states in q^{th} partition can be defined as

$$\#\mathbf{L}_q = \sum_j \frac{b!}{n_0^{(j)}! n_1^{(j)}! \cdots n_{M-1}^{(j)}!} \ , \tag{4.57}$$

where j is the number of combinations for $n_i^{(j)}$ which satisfies both (4.55) and (4.56).

We then present the concept of lumpability to form an aggregated state $\mathbf{L}$ from multiple atomic states of an FSMC and obtain its eventual transition matrix.

Definition 4.3. *For the partitions, $\mathbf{L} = \{\mathbf{L}_0, \mathbf{L}_1, \ldots, \mathbf{L}_{Q-1}\}$, assume that the chain before lumping has $R = M^b$ states and after lumping has $Q = [(M-1)b + 1]$ states. Let $\mathbf{U}$ be the $(Q \times R)$ matrix whose i^{th} row is the probability vector having equal components for states in $\mathbf{L}_i$ and 0 for the remaining states. Let $\mathbf{V}$ be the $(R \times Q)$ matrix with the j^{th} column being a vector with 1's in the components corresponding to states in $\mathbf{L}_j$ and 0's otherwise. Given that the transition matrix of the M^b-state Markov chain is $\mathbf{A}_s$, the lumped transition matrix [53] is defined as*

$$\mathbf{A}_l = \mathbf{U}\mathbf{A}_s\mathbf{V}, \tag{4.58}$$

where $\mathbf{A}_l = [a_{\mathbf{L}_x, \mathbf{L}_y}]$ is a $(Q \times Q)$ matrix, for $x, y = 0, 1, \ldots, Q-1$, and $a_{\mathbf{L}_x, \mathbf{L}_y}$ denotes the state transition probability from the x^{th} partition to the y^{th} partition.

Definition 4.4. *Given that the steady-state vector of the M^b-state Markov chain is $\boldsymbol{\pi}_s$, the lumped steady-state probability vector is defined as*

$$\boldsymbol{\pi}_l = \boldsymbol{\pi}_s \mathbf{V}, \tag{4.59}$$

where $\boldsymbol{\pi}_l = [\pi_{\mathbf{L}_q}]$, for $q = 0, 1, \ldots, Q-1$, and $\pi_{\mathbf{L}_q}$ denotes the steady-state probability for the q^{th} partition. Since the sum of all steady-state probabilities in $\boldsymbol{\pi}_s$ is 1, the sum of all steady-state probabilities in $\boldsymbol{\pi}_l$ must also be 1.

4.4.3 An Example of Lumpable 2^4-state Markov Channel

Consider a practical OFDMA system with $N = 512$ sub-carriers. For simplicity, each sub-channel is modelled as a Gilbert-Elliott channel with only $M = 2$ states distinguishing a good state and a bad state. Due to the different level crossing rate and transmission rate for different sub-carriers, each sub-channel has its own transition matrix $\mathbf{A}^{(n)}$, for $n = 1, 2, \ldots, N$, which is given as

$$\mathbf{A}^{(n)} = \begin{bmatrix} a_{0,0}^{(n)} & a_{0,1}^{(n)} \\ a_{1,0}^{(n)} & a_{1,1}^{(n)} \end{bmatrix}, \tag{4.60}$$

where the transition probabilities $a_{i,j}^{(n)}$, for $i, j = \{0, 1\}$, are defined in (4.34)-(4.38).

Assuming that the coherent bandwidth of the channel, B_c, is less than the signal bandwidth, B, such that b can be chosen as 4. Thus, 512 sub-channels can be subdivided into $N/b = 512/4 = 128$ parallel sub-bands, where each sub-band is modelled as a 2^4-state Markov channel with states $\mathbf{s}_0 = (0000), \mathbf{s}_1 = (0001), \ldots, \mathbf{s}_{15} = (1111)$. An example of a 2^4-state Markov chain is illustrated in the upper part of Figure 4.4. With *Definition 4.1*, all 16 states can be divided into $Q = 5$ lumpable partitions, as shown in Table 4.1. The demonstration of determining the number of lumpable states, $\#\mathbf{L}_q$, in any q^{th} partition, according to *Definition 4.2*, can be found in Table 4.2. It is shown that each $\#\mathbf{L}_q$ has verified the number of lumpable states in the q^{th} partition. Thus, the lumped Markov model is given as the uni-chain birth-death Markov process in the lower part of Figure 4.4.

Table 4.1. 2^4-state Markov channel with 5 lumpable partitions

States, $\mathbf{s}_i = (s_{i1}s_{i2}s_{i3}s_{i4})$	*Index*, $q = \sum_k s_{ik}$	*Partitions*, $\mathbf{L}_q$
$\mathbf{s}_0 = (0000)$	0	$\mathbf{L}_0$
$\mathbf{s}_1 = (0001)$	1	$\mathbf{L}_1$
$\mathbf{s}_2 = (0010)$	1	
$\mathbf{s}_3 = (0100)$	1	
$\mathbf{s}_4 = (1000)$	1	
$\mathbf{s}_5 = (0011)$	2	$\mathbf{L}_2$
$\mathbf{s}_6 = (0101)$	2	
$\mathbf{s}_7 = (0110)$	2	
$\mathbf{s}_8 = (1001)$	2	
$\mathbf{s}_9 = (1010)$	2	
$\mathbf{s}_{10} = (1100)$	2	
$\mathbf{s}_{11} = (0111)$	3	$\mathbf{L}_3$
$\mathbf{s}_{12} = (1011)$	3	
$\mathbf{s}_{13} = (1101)$	3	
$\mathbf{s}_{14} = (1110)$	3	
$\mathbf{s}_{15} = (1111)$	4	$\mathbf{L}_4$

Table 4.2. Number of states in each lumpable partition

Index, q	*Combinations for* $n_i, \forall i = 0, 1$	$\#\mathbf{L}_q$
0	$n_1 = 0, \therefore n_0 = 4$	$\frac{4!}{4!0!} = 1$
1	$n_1 = 1, \therefore n_0 = 4 - 1 = 3$	$\frac{4!}{3!1!} = 4$
2	$n_1 = 2, \therefore n_0 = 4 - 2 = 2$	$\frac{4!}{2!2!} = 6$
3	$n_1 = 3, \therefore n_0 = 4 - 3 = 1$	$\frac{4!}{1!3!} = 4$
4	$n_1 = 4, \therefore n_0 = 4 - 4 = 0$	$\frac{4!}{0!4!} = 1$

The state transition probabilities of the 2^4-state Markov chain can be obtained in the similar form as (4.53),

$$\begin{aligned}
\hat{a}_{\mathbf{s}_0,\mathbf{s}_1} &= \frac{a_{0,1}^{(w)}}{4}, \\
\hat{a}_{\mathbf{s}_0,\mathbf{s}_2} &= \frac{a_{0,1}^{(x)}}{4}, \\
\hat{a}_{\mathbf{s}_0,\mathbf{s}_3} &= \frac{a_{0,1}^{(y)}}{4}, \\
\hat{a}_{\mathbf{s}_0,\mathbf{s}_4} &= \frac{a_{0,1}^{(z)}}{4}, \\
\hat{a}_{\mathbf{s}_0,\mathbf{s}_0} &= 1 - \hat{a}_{\mathbf{s}_0,\mathbf{s}_1} - \hat{a}_{\mathbf{s}_0,\mathbf{s}_2} - \hat{a}_{\mathbf{s}_0,\mathbf{s}_3} - \hat{a}_{\mathbf{s}_0,\mathbf{s}_4}, \\
&\vdots \\
\hat{a}_{\mathbf{s}_{15},\mathbf{s}_{11}} &= \frac{a_{1,0}^{(z)}}{4}, \\
\hat{a}_{\mathbf{s}_{15},\mathbf{s}_{12}} &= \frac{a_{1,0}^{(y)}}{4}, \\
\hat{a}_{\mathbf{s}_{15},\mathbf{s}_{13}} &= \frac{a_{1,0}^{(x)}}{4}, \\
\hat{a}_{\mathbf{s}_{15},\mathbf{s}_{14}} &= \frac{a_{1,0}^{(w)}}{4}, \\
\hat{a}_{\mathbf{s}_{15},\mathbf{s}_{15}} &= 1 - \hat{a}_{\mathbf{s}_{15},\mathbf{s}_{11}} - \hat{a}_{\mathbf{s}_{15},\mathbf{s}_{12}} - \hat{a}_{\mathbf{s}_{15},\mathbf{s}_{13}} - \hat{a}_{\mathbf{s}_{15},\mathbf{s}_{14}},
\end{aligned}$$

where w, x, y, z indicates the index of four arbitrary sub-channels.

With *Definition 4.3*, we can determine $\mathbf{U}$ and $\mathbf{V}$ operators prior to computing the lumped transition matrix,

$$\mathbf{U} = \begin{bmatrix}
1 & 0 & 0 & 0 & 0 & 0 & 0 & 0 & 0 & 0 & 0 & 0 & 0 & 0 & 0 & 0 \\
0 & \frac{1}{4} & \frac{1}{4} & \frac{1}{4} & \frac{1}{4} & 0 & 0 & 0 & 0 & 0 & 0 & 0 & 0 & 0 & 0 & 0 \\
0 & 0 & 0 & 0 & 0 & \frac{1}{6} & \frac{1}{6} & \frac{1}{6} & \frac{1}{6} & \frac{1}{6} & \frac{1}{6} & 0 & 0 & 0 & 0 & 0 \\
0 & 0 & 0 & 0 & 0 & 0 & 0 & 0 & 0 & 0 & 0 & \frac{1}{4} & \frac{1}{4} & \frac{1}{4} & \frac{1}{4} & 0 \\
0 & 0 & 0 & 0 & 0 & 0 & 0 & 0 & 0 & 0 & 0 & 0 & 0 & 0 & 0 & 1
\end{bmatrix}, \quad \mathbf{V} = \begin{bmatrix}
1 & 0 & 0 & 0 & 0 \\
0 & 1 & 0 & 0 & 0 \\
0 & 1 & 0 & 0 & 0 \\
0 & 1 & 0 & 0 & 0 \\
0 & 1 & 0 & 0 & 0 \\
0 & 0 & 1 & 0 & 0 \\
0 & 0 & 1 & 0 & 0 \\
0 & 0 & 1 & 0 & 0 \\
0 & 0 & 1 & 0 & 0 \\
0 & 0 & 1 & 0 & 0 \\
0 & 0 & 1 & 0 & 0 \\
0 & 0 & 0 & 1 & 0 \\
0 & 0 & 0 & 1 & 0 \\
0 & 0 & 0 & 1 & 0 \\
0 & 0 & 0 & 1 & 0 \\
0 & 0 & 0 & 0 & 1
\end{bmatrix}.$$

Thus, the lumped state transition probability matrix, $\mathbf{A}_l$, can be computed by

$$\mathbf{A}_l = \mathbf{U}\mathbf{A}_s\mathbf{V} = \begin{bmatrix}
a_{\mathbf{L}_0,\mathbf{L}_0} & a_{\mathbf{L}_0,\mathbf{L}_1} & 0 & 0 & 0 \\
a_{\mathbf{L}_1,\mathbf{L}_0} & a_{\mathbf{L}_1,\mathbf{L}_1} & a_{\mathbf{L}_1,\mathbf{L}_2} & 0 & 0 \\
0 & a_{\mathbf{L}_2,\mathbf{L}_1} & a_{\mathbf{L}_2,\mathbf{L}_2} & a_{\mathbf{L}_2,\mathbf{L}_3} & 0 \\
0 & 0 & a_{\mathbf{L}_3,\mathbf{L}_2} & a_{\mathbf{L}_3,\mathbf{L}_3} & a_{\mathbf{L}_3,\mathbf{L}_4} \\
0 & 0 & 0 & a_{\mathbf{L}_4,\mathbf{L}_3} & a_{\mathbf{L}_4,\mathbf{L}_4}
\end{bmatrix}, \tag{4.61}$$

where

$$
\begin{aligned}
a_{\mathbf{L}_0,\mathbf{L}_0} &= \hat{a}_{\mathbf{s}_0,\mathbf{s}_0}, \\
a_{\mathbf{L}_0,\mathbf{L}_1} &= \hat{a}_{\mathbf{s}_0,\mathbf{s}_1} + \hat{a}_{\mathbf{s}_0,\mathbf{s}_2} + \hat{a}_{\mathbf{s}_0,\mathbf{s}_3} + \hat{a}_{\mathbf{s}_0,\mathbf{s}_4}, \\
a_{\mathbf{L}_1,\mathbf{L}_0} &= \tfrac{1}{4}\left(\hat{a}_{\mathbf{s}_1,\mathbf{s}_0} + \hat{a}_{\mathbf{s}_2,\mathbf{s}_0} + \hat{a}_{\mathbf{s}_3,\mathbf{s}_0} + \hat{a}_{\mathbf{s}_4,\mathbf{s}_0}\right), \\
a_{\mathbf{L}_1,\mathbf{L}_1} &= \tfrac{1}{4}\left(\hat{a}_{\mathbf{s}_1,\mathbf{s}_1} + \hat{a}_{\mathbf{s}_2,\mathbf{s}_2} + \hat{a}_{\mathbf{s}_3,\mathbf{s}_3} + \hat{a}_{\mathbf{s}_4,\mathbf{s}_4}\right), \\
a_{\mathbf{L}_1,\mathbf{L}_2} &= \tfrac{1}{4}\left(\hat{a}_{\mathbf{s}_1,\mathbf{s}_5} + \hat{a}_{\mathbf{s}_1,\mathbf{s}_6} + \hat{a}_{\mathbf{s}_1,\mathbf{s}_8} + \hat{a}_{\mathbf{s}_2,\mathbf{s}_5} + \hat{a}_{\mathbf{s}_2,\mathbf{s}_7} + \hat{a}_{\mathbf{s}_2,\mathbf{s}_9} + \right. \\
&\quad \left. \hat{a}_{\mathbf{s}_3,\mathbf{s}_6} + \hat{a}_{\mathbf{s}_3,\mathbf{s}_7} + \hat{a}_{\mathbf{s}_3,\mathbf{s}_{10}} + \hat{a}_{\mathbf{s}_4,\mathbf{s}_8} + \hat{a}_{\mathbf{s}_4,\mathbf{s}_9} + \hat{a}_{\mathbf{s}_4,\mathbf{s}_{10}}\right), \\
a_{\mathbf{L}_2,\mathbf{L}_1} &= \tfrac{1}{6}\left(\hat{a}_{\mathbf{s}_5,\mathbf{s}_1} + \hat{a}_{\mathbf{s}_6,\mathbf{s}_1} + \hat{a}_{\mathbf{s}_8,\mathbf{s}_1} + \hat{a}_{\mathbf{s}_5,\mathbf{s}_2} + \hat{a}_{\mathbf{s}_7,\mathbf{s}_2} + \hat{a}_{\mathbf{s}_9,\mathbf{s}_2} + \right. \\
&\quad \left. \hat{a}_{\mathbf{s}_6,\mathbf{s}_3} + \hat{a}_{\mathbf{s}_7,\mathbf{s}_3} + \hat{a}_{\mathbf{s}_{10},\mathbf{s}_3} + \hat{a}_{\mathbf{s}_8,\mathbf{s}_4} + \hat{a}_{\mathbf{s}_9,\mathbf{s}_4} + \hat{a}_{\mathbf{s}_{10},\mathbf{s}_4}\right), \\
a_{\mathbf{L}_2,\mathbf{L}_2} &= \tfrac{1}{6}\left(\hat{a}_{\mathbf{s}_5,\mathbf{s}_5} + \hat{a}_{\mathbf{s}_6,\mathbf{s}_6} + \hat{a}_{\mathbf{s}_7,\mathbf{s}_7} + \hat{a}_{\mathbf{s}_8,\mathbf{s}_8} + \hat{a}_{\mathbf{s}_9,\mathbf{s}_9} + \hat{a}_{\mathbf{s}_{10},\mathbf{s}_{10}}\right), \\
a_{\mathbf{L}_2,\mathbf{L}_3} &= \tfrac{1}{6}\left(\hat{a}_{\mathbf{s}_5,\mathbf{s}_{11}} + \hat{a}_{\mathbf{s}_5,\mathbf{s}_{12}} + \hat{a}_{\mathbf{s}_6,\mathbf{s}_{11}} + \hat{a}_{\mathbf{s}_6,\mathbf{s}_{13}} + \hat{a}_{\mathbf{s}_7,\mathbf{s}_{11}} + \hat{a}_{\mathbf{s}_7,\mathbf{s}_{14}} \right. \\
&\quad \left. + \hat{a}_{\mathbf{s}_8,\mathbf{s}_{12}} + \hat{a}_{\mathbf{s}_8,\mathbf{s}_{13}} + \hat{a}_{\mathbf{s}_9,\mathbf{s}_{12}} + \hat{a}_{\mathbf{s}_9,\mathbf{s}_{14}} + \hat{a}_{\mathbf{s}_{10},\mathbf{s}_{13}} + \hat{a}_{\mathbf{s}_{10},\mathbf{s}_{14}}\right), \\
a_{\mathbf{L}_3,\mathbf{L}_2} &= \tfrac{1}{4}\left(\hat{a}_{\mathbf{s}_{11},\mathbf{s}_5} + \hat{a}_{\mathbf{s}_{12},\mathbf{s}_5} + \hat{a}_{\mathbf{s}_{11},\mathbf{s}_6} + \hat{a}_{\mathbf{s}_{13},\mathbf{s}_6} + \hat{a}_{\mathbf{s}_{11},\mathbf{s}_7} + \hat{a}_{\mathbf{s}_{14},\mathbf{s}_7} \right. \\
&\quad \left. + \hat{a}_{\mathbf{s}_{12},\mathbf{s}_8} + \hat{a}_{\mathbf{s}_{13},\mathbf{s}_8} + \hat{a}_{\mathbf{s}_{12},\mathbf{s}_9} + \hat{a}_{\mathbf{s}_{14},\mathbf{s}_9} + \hat{a}_{\mathbf{s}_{13},\mathbf{s}_{10}} + \hat{a}_{\mathbf{s}_{14},\mathbf{s}_{10}}\right), \\
a_{\mathbf{L}_3,\mathbf{L}_3} &= \tfrac{1}{4}\left(\hat{a}_{\mathbf{s}_{11},\mathbf{s}_{11}} + \hat{a}_{\mathbf{s}_{12},\mathbf{s}_{12}} + \hat{a}_{\mathbf{s}_{13},\mathbf{s}_{13}} + \hat{a}_{\mathbf{s}_{14},\mathbf{s}_{14}}\right), \\
a_{\mathbf{L}_3,\mathbf{L}_4} &= \tfrac{1}{4}\left(\hat{a}_{\mathbf{s}_{11},\mathbf{s}_{15}} + \hat{a}_{\mathbf{s}_{12},\mathbf{s}_{15}} + \hat{a}_{\mathbf{s}_{13},\mathbf{s}_{15}} + \hat{a}_{\mathbf{s}_{14},\mathbf{s}_{15}}\right), \\
a_{\mathbf{L}_4,\mathbf{L}_3} &= \hat{a}_{\mathbf{s}_{15},\mathbf{s}_{11}} + \hat{a}_{\mathbf{s}_{15},\mathbf{s}_{12}} + \hat{a}_{\mathbf{s}_{15},\mathbf{s}_{13}} + \hat{a}_{\mathbf{s}_{15},\mathbf{s}_{14}}, \\
a_{\mathbf{L}_4,\mathbf{L}_4} &= \hat{a}_{\mathbf{s}_{15},\mathbf{s}_{15}}.
\end{aligned}
$$

Furthermore, the lumped steady-state probability vector, $\boldsymbol{\pi}_l$, can be determined with *Definition 4.4*, which is given as

$$
\begin{aligned}
\boldsymbol{\pi}_l &= \boldsymbol{\pi}_s \mathbf{V} \\
&= \begin{bmatrix} \pi_{\mathbf{L}_0} & \pi_{\mathbf{L}_1} & \pi_{\mathbf{L}_2} & \pi_{\mathbf{L}_3} & \pi_{\mathbf{L}_4} \end{bmatrix} \\
&= \begin{bmatrix} \hat{\pi}_{\mathbf{s}_0} & (\hat{\pi}_{\mathbf{s}_1}+\hat{\pi}_{\mathbf{s}_2}+\hat{\pi}_{\mathbf{s}_3}+\hat{\pi}_{\mathbf{s}_4}) & (\hat{\pi}_{\mathbf{s}_5}+\hat{\pi}_{\mathbf{s}_6}+\hat{\pi}_{\mathbf{s}_7}+\hat{\pi}_{\mathbf{s}_8}+\hat{\pi}_{\mathbf{s}_9}+\hat{\pi}_{\mathbf{s}_{10}}) & (\hat{\pi}_{\mathbf{s}_{11}}+\hat{\pi}_{\mathbf{s}_{12}}+\hat{\pi}_{\mathbf{s}_{13}}+\hat{\pi}_{\mathbf{s}_{14}}) & \hat{\pi}_{\mathbf{s}_{15}} \end{bmatrix}. \qquad (4.62)
\end{aligned}
$$

With *Theorem 4.1*, we can verify that

$$
\sum_{i=0}^{4} \pi_{\mathbf{L}_i} = \sum_{j=0}^{15} \pi_{\mathbf{s}_j} = 1, \qquad (4.63)
$$

which indicates that the lumped Markov chain remains similar state dynamics as the ordinary Markov chain.

By comparing the expanded Markov model to the lumped Markov model, as shown in the lower and upper parts of Figure 4.4, we observe that an expanded Markov channel

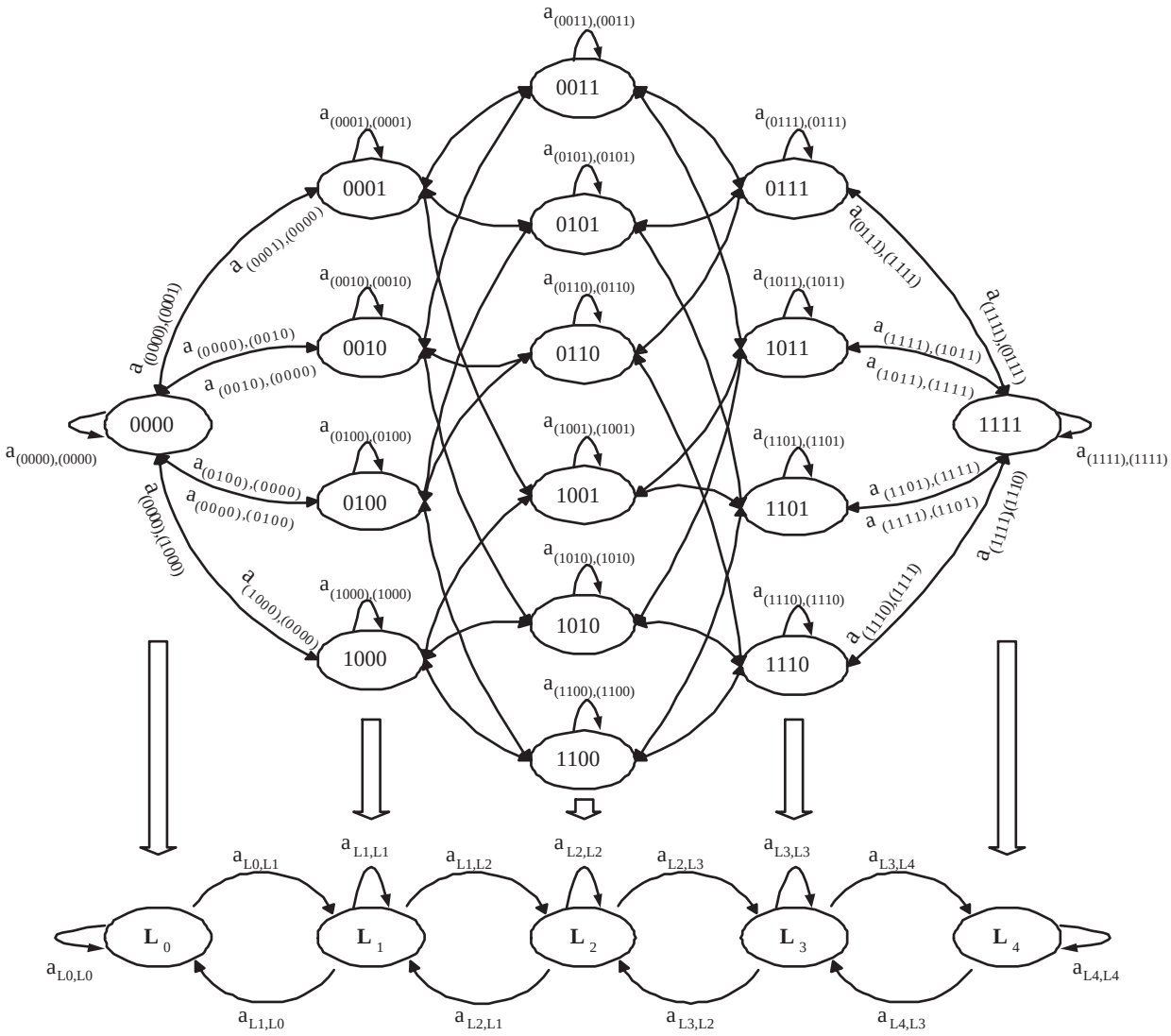

Figure 4.4. Illustration of 2^4-state Markov chain and its reduced model after lumping.

actually satisfies *slow fading* assumption (as explained in Section 4.3.2) while the lumped Markov channel satisfies *moderate fading* assumptions. The lumped Markov channel in Figure 4.4 illustrates that one or more sub-channels can vary simultaneously to one quantised level in either direction. For example, state $\mathbf{s}_1 = (0001)$, which belongs to partition $\mathbf{L}_1$, can transit to state $\mathbf{s}_{10} = (1100)$ of partition $\mathbf{L}_2$ with three sub-states vary simultaneously. Intuitively, we expect the lumped Markov model to describe the channel variation slightly more accurate than the expanded Markov model for any arbitrary fading channel that subjects to slow, moderate or fast fading.

4.5 Resource Allocation with Predicted Channel

To utilise the proposal of FSMC, the term $\gamma_{k,n}$ in (4.5) of problem (P1) and (4.17) of problem (P2) can be replaced by the predicted channel state. Throughout this chapter, the receiver is assumed to estimate the instantaneous channel conditions perfectly and then the received SNR is used to estimate the average SNR for the time-varying channel. The change in average SNR, $\bar{\gamma}$, will directly change (4.31)-(4.33). Hence, the receiver is required to compute a new set of state transition probability matrix and steady-state probability vector for each transmission cycle in order to perform channel prediction.

4.5.1 Full Feedback with States of Sub-bands

At an arbitrary receiver with N sub-carriers, there are N/b sub-bands and each sub-band has its $(M^b \times M^b)$ transition matrix, $\mathbf{A}_s^{(z)}$, and its $(M^b \times 1)$ steady-state probability vector, $\boldsymbol{\pi}_s^{(z)}$, for $z = 1, 2, \ldots, N/b$. Let $S_t = \mathbf{s}_i$ be the current state of channel condition where $\mathbf{s}_i = (s_{i1} s_{i2} \cdots s_{ib})$ and $S_{t+1} = \mathbf{s}_j$ be one of the potential states at the next time frame with a probability of

$$\begin{aligned} \Pr(S_{t+1} = \mathbf{s}_j) &= \Pr(S_{t+1} = \mathbf{s}_j | S_t = \mathbf{s}_i) \cdot \Pr(S_t = \mathbf{s}_i) \\ &= \hat{a}_{\mathbf{s}_i, \mathbf{s}_j} \hat{\pi}_{\mathbf{s}_i}. \end{aligned} \tag{4.64}$$

Policy 4.1. *At the next transmission time frame, there are multiple potential states to describe the channel condition. Among all possible states, the state* $\mathbf{s}_u$ *with the highest probability, such that* $\Pr(S_{t+1} = \mathbf{s}_u) > \Pr(S_{t+1} = \mathbf{s}_j)$*, for all* $j \neq u$*, is recognised as the predicted state.*

With the predicted channel condition observed at state $\mathbf{s}_u$, the receiver is able to retrieve each sub-channel condition, i.e. sub-state s_{uv}, of one sub-band in terms of a finite integer within the range of 0 to $M-1$. In other words, the receiver requires to feedback N finite integers, which is equivalent to $\lceil \log_2 (M) \rceil$ bits per sub-carrier, where $\lceil \cdot \rceil$ indicates the ceiling function. The SNR term $\gamma_{k,n}$ in (4.11) and (4.23) can now be replaced by a normalised predicted channel condition,

$$\hat{\gamma}_{k,n} = \frac{s_{uv}^{(k,z)} + 1}{M} \ , \tag{4.65}$$

where $z \in \{1, 2, \ldots, N/b\}$ is the index of the sub-band which accommodates sub-channel n, and $s_{uv}^{(k,z)} \in \{0, 1, \ldots, M-1\}$ is the predicted sub-state which corresponds to user k at sub-channel $n = \frac{N}{b}(z-1) + v$. Note that the term $+1$ is introduced in (4.65) mainly for avoiding $\hat{\gamma}_{k,n} = 0$; in other words, we want to ensure that $\hat{\gamma}_{k,n} \in [1/M, 1]$. Besides replacing $\gamma_{k,n}$ to $\hat{\gamma}_{k,n}$, the sub-channel and power allocation schemes in (4.11) and (4.23), respectively, remain unchanged.

4.5.2 Limited Feedback with Lumpable States

For the same receiver model, the M^b-state Markov channel can be reduced to a $[(M-1)b+1]$-state Markov channel, and hence it reduces the size of the feedback information. Let $S_t = \mathbf{s}_i$ and $\tilde{S}_t = \mathbf{L}_q$ be the current state and current partition of channel condition, respectively, where $\mathbf{s}_i$ is one of the aggregated states belonging to partition $\mathbf{L}_q$. At the next transmission time frame, the channel state is predicted to be $S_{t+1} = \mathbf{s}_j$, where $\mathbf{s}_j \subset \mathbf{L}_r$, with a probability of

$$\begin{aligned} \Pr(S_{t+1} = \mathbf{s}_j) &= \Pr(\tilde{S}_{t+1} = \mathbf{L}_r) \\ &= \Pr(\tilde{S}_{t+1} = \mathbf{L}_r | \tilde{S}_t = \mathbf{L}_q) \cdot \Pr(\tilde{S}_t = \mathbf{L}_q) \\ &= a_{\mathbf{L}_q, \mathbf{L}_r} \pi_{\mathbf{L}_q}. \end{aligned} \tag{4.66}$$

Since the reduced model of the $[(M-1)b+1]$-state Markov channel is a typical birth-death process, there are no more than three situations at the next transmission time frame. The three cases are: (i) transit to a set of lumpable states of higher order, (ii) transit to a set of lumpable states of lower order, and (iii) remain in the same set of lumpable states. A specific selection policy is applied to obtain the predicted partition, $\mathbf{L}_u$.

Policy 4.2. *Among all possible situations, there exists a partition* $\mathbf{L}_u$ *such that the probability of* $\Pr(\tilde{S}_{t+1} = \mathbf{L}_u) > \Pr(\tilde{S}_{t+1} = \mathbf{L}_r)$*, for all* $r \neq u$*, in order for the partition* $\mathbf{L}_u$ *to be recognised as the predicted partition.*

With the predicted partition $\mathbf{L}_u$ that might consist of more than one atomic state, the receiver is not able to retrieve each sub-channel condition of one sub-band. However, the receiver can quantise the sub-band condition in terms of a finite integer within the range of 0 to $(M-1)b$, where 0 indicates that all sub-channels within the sub-band are experiencing

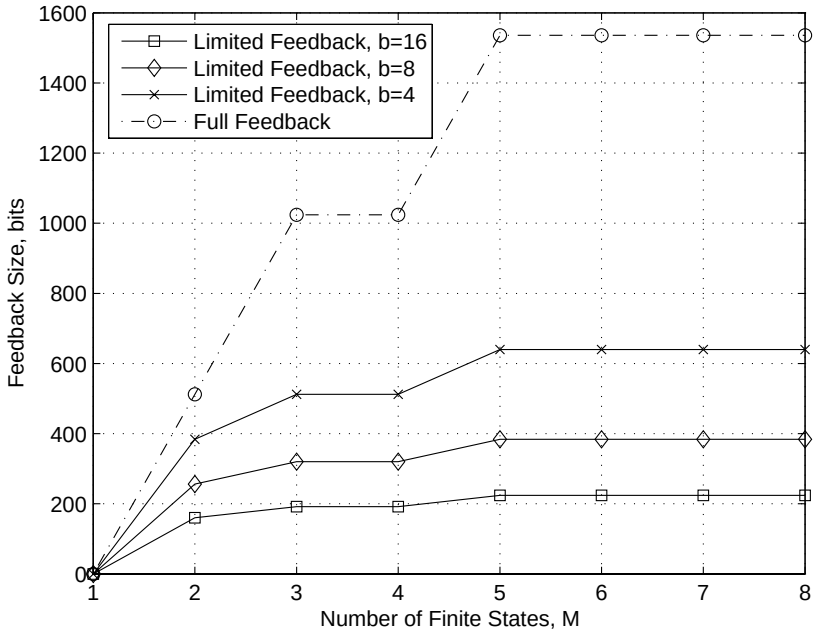

Figure 4.5. Number of feedback bits required for an OFDMA system with 512 sub-carriers.

worst fading and $(M-1)b$ indicates otherwise. In other words, the receiver can feed back less information with N/b finite integers, equivalent to $\left\lceil \log_2 \left[(M-1)b+1 \right] \right\rceil$ bits per sub-band. Figure 4.5 shows the comparison of feedback bits required for an OFDMA system of 512 sub-carriers with full feedback (*Policy 4.1*) and limited feedback (*Policy 4.2*). It is verified in Figure 4.5 that the full feedback scheme required much higher feedback overheads than the limited feedback scheme as the sub-band size, b, increases.

For the case of limited feedback with lumpable states, all sub-channel conditions $\gamma_{k,1}, \gamma_{k,2}, \ldots, \gamma_{k,N}$ are grouped into N/b sub-bands. The normalised sub-band condition of user k at sub-band z is represented by the index of its predicted state, $\mathbf{L}_u^{(k,z)}$, which is expressed as

$$\hat{\gamma}_{k,z} = \frac{u^{(k,z)}+1}{(M-1)b+1} \ , \tag{4.67}$$

where $u^{(k,z)} \in \{0, 1, \ldots, (M-1)b\}$ is the index of the predicted state. The definition of the sub-carrier assignment vector, $\boldsymbol{\beta}_k = \{\beta_{k,n}\}$, is redefined as the sub-band assignment vector, $\boldsymbol{\beta}_k = \{\beta_{k,z}\}$. Hence, the term $\beta_{k,z}$ shall be used in the sub-channel and power allocation schemes which are given in (4.11)-(4.16) and (4.23)-(4.28).

4.6 Simulation and Discussion

There are two main objectives of these simulations. Firstly, we obtain the performance of the channel prediction scheme for a range of frequency-selective fading channels and show, or otherwise, that the proposed limited feedback channel predictor is performing equally well in slow and in moderate fading environments. Then we investigate the performance of the sub-channel and power allocation scheme based on the predicted channel information.

4.6.1 Channel Model

The system is configured to have 512 sub-carriers and a received bandwidth of 5.12MHz, such that the sub-carrier spacing is determined as $\Delta f = 10$kHz. The carrier frequency is taken as $f_c = 2.4$GHz. Assume that the cyclic prefix is 11μs, the symbol period which ensures orthogonality among sub-channels is obtained as

$$T = \frac{1}{\Delta f} + 11 = 111\mu\text{s}. \tag{4.68}$$

The frequency-selective fading channel is generated using a four-ray Rayleigh fading channel model [78] with the impulse response of the model given as

$$h(t) = \sum_{l=1}^{4} A_l \psi_l(t) \delta(t - \tau_l), \tag{4.69}$$

where A_l and τ_l are the amplitude and time delay of the l^{th} ray, respectively, and $\psi_l(t)$ is a Rayleigh distributed random variable. The classical Jakes model [47] shows that the time-domain correlation of $\psi_l(t)$, for all l, is defined as $J_0(2\pi f_d T)$, where $J_0(\cdot)$ is the zeroth order Bessel function and f_d is the maximum Doppler frequency. Throughout this section, the size of sub-band is fixed at $b = 4$.

4.6.2 Channel Prediction

By varying the vehicular speed of mobile users from 10km/h to 100km/h, we generated 10^5 sets of frequency-selective fading channels ranging from slow ($f_d T = 0.0025$) to moderate ($f_d T = 0.01$), and to fast ($f_d T = 0.025$) fading. For each set of the frequency-selective fading channels, we compare a set of predicted channel states to the quantised set of

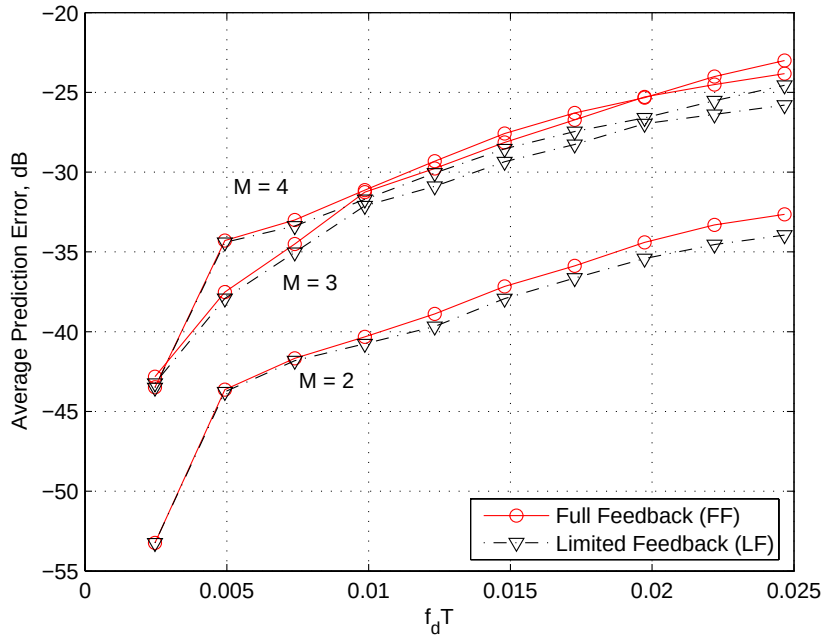

Figure 4.6. Prediction error of M^4-state Markov channels for channel variation in terms of f_dT.

generated channels for the next time frame. Average prediction error is defined as the ratio of the number of errors observed in comparison to the number of sample channels. The average prediction errors of M^b-state Markov channels for $M = 2, 3, 4$ are illustrated in Figure 4.6. As explained in Sections 4.3.2 and 4.4.2, the system with full feedback works well in a slow fading environment but the one with limited feedback works well in slow and moderate fading environments. Therefore, as f_dT increases from 0.0025 to 0.01, both schemes work similarly well but as f_dT increases from 0.01 to 0.025, limited feedback experiences up to 3 dB less error than full feedback. Since FSMC is an equivalent quantisation of the real channel, it is understandable that the larger the size of M, the more accurate the real channel is represented by M-state Markov channel. On the contrary, the smaller the size of M, the lesser the room for error. Hence, it explains the phenomena of higher M experiencing slightly higher prediction error in Figure 4.6.

The prediction policies are then put into an experiment to investigate the performance of channel prediction in several symbol durations ahead. We consider a simple multi-step predictor. Based on the information of the current channel state condition, we can obtain the outcome of one-step prediction as explained in Section 4.5. If we treat this outcome as the virtual channel state condition for the next time frame, we can predict the

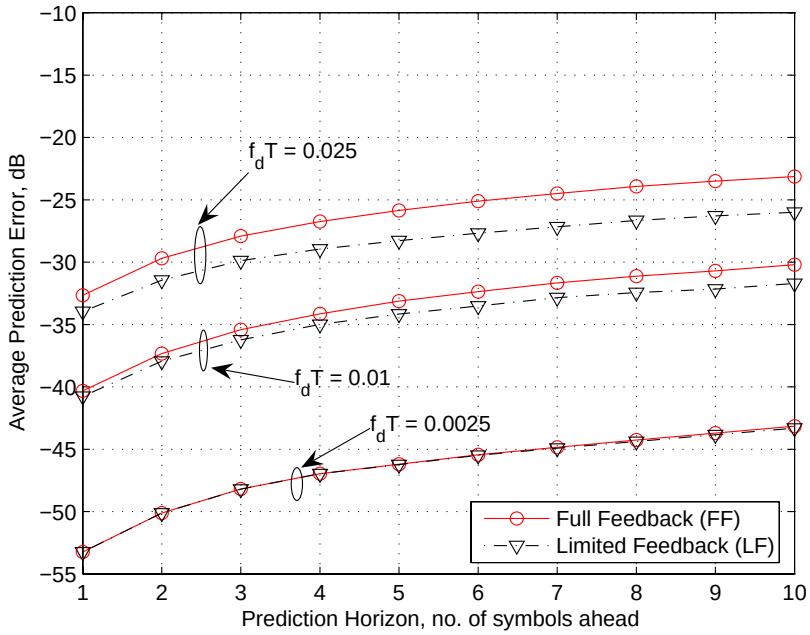

Figure 4.7. Prediction error of 2^4-state Markov channel for prediction horizon of 1 to 10 symbols ahead.

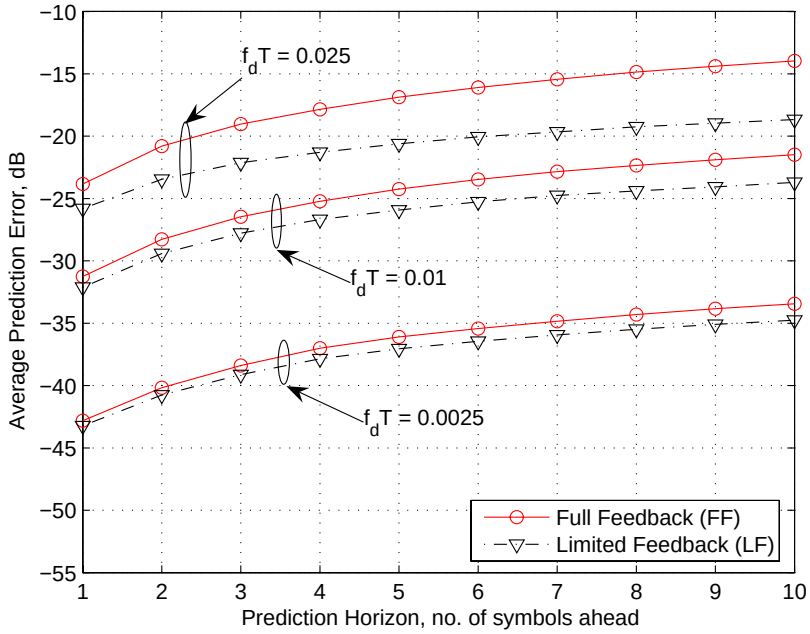

Figure 4.8. Prediction error of 3^4-state Markov channel for prediction horizon of 1 to 10 symbols ahead.

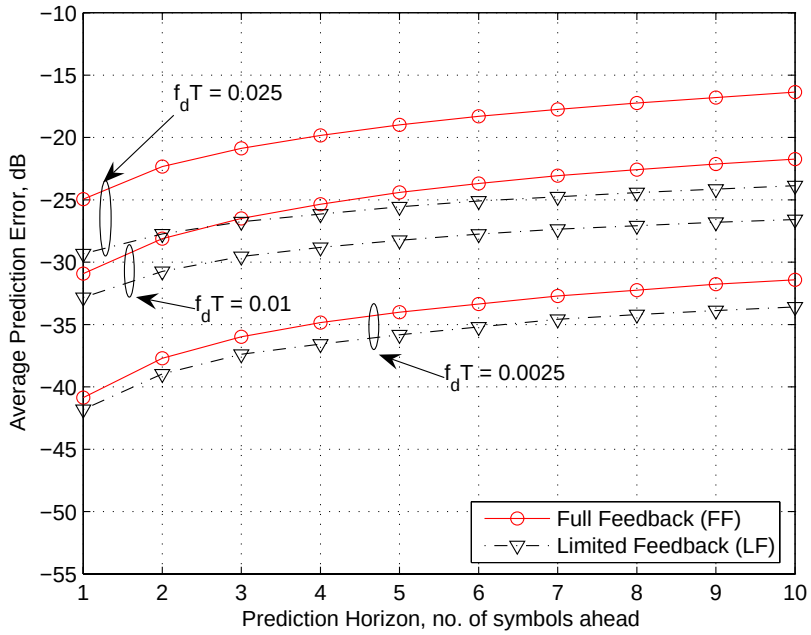

Figure 4.9. Prediction error of 4^4-state Markov channel for prediction horizon of 1 to 10 symbols ahead.

channel state at the two-step horizon. Similarly up to 10-step horizon of prediction can be derived with this prediction scheme. Figures 4.7, 4.8 and 4.9 show the prediction error of 2^b-state, 3^b-state and 4^b-state Markov channels, respectively, for a prediction depth of 1 to 10 symbol durations ahead for slow ($f_dT = 0.0025$), moderate ($f_dT = 0.01$) and fast ($f_dT = 0.025$) fading channels. We observe that the prediction error for full feedback and limited feedback schemes are seemingly very close for a slow fading channel, but the gap in prediction error progressively increases as the channel becomes a moderate and fast fading channel. Similarly, the gaps in average prediction error between the limited and full feedback schemes for all three channel models increase gradually as the depth of prediction increases. For comparison purposes, a prediction is taken as if its prediction error is less than -30 dB. For the system with 128 parallel 2^4-state Markov channels as shown in Figure 4.7, the system achieves 10-step reliable prediction for slow and moderate fading but can only attains three-step reliable prediction for fast fading. As M increases to 3 and 4, as shown in Figures 4.8 and 4.9, the system achieves 10-step reliable prediction only for slow fading; its performance degrades for moderate and fast fading. The results indicate that both feedback schemes perform well in a slow fading environment but the limited feedback scheme outperforms the full feedback scheme in moderate and fast fading

environments. This verifies our remark made in Section 4.4.3 that the expanded Markov model works well in a slow fading environment and the lumpable Markov model works well in slow and moderate fading environments.

4.6.3 Sub-channel and Power Allocation

With the same channel model as described in Section 4.6.1, the system now accommodates 4 users. Given that the system is constrained by a total power budget, each user is allocated a number of sub-channels such that each sub-channel can only be allocated for one user at any time instant. The achievable capacity is computed for slow ($f_dT = 0.0025$), moderate ($f_dT = 0.01$) and fast ($f_dT = 0.025$) fading channels with different feedback types:

1. *Optimum* - Assume perfect feedback (exact channel condition), where feedback size could be infinitely large, an optimum achievable capacity is computed based on (4.16) and (4.28).

2. *Full feedback* - Assume full feedback (quantised channel condition) with predicted states of sub-bands, where each sub-channel state is retrieved to compute an achievable capacity.

3. *Limited feedback* - Assume limited feedback (quantised channel condition) with predicted partitions (lumpable states), where each sub-band state is retrieved to compute an achievable capacity.

4. *Convention* - Assume no feedback and each user is pre-assigned to use a regular set of sub-carriers, an achievable capacity is computed based on average power.

By varying the transmitted SNR, the ratio of the achievable capacities with limited feedback, full feedback and conventional schemes with respect to the optimum achievable capacity of M^b-state Markov channels for $M = 2, 3, 4$ are illustrated in Figures 4.10, 4.11 and 4.12, respectively. These figures show that the conventional schemes often act as the lower benchmark for slow, moderate and fast fading channels. Since a slow fading channel experiences less average prediction error, followed by moderate and fast fading channels, it is expected that the system is capable of achieving higher capacity for slow

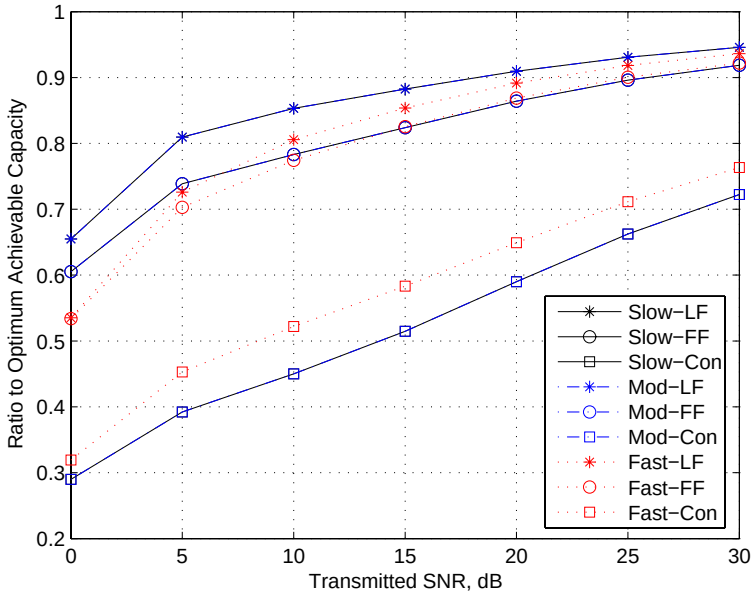

Figure 4.10. Ratio of achievable capacities with limited feedback (LF), full feedback (FF) and conventional (Con) schemes with respect to optimum capacity, for slow, moderate and fast fading of 2^4-state Markov channels.

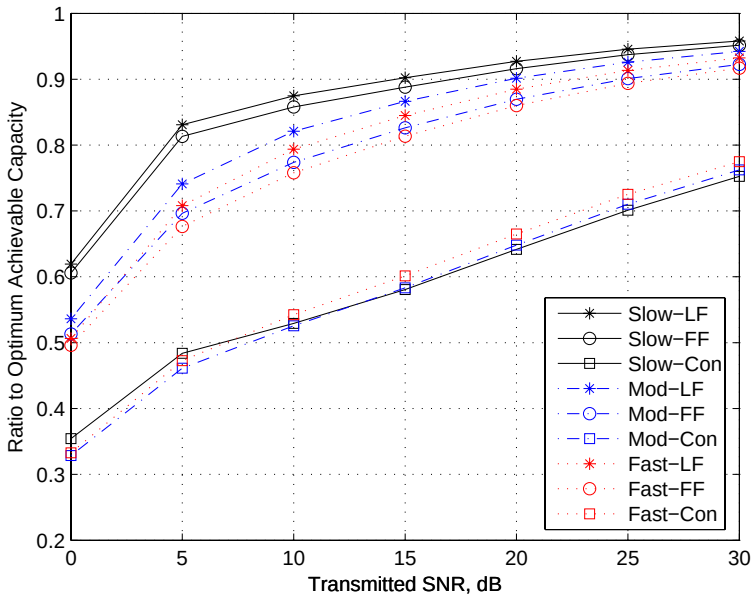

Figure 4.11. Ratio of achievable capacities with limited feedback (LF), full feedback (FF) and conventional (Con) schemes with respect to optimum capacity, for slow, moderate and fast fading of 3^4-state Markov channels.

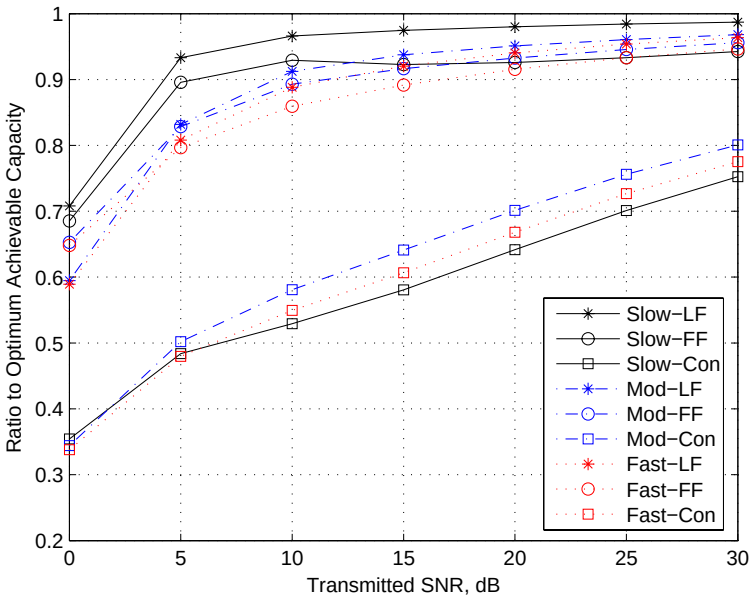

Figure 4.12. Ratio of achievable capacities with limited feedback (LF), full feedback (FF) and conventional (Con) schemes with respect to optimum capacity, for slow, moderate and fast fading of 4^4-state Markov channels.

Table 4.3. Ratio of achievable capacities with limited and full feedback schemes with respect to optimum capacity for M^4-state Markov channels

	Limited feedback scheme		*Full feedback scheme*	
M	*Ratio to optimum*	*Feedback size*	*Ratio to optimum*	*Feedback size*
2	94.6%	384 bits	91.9%	512 bits
3	95.8%	512 bits	95.1%	1024 bits
4	97.1%	512 bits	95.6%	1024 bits

fading channels, followed by moderate and fast fading channels. These phenomena can be observed when comparing Figures 4.10, 4.11 and 4.12. The numerical comparison of the ratio of achievable capacities with limited and full feedback schemes with respect to optimum capacity for M=2,3,4 is tabulated in Table 4.3.

By intuition, limited feedback and full feedback schemes approach the optimum achievable capacity as M increases. Both feedback schemes achieve reasonably high capacity in slow fading environment. On closer look, the limited feedback scheme always

outperforms full feedback scheme in moderate and fast fading environments. These phenomena are within our expectation because we have shown that the average prediction error for a limited feedback scheme is always marginally better than full feedback. Hence, it is reasonable that a limited feedback scheme is slightly better to exploit the benefit of sub-channel (sub-band) and power allocation schemes than a full feedback scheme.

4.7 Conclusion

This chapter presented a sub-optimal sub-channel and an optimal power allocation schemes that incorporate channel prediction. The implementation of these schemes in an OFDMA system incurs two main issues, namely the size of feedback information and imperfect CSI due to feedback delay. Conventionally, CSI is constructed with detailed current channel conditions in the form of amplitude or SNR. In this chapter, the Rayleigh fading channel is modelled as a FSMC by partitioning the received SNR into several quantised levels. With the aid of sub-band formation and lumpability, the size of feedback information is reduced from $N \cdot \lceil \log_2(M) \rceil$ bits to $\frac{N}{b} \cdot \left\lceil \log_2[(M-1)b+1] \right\rceil$ bits, where N, M and b are the number of sub-carriers, number of states and size of sub-band, respectively. The reliability of the proposed channel prediction scheme with limited and full feedbacks are shown in the simulation results. The prediction of CSI is obtained multiple symbol durations in advance to mitigate the effect of imperfect CSI due to the feedback delay. By obtaining the sub-optimal outcomes of sub-channel (sub-band) and power allocations, we show that the integration of channel prediction with limited feedback in these adaptive schemes is able to achieve a near-optimum capacity.

This page is blank

Chapter 5

A Game Theoretic Framework for Resource Allocation

The resource allocation problem in an orthogonal frequency division multiple access (OFDMA) system is studied under the framework of cooperative and non-cooperative games. The investigation aims to find solutions to enhance the fairness of the achievable rates among all users. In a non-cooperative resource allocation game approach, each user competes for a set of sub-carriers that maximises its achievable rate such that the outcome of this game is a Nash equilibrium. In a cooperative resource allocation game approach, the key is for all users to participate in a bargaining model for the use of sub-carriers to achieve a Pareto optimal outcome. Simulation results show that the cooperative approach outperforms the non-cooperative approach under the same system with the same wireless resources for sharing.

5.1 Introduction

Minimising the total transmit power in a dynamic sub-carrier, bit and power allocation scheme for an OFDM system with the Lagrangian relaxation method is proposed in [105]. While it achieves good performance over fixed assignment strategies, the algorithm is computationally intensive and difficult to implement. This strategy also could not resolve the scenario where the best sub-carrier of one user may also be the best sub-carrier of another user. The best sub-carrier in this context is the one with the highest effective channel gain. To resolve this issue, an approach other than implementing user-prioritisation is through the notion of fairness among users.

Solving the resource allocation problem for multi-user wireless networks is an active research area [58,64,86,87,120]. Zhang and Letaief in [120] proposed a reduced-complexity algorithm that can decouple the multi-user resource allocation problem into single-user bit-and-power-allocation problems and achieve power and diversity gains. Opportunistic scheduling is another way to maximise system performance by exploiting the variations of channel conditions while satisfying certain constraints and requirements. Liu *et al.* in [64] presented a framework for opportunistic scheduling of user transmissions to exploit the multi-user diversity with two fairness requirements (temporal fairness and utilitarian fairness) and a minimum performance constraint. In recent years, some existing work [58,108] applied microeconomic theories to resource allocation taking into account notions of utility and pricing. On the one hand, Yaïche *et al.* in [108] proposed to decentralise a centralised problem so that a greedy distributed algorithm can yield an optimal and fair bandwidth allocation. On the other hand, Lee *et al.* in [58] applied the concept of utility and pricing to develop a simple algorithm and obtain a power allocation that is asymptotically optimal in the number of users. However, the main difficulty in solving a utility- and pricing-based resource allocation problem is that neither the Karush-Kuhn-Tucker (KKT) conditions nor the duality theorem provides sufficient conditions to obtain an optimal solution.

To enhance fairness criteria, game theory is an appropriate approach. A game theoretic framework for resource allocation problem has been considered in many studies [36–38, 71, 91, 108]. Due to the difficulty in implementing centralised algorithms for power allocation, most researchers emphasised distributed algorithms [36,38,91]. This approach belongs to the domain of the non-cooperative game. Each user is only interested

in achieving their own goals. Each user adjusts its power on the basis of local information where the base station does not keep track of the channel information of the entire system. A distributed algorithm is the key to obtaining a Nash equilibrium, which is often perceived to be inefficient from the point of view of the overall system throughput. Johari *et al.* in [48] considered a non-cooperative resource allocation problem that maximises each user's cost and utility functions under a total rate constraint and established the existence of Nash equilibria. The authors have shown that the Nash equilibria suffered some efficiency loss compared to the optimal aggregate surplus. Cao *et al.* in [8] also demonstrated that the non-cooperative game may lead to a solution that is not Pareto optimal and may not be fair to all users. A set of solutions is considered as Pareto optimal if there is no wasted utility such that no party can be better off without making any other worse off.

Inspired by the existing work in non-cooperative resource allocation, we model a non-cooperative resource allocation game, which focuses on individual rationality and individual optimal strategy, and investigate the efficiency loss of the Nash equilibria. In this chapter, we also propose to model the resource allocation problem using the cooperative game [72], which emphasises collective rationality and fairness. With this approach, we attempt to distribute Pareto optimal rates among users with two bargaining outcomes: Nash bargaining solution (NBS) and Raiffa-Kalai-Smorodinsky [7] bargaining solution (RBS). Closed-form expressions of Pareto optimal rates for the NBS and RBS are derived in this chapter. We propose a sub-carrier and power allocation scheme to achieve these rates based on the perfect feedback channel state information (CSI) at each OFDMA transmission cycle. Thus, the main contribution of this chapter is to highlight the performance difference between non-cooperative and cooperative resource allocation schemes and to quantify the efficiency losses in Pareto optimal rates for both schemes. A few recent works have been attentive to the idea of using the NBS in the context of the resource allocation problem [37, 108]. A generalised proportional fair scheme based on NBS and coalitions to allocate sub-carrier, rate and power for a multi-user OFDMA system has been proposed in [37]. The authors developed a multi-user bargaining algorithm based on optimal coalition pairs among users that can achieve comparable overall system rate as the maximal-rate scheme that maximises the total rate without considering fairness. However, the only disadvantage is the involvement of highly complex computations. In

contrast, we propose a reduced complexity algorithm to allocate sub-carrier, rate and power for a multi-user OFDMA system.

This chapter is organised as follows. We provide the system model of an OFDMA system in Section 5.2. The model is the same as that in Chapter 4 and is included here for completeness. We then present the basic concepts of non-cooperative and cooperative games followed by the formulation of the game-theoretic resource allocation problem in Sections 5.3 and 5.4. A simple algorithm to perform non-cooperative resource allocation is proposed in Section 5.3.1 and a reduced complexity algorithm to perform cooperative resource allocation is proposed in Section 5.4.4. Simulation results are then presented in Section 5.5 followed by a conclusion in Section 5.6.

5.2 System Model

Consider a single-cell OFDMA system of N sub-carriers with a frequency-selective fading channel. There are K users randomly located within this cell. Each user is assigned a subset of sub-carriers for use, and each sub-carrier is assigned exclusively to one user. The entire bandwidth B is shared among N sub-carriers and this allows all users to transmit simultaneously. Assuming that the sub-carrier separation is smaller than the coherent bandwidth, each sub-carrier can be considered as a flat fading sub-channel. Assuming unity average transmission power, a general downlink received signal for an arbitrary k^{th} user at its n^{th} sub-carrier is modelled as

$$y_{k,n} = x_{k,n} h_{k,n} + n_{k,n}, \tag{5.1}$$

where $x_{k,n}$ and $y_{k,n}$ are the transmitted and received signals, respectively, $n_{k,n}$ is the additive white Gaussian noise (AWGN) and $h_{k,n}$ is extracted from the channel vector $\mathbf{h}_k = [h_{k,1}, \ldots, h_{k,N}]$. The corresponding SNR for the k^{th} user's n^{th} sub-channel is expressed as $\gamma_{k,n} = |h_{k,n}|^2/\sigma_{k,n}^2$, where $\sigma_{k,n}^2$ is the noise variance of AWGN. As the overall bandwidth, B, is evenly allocated to each sub-channel, the noise variance of any arbitrary user k at all sub-channels are identical, i.e. $\sigma_{k,n}^2 = \sigma_k^2/N$. Assuming that user k occupies all sub-channels and unit power for each sub-channel, the Shannon's capacity for user k is defined as

$$C_k = \sum_{n=1}^{N} \frac{B}{N} \log_2 (1 + \gamma_{k,n}) . \tag{5.2}$$

One goal of this study is to optimise the spectral efficiency while *fairly* allocating transmission power and assign sub-carriers among all users. We define the optimisation variables as the instantaneous transmission power of user k, $\mathbf{P}_k = [P_{k,1}, \ldots, P_{k,N}]$, and the sub-carrier assignment vector of user k, $\boldsymbol{\beta}_k = [\beta_{k,1}, \ldots, \beta_{k,N}]$, where $P_{k,n} \geq 0$ and $\beta_{k,n}$ indicates the assignment of sub-carrier n to user k, such that

$$\beta_{k,n} = \begin{cases} 1, & \text{if sub-carrier } n \text{ is assigned to user } k, \\ 0, & \text{otherwise.} \end{cases} \tag{5.3}$$

There are two criteria that must be met. Firstly, the sum of all transmission power is bounded by a total power budget, i.e. $\sum_{k=1}^{K}\sum_{n=1}^{N} \beta_{k,n} P_{k,n} \leq P^{\max}$. Secondly, not more than one user is permitted to transmit in any n^{th} sub-carrier, i.e. $\sum_{k=1}^{K} \beta_{k,n} \leq 1$. Assuming that the sub-channel conditions, $\gamma_{k,n}$ for all k and n, are perfectly estimated, the transmission rate for user k is denoted as

$$R_k = \sum_{n=1}^{N} \frac{B}{N} \log_2 \left(1 + \beta_{k,n} P_{k,n} \gamma_{k,n}\right). \tag{5.4}$$

The non-cooperative game approach is one conservative approach that is used by many [36, 38, 71, 91] to optimise the users' rate individually where each user attempts to maximise his own degree of satisfaction and does not care about other users in the system. From the perspective of resource sharing, one important criterion is the notion of fairness. The common issue in a power and sub-carrier allocation problem is the usage of any sub-carrier that appears to be good for more than one user at any transmission cycle. Dealing with fairness while satisfying different requirements from users might be challenging. A well-known approach that provides a satisfactory outcome in resource allocation is to use the fairness criteria from cooperative game theory [37]. The bargaining problem in [37] depends on a transmission rate as a function of bit-error rate (BER) which is approximated by

$$R_k = \sum_{n=1}^{N} \frac{B}{N} \log_2 \left(1 + P_{k,n} \gamma_{k,n} \frac{1.5}{\ln\left(\frac{0.2}{\text{BER}}\right)}\right), \tag{5.5}$$

where BER is assumed fixed and identical for all users in all sub-carriers. In other words, the bargaining outcomes in [37] adopted a specific BER and M-ary quadrature amplitude modulation (MQAM) scheme. In this chapter, we propose to solve a more general resource allocation problem based on the Shannon's capacity. It is assumed that once the capacity is determined, a suitable pair of modulation scheme and channel code is to be found to achieve the capacity.

5.3 Non-cooperative Resource Allocation Game

In general, game theory is the study of interactive decision making. The object of study in non-cooperative game theory is the *game*, which is a formal model of an interactive situation that involves several *players*. A central assumption in game theory is that all players are rational and always chooses an action which gives the outcome he most prefers, given what he expects his opponents to do. This common knowledge of rationality is the key to achieving an equilibrium point. Non-cooperative game means this branch of game theory explicitly models the process of players making choices out of their own interest to achieve a Nash equilibrium. A Nash equilibrium, also called a strategic equilibrium, is a set of strategies (one for each player) such that no player can unilaterally improve his own utility by changing his strategy. Non-cooperative games can be divided into two categories: static and dynamic games. In a static game, players make decisions simultaneously without knowing the decisions of other players. This is known as the strategic form of a game. Players in a dynamic game are governed by a strict order of play such that each player takes turn to make their decisions with the knowledge of the decisions of all previous players. This type of game is often referred as the extensive form [98].

5.3.1 Non-cooperative Resource Allocation Algorithm

In the non-cooperative game-theoretic framework, we define the throughput optimisation of individual user as the game and all mobile users as the players. Each user competes with others for the wireless resources to maximise his performance. This approach leads the system to reach one or more Nash equilibria. Depending on the game rules, some or all of the Nash equilibria are not optimal. To pose the sub-carrier allocation problem as a non-cooperative game, we need to define a utility function that best describes the gain in throughput of one user as more sub-carriers are allocated to that user. Motivated by the concept of sigmoid utility in [107], our utility function is defined as

$$u_k = \frac{R_k}{\lceil N/K \rceil - \sum_{n=1}^{N} \beta_{k,n}}, \tag{5.6}$$

where R_k is given as (5.4), $\lceil N/K \rceil$ denotes the maximum number of sub-carriers that one user can occupy and $\lceil \cdot \rceil$ indicates the ceiling function. Figure 5.1 illustrates the

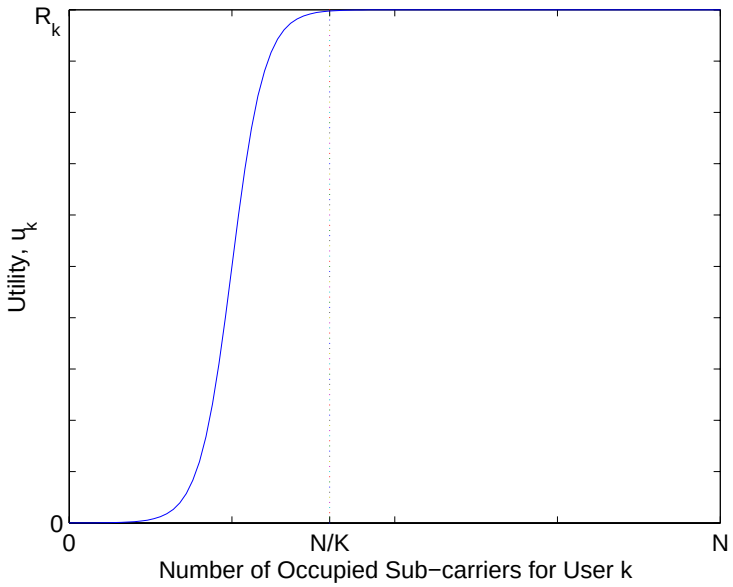

Figure 5.1. Sigmoid-like utility versus number of occupied sub-carriers for user k.

sigmoid utility function, u_k in (5.6) satisfying the following: $u_k^{\min} = 0$, $u_k^{\max} = R_k$ and u_k increases monotonically as $\sum_{n=1}^{N} \beta_{k,n} \leq \lfloor N/K \rfloor$, where $\lfloor \cdot \rfloor$ indicates the floor function. For one special case when the term $N/K \in \mathbb{Z}^+$, we observe that $u_k^{\max} \to \infty$; however, this phenomenon does not affect the property of u_k in (5.6) as u_k is still maximised when $\sum_{n=1}^{N} \beta_{k,n} = N/K$.

The idea of competing sub-carriers simultaneously by all users may not give us any rational outcome because some sub-carriers may be perceived to be good channel by multiple users at one time instant. To avoid this to happen, we model this game as a dynamic game. We set a game rule whereby the system will pre-specify the order of users to choose a set of sub-carriers from the available sub-carriers that maximises their own utilities. Note that each user is allowed to occupy a disjoint set of sub-carriers of the same size. Except in cases where the number of sub-carriers cannot be evenly divided, then the top few users in the pre-specified order may occupy one extra sub-carrier than others, where the maximum utility may approach infinity for these users. This game rule exhibits the property called the *first mover advantage* [98]. The first user who gets to choose his set of sub-carriers from all sub-carriers often has the benefit of maximising his utility. The sequential users can only choose among the remaining sub-carriers. In other

words, this problem can be formulated as (P1):

$$\begin{aligned} \max_{\beta_k} \quad & u_k(\boldsymbol{\beta}_k \mid \boldsymbol{\beta}_{-k}), \\ \text{subject to} \quad & \sum_{k=1}^{K} \beta_{k,n} \leq 1, \end{aligned} \tag{5.7}$$

where $\beta_{k,n} \in \{0,1\}$, for all k and n, and $\boldsymbol{\beta}_k \mid \boldsymbol{\beta}_{-k}$ indicates the set of sub-carriers chosen for user k depends on sub-carrier selection of other users with $\boldsymbol{\beta}_{-k}$ defines by $\boldsymbol{\beta}_{-k} = [\boldsymbol{\beta}_1, \ldots, \boldsymbol{\beta}_{k-1}, \boldsymbol{\beta}_{k+1}, \ldots, \boldsymbol{\beta}_K]^T$. To solve this problem, we propose the following algorithm:

Algorithm 5.1. *Given a pre-specified order of users to select sub-carriers, the outcome of the non-cooperative adaptive sub-carrier allocation scheme for one transmission cycle is given by $\boldsymbol{\beta}_k^* = \{\beta_{k,n}^*\}, \forall k, n$. Note that the notation 'user (1)' indicates the first user in the pre-specified order and 'user (K)' indicates the last user.*

1. *Initialise $\beta_{k,n}^* = 0, \forall k, n$. Sort all users according to the pre-specified order, such that user (1) gets to select sub-carriers first and user (K) selects last.*

2. *User (1) selects a set of $\lceil N/K \rceil$ sub-carriers to maximise (5.6), i.e. $\beta_{(1),n}^* = 1$ for the chosen sub-carrier n. Based on the knowledge of sub-carriers that occupied by previous users, the subsequent user (k) obtains $\boldsymbol{\beta}_{(k)}^*$.*

Remark 5.1. *This algorithm only requires K iterations to accomplish the task of allocating N sub-carriers to K users. To be specific, User (1) gets to select a set of $\lceil N/K \rceil$ sub-carriers from the pool of N available sub-carriers; the next user is left with a pool of $N - \lceil N/K \rceil$ available sub-carriers to choose from; and subsequently for the remaining users. A change in pre-specified order of users expects a different allocation outcome.*

We can randomly choose any pre-specified order which produces a unique Nash equilibrium with *Algorithm 5.1*, which is verified by the following definition.

Definition 5.1. *Given a pre-specified order of users to select sub-carriers, the non-cooperative resource allocation game in (P1) converges to a unique Nash equilibrium when $u_k(\boldsymbol{\beta}_k^* \mid \boldsymbol{\beta}_{-k}^*) \geq u_k(\boldsymbol{\beta}_k \mid \boldsymbol{\beta}_{-k}^*), \forall k$, such that no user can unilaterally improve his utility by selecting another set of sub-carriers.*

However, a Nash equilibrium may not necessarily be Pareto optimal. In a repeated game, we can repeat the non-cooperative game with all $K!$ combinations of pre-specified order, so that all users have the chance to be the *first mover*. Among the $K!$ Nash equilibria, we shall distinguish the best and the worst cases. However, the existence of one Nash equilibrium that is Pareto optimal is never guaranteed. Moreover, the computational complexity will rise substantially as the number of users, K, increases. Thus, we do not consider repeated game in this study.

Based on the outcome of the non-cooperative game in sub-carrier assignment, $\boldsymbol{\beta}_k^*, \forall k$, we modify the power allocation scheme described in earlier chapters, which is inspired by the water-filling technique to distribute the transmission power for each user. We compute the transmission power of any k^{th} user by considering the conditions of the l assigned sub-channels, where $l = \sum_{j=1}^{N} \beta_{k,j}^*$. The water-filling like transmission power of user k at sub-channel n can then be expressed as

$$P_{k,n}^* = \begin{cases} \dfrac{P_k^{\max} + \sum_{i=1}^{K} \sum_{j=1}^{N} \frac{\beta_{i,j}^*}{\gamma_{i,j}}}{\sum_{j=1}^{N} \beta_{k,j}^*} - \dfrac{1}{\beta_{k,n}^* \gamma_{k,n}}, & \text{for } \beta_{k,n}^* = 1; \\ 0, & \text{otherwise;} \end{cases} \tag{5.8}$$

where the pro rata power budget for each user is determined based on the number of assigned sub-carriers, $P_k^{\max} = \frac{P^{\max}}{N} \sum_{j=1}^{N} \beta_{k,j}^*$ while $P^{\max} = \sum_{k=1}^{K} P_k^{\max}$.

5.3.2 Price of Anarchy

The Nash equilibria of a non-cooperative game may not be optimal [48, 49]. This is because the nature of non-cooperative game often leads to selfish behaviour which affects the system efficiency. More attention has been attracted to quantify the loss in efficiency of Nash equilibria. The degree of efficiency loss is known as the *price of anarchy* (PoA). The general definition of PoA is taken as the ratio of an aggregate utility to the maximum possible aggregate utility. As the utility of the non-cooperative resource allocation game is a function of achievable rate, without loss of generality, we alter the model of the PoA to take the form of

$$\text{PoA} = \frac{\text{aggregate achievable rate}}{\text{maximum possible aggregate achievable rate}}, \tag{5.9}$$

where the maximum possible aggregate achievable rate is best represented by the aggregate of Pareto optimal rates. Such a definition suggests that a Pareto optimal point is

essential to quantify the efficiency loss of an outcome from the non-cooperative game. The discussion of obtaining Pareto optimal rates for the same resource allocation problem is presented in the next section.

5.4 Cooperative Resource Allocation Game

The object of study in the cooperative game theory is also the *game*, which is a formal model of an interactive situation that similarly involves several *players*. All players are assumed rational and each of them always chooses an action which gives the outcome he most prefers, given what he expects his opponents to do. A cooperative game is a high-level description, specifying what payoffs each potential group can obtain by the cooperation of its members. Nash bargaining model fits within the cooperative framework in that the solution does not define a specific timeline of offers and counteroffers, but rather focuses solely on the outcome of the bargaining process.

5.4.1 Nash Bargaining Solution (NBS)

In the bargaining framework, we define the throughput optimisation as the game and the corresponding players in our problem are the mobile users. Define $\mathcal{S}$ be a closed and convex subset of $\mathbb{R}^K$ to represent the feasible set of all possible bargaining outcomes. Let $R_k^{\min}$ be the minimal rate required by user k without any cooperation in order to participate in the game. Note that user k shall not participate in the game if this is not attainable, i.e. the achievable rate, $R_k < R_k^{\min}$. Let $\mathbf{R}^{\min} = [R_1^{\min}, \ldots, R_K^{\min}]$ such that $(\mathcal{S}, \mathbf{R}^{\min})$ is defined as the bargaining problem and $f(\mathcal{S}, \mathbf{R}^{\min})$ is the bargaining outcome of the game. There might be more than one Pareto optimal points, but NBS provides a unique and fair Pareto optimal operation point.

Let $\mathbf{r} = f(\mathcal{S}, \mathbf{R}^{\min})$ be an NBS that satisfies the following four axioms [72]:

A1 *Pareto Optimality*: For every $\mathbf{r}' \in \mathcal{S}$, if $\sum_{n=1}^{N} r'_{k,n} \geq \sum_{n=1}^{N} r_{k,n}$, $\forall k$, and $\sum_{n=1}^{N} r'_{m,n} > \sum_{n=1}^{N} r_{m,n}$, $\forall m \neq k$, then the outcome $f(\mathcal{S}, \mathbf{R}^{\min}) \neq \mathbf{r}$.

A2 *Independence of Linear Transformations*: Let $y(\cdot)$ be any positive affine transformation, $y(\mathbf{r}) = f\big(y(\mathcal{S}), y(\mathbf{R}^{\min})\big)$.

A3 *Symmetry*: For any user k and m where $R_k^{\min} = R_m^{\min}$, then $f_k(\mathcal{S}, \mathbf{R}^{\min}) = f_m(\mathcal{S}, \mathbf{R}^{\min})$.

A4 *Independence of Irrelevant Alternatives*: For any $\mathbf{r}' \in \mathcal{S}'$ where $\mathbf{r}' = f(\mathcal{S}', \mathbf{R}^{\min})$, if $\mathcal{S} \subseteq \mathcal{S}'$, then $f(\mathcal{S}, \mathbf{R}^{\min}) = \mathbf{r}'$.

In the Nash bargaining model, the utility function for user k is commonly defined as

$$u_k = R_k - R_k^{\min}. \tag{5.10}$$

To ensure fairness, the bargaining outcome $\mathbf{u}^*$ can be solved via an optimisation problem, which is defined as problem (P2):

$$\mathbf{u}^* = \arg\max_{\mathbf{R}} \prod_{k=1}^{K} u_k \tag{5.11}$$

$$\text{subject to} \quad \sum_{k=1}^{K} R_k \leq R^{\text{tot}}, \tag{5.12}$$
$$R_k \geq R_k^{\min},$$

where R^{tot} represents the total transmission rate achievable by the system. As R^{tot} is affected by the total power budget and the channel quality of all users, it can be approximated by

$$R^{\text{tot}} = \sum_{i=1}^{N} \frac{B}{N} \log_2(1 + P_i^* \tilde{\gamma}_i), \tag{5.13}$$

where $\tilde{\gamma}_i$ is one of the best N sub-channels among all the possible $K \times N$ sub-channels in the system, P_i^* is the water-filling transmission power defined as

$$P_i^* = \frac{P^{\max} + \sum_{j=1}^{N} \frac{1}{\tilde{\gamma}_j}}{N} - \frac{1}{\tilde{\gamma}_i}, \tag{5.14}$$

where $\sum_i P_i^* \leq P^{\max}$ and $P^{\max}$ is the total power budget.

If problem (P2) has a unique solution, applying logarithmic function onto the objective function of (P2) converts (P2) into a convex optimisation problem that also has a unique solution. Kelly in [52] showed that if the user utility functions are logarithmic, then the maximisation of the sum of these utility functions leads to an allocation which has been termed as proportionally fair. In order to adopt this approach, we need to firstly establish a proof that (5.11) is a log-concave function. Under the conditions of $\mathbf{R}$ as stated in (5.12), the first derivative of $\ln \mathbf{u}^*$, i.e. $\partial \ln \mathbf{u}^* / \partial R_k = \left(R_k - R_k^{\min}\right)^{-1}$,

indicates a monotonic decreasing function; whereas the second derivative of $\ln \mathbf{u}^*$, i.e. $\partial^2 \ln \mathbf{u}^* / \partial R_k^2 = -\left(R_k - R_k^{\min}\right)^{-2}$, indicates a strictly negative function. The first and second derivative tests sufficiently prove that (5.11) is indeed a log-concave function. Thus, the problem (P2) can now be rewritten as

$$\max_{\mathbf{R}} \quad \sum_{k=1}^{K} \ln\left(R_k - R_k^{\min}\right) \tag{5.15}$$

$$\text{subject to} \quad \sum_{k=1}^{K} R_k \leq R^{\text{tot}}, \tag{5.16}$$

$$R_k \geq R_k^{\min}.$$

Using Lagrangian and duality methods, we derive a set of NBS on the Pareto boundary.

Proposition 5.1. *To obtain feasible bargaining outcomes,* $R^{\text{tot}} \geq \sum_{k=1}^{K} R_k^{\min}$ *must be attained. Assuming that* $\sum_{k=1}^{K} R_k = R^{\text{tot}}$*, the NBS for user* k *is given as*

$$R_k^* = \frac{R^{\text{tot}} - \sum_{j=1}^{K} R_j^{\min}}{K} + R_k^{\min}. \tag{5.17}$$

Proof. To attain $R^{\text{tot}} \geq \sum_{k=1}^{K} R_k^{\min}$, $\sum_{k=1}^{K} R_k \geq \sum_{k=1}^{K} R_k^{\min}$ must also be attained. Intuitively, we can obtain $R_k^* \geq R_k^{\min}$. Therefore, the second constraint in (5.16) is redundant. The Lagrangian is then formulated as:

$$L(\mathbf{R}, \lambda) \;=\; \sum_{k=1}^{K} \ln\left(R_k - R_k^{\min}\right) + \lambda \left(R^{\text{tot}} - \sum_{k=1}^{K} R_k \right),$$

where λ is the Lagrangian multiplier. We take the derivative of $L(\mathbf{R}, \lambda)$ with respect to R_k and equate it to zero to obtain

$$\frac{1}{R_k - R_k^{\min}} - \lambda = 0 \;\Rightarrow\; R_k = \frac{1}{\lambda} + R_k^{\min}. \tag{5.18}$$

Since $\sum_{k=1}^{K} R_k = R^{\text{tot}}$, we can obtain λ explicitly in terms of R^{tot}

$$\lambda = \frac{K}{R^{\text{tot}} - \sum_{j=1}^{K} R_j^{\min}}. \tag{5.19}$$

Substituting (5.19) into (5.18), we obtain the closed-form solution of R_k^* as shown in (5.17). □

5.4.2 Raiffa-Kalai-Smorodinsky Bargaining Solution (RBS)

One main drawback of Nash's fairness criteria is that each user does not care about how much the others have given up but only takes into account of the individual's gain. *Axiom A4* in Section 5.4.1 asserts that the NBS should not be affected even if the feasible solutions belong to a subset of a larger domain. However, Raiffa [77], Kalai and Smorodinsky [51] inferred that a user's gain in rate should be proportional not only to his minimal rate but also to his maximal rate. In other words, RBS emphasises the importance of one's gain and others' losses. Since this does not consider in NBS, they proposed to modify *Axiom A4* into a new axiom:

A4' *Monotonicity*: For any $\mathbf{r}' \in \mathcal{S}'$ where $\mathbf{r}' = f(\mathcal{S}', \mathbf{R}^{\min})$, if $\mathcal{S} \subseteq \mathcal{S}'$ and $\sum_{n=1}^{N} r'_{k,n} \geq \sum_{n=1}^{N} r_{k,n}$, then $f_k(\mathcal{S}', \mathbf{R}^{\min}) \geq f_k(\mathcal{S}, \mathbf{R}^{\min})$.

A set of solutions was proposed in [7] that represents the concerns of each user for how much he gets as well as how much the others give up with a weighting factor, α, whose value indicates the tradeoff between those two concerns. By normalising the minimum and maximum transmission rates to zero and one, $\hat{\mathbf{R}}^{\min} = \mathbf{0}$ and $\hat{\mathbf{R}}^{\max} = \mathbf{1}$, the normalised utility function for user k is expressed as

$$\hat{u}_k(\alpha) = \hat{R}_k + \frac{\alpha}{K-1} \sum_{j \neq k} \left(1 - \hat{R}_j\right), \tag{5.20}$$

where $\hat{R}_k$ is the normalised transmission rate for user k. Hence, a set of bargaining solutions parameterised by α can be obtained from [44]

$$\hat{\mathbf{u}}^*(\alpha) = \arg\max_{\mathbf{R}} \prod_{k=1}^{K} \hat{u}_k(\alpha), \tag{5.21}$$

$$\text{subject to} \quad \sum_{k=1}^{K} \hat{R}_k \leq \hat{R}^{\text{tot}}, \tag{5.22}$$

$$0 \leq \hat{R}_k \leq 1,$$

where $-1 \leq \alpha \leq 1$ such that $\alpha = 0$ infers the Nash bargaining model, $\alpha = 1$ for the Raiffa-Kalai-Smorodinsky model and $\alpha = -1$ for the modified Thomson model [7]. Since both the NBS and RBS are Pareto optimal, the selection of α does not need to be constrained only to 0 or 1. It is shown in [44] that the selection of $\alpha \in [0, 1]$ can be arbitrary while the bargaining outcomes are feasible and remain as Pareto optimal.

As we are focusing on RBS, we only need $\alpha = 1$. Under the conditions of $\hat{\mathbf{R}}$ as stated in (5.22), the first and second derivatives of $\ln \hat{\mathbf{u}}^*$ can be obtained in such forms: $\partial \ln \hat{\mathbf{u}}^*/\partial R_k = g\big(\hat{R}_k\big) - \frac{1}{K-1}\sum_{j\neq k} g\big(\hat{R}_j\big)$ and $\partial^2 \ln \mathbf{u}^*/\partial R_k^2 = -\big[g\big(\hat{R}_k\big)\big]^2$, where $g\big(\hat{R}_k\big) = \Big[\hat{R}_k + \frac{1}{K-1}\sum_{j\neq k}\big(1-\hat{R}_j\big)\Big]^{-1}$. Since the first and second derivative tests indicate a monotonic decreasing function and a strictly negative function, respectively, it is suffice to imply that (5.21) is also a log-concave function. Thus, we define an optimisation problem (P3) to obtain the bargaining outcome of the Raiffa-Kalai-Smorodinsky model:

$$\max_{\hat{\mathbf{R}}} \quad \sum_{k=1}^{K} \ln\left[\hat{R}_k + \frac{1}{K-1}\sum_{j\neq k}\big(1-\hat{R}_j\big)\right] \tag{5.23}$$

$$\text{subject to} \quad \sum_{k=1}^{K} \hat{R}_k \leq \hat{R}^{\text{tot}}, \tag{5.24}$$

$$0 \leq \hat{R}_k \leq 1,$$

where $\hat{R}^{\text{tot}}$ represents the normalised total transmission rate achievable by the system and it can be expressed as a function of R^{tot}. Using Lagrangian method, we derive a set of normalised RBS.

Proposition 5.2. *To obtain feasible bargaining outcomes, $0 \leq \hat{R}^{\text{tot}} \leq K$ must be attained. Assuming that $\sum_{k=1}^{K} \hat{R}_k = \hat{R}^{\text{tot}}$, the normalised RBS for user k is given as*

$$\hat{R}_k^* = \frac{\hat{R}^{\text{tot}}}{K}\,. \tag{5.25}$$

Proof. To attain $0 \leq \hat{R}^{\text{tot}} \leq K$, $\sum_{k=1}^{K} \hat{R}_k \geq 0$ and $\sum_{k=1}^{K} \hat{R}_k \leq K$ must also be attained. Intuitively, we expect $0 \leq \sum_{k=1}^{K} \hat{R}_k^* \leq K$. Therefore, the second constraint in (5.24) is redundant. The Lagrangian is then formulated as:

$$L(\hat{\mathbf{R}}, \nu) \;=\; \sum_{k=1}^{K} \ln\left[\hat{R}_k + \frac{1}{K-1}\sum_{j\neq k}\big(1-\hat{R}_j\big)\right] + \nu\left(\hat{R}^{\text{tot}} - \sum_{k=1}^{K}\hat{R}_k\right),$$

where ν is the Lagrangian multiplier. We take the derivative of $L(\hat{\mathbf{R}}, \nu)$ with respect to $\hat{R}_k$ and equate it to zero to obtain

$$g\big(\hat{R}_k\big) - \frac{1}{K-1}\sum_{j\neq k} g\big(\hat{R}_j\big) - \nu = 0, \tag{5.26}$$

where $g\big(\hat{R}_k\big) = \Big[\hat{R}_k + \frac{1}{K-1}\sum_{j\neq k}\big(1-\hat{R}_j\big)\Big]^{-1}$. For the cases of $k = 1$ and $k = 2$, (5.26) are given by

$$g\big(\hat{R}_1\big) - \frac{1}{K-1}\Big[g\big(\hat{R}_2\big) + g\big(\hat{R}_3\big) + \ldots + g\big(\hat{R}_K\big)\Big] = \nu, \tag{5.27}$$

$$g\big(\hat{R}_2\big) - \frac{1}{K-1}\Big[g\big(\hat{R}_1\big) + g\big(\hat{R}_3\big) + \ldots + g\big(\hat{R}_K\big)\Big] = \nu, \tag{5.28}$$

respectively. Subtracting (5.27) from (5.28) produces $g\big(\hat{R}_1\big) = g\big(\hat{R}_2\big)$, which can also be expressed as

$$\hat{R}_1 + \frac{1}{K-1}\sum_{j\neq 1}\big(1-\hat{R}_j\big) = \hat{R}_2 + \frac{1}{K-1}\sum_{j\neq 2}\big(1-\hat{R}_j\big). \tag{5.29}$$

Rearranging (5.29) results in $\hat{R}_1 = \hat{R}_2$. By repeating the same process for all other k, we can show that $\hat{R}_i = \hat{R}_j, \forall i \neq j$. Since $\sum_{k=1}^{K}\hat{R}_k = \hat{R}^{\text{tot}}$, we obtain the expression of $\hat{R}_k^*$ as shown in (5.25). □

Assume that all users have equal bargaining power. With $\mathbf{R}^{\min}$ and $\mathbf{R}^{\max}$ correspond to the users' requirement for the minimum and maximum transmission rates, respectively, we define R_k as the non-normalised transmission rate for user k such that

$$\hat{R}_k = \frac{R_k - R_k^{\min}}{R_k^{\max} - R_k^{\min}}, \tag{5.30}$$

where $\sum_{k=1}^{K} R_k = R^{\text{tot}}$. Therefore, we can derive the Pareto optimal rate, $\mathbf{R}^*$ from the optimal solution of the normalised transmission rate, $\hat{\mathbf{R}}^*$.

Proposition 5.3. *To obtain feasible bargaining outcomes, $\sum_{k=1}^{K} R_k^{\min} \leq R^{\text{tot}} \leq \sum_{k=1}^{K} R_k^{\max}$ must be attained. Assume that $\sum_{k=1}^{K} R_k = R^{\text{tot}}$, the RBS for user k is given as*

$$R_k^* = \frac{\big(R^{\text{tot}} - \sum_{j=1}^{K} R_j^{\min}\big)\big(R_k^{\max} - R_k^{\min}\big)}{\sum_{i=1}^{K}\big(R_i^{\max} - R_i^{\min}\big)} + R_k^{\min}. \tag{5.31}$$

Proof. Substituting (5.30) into (5.25), we can obtain

$$R_k^* = \frac{\hat{R}^{\text{tot}}}{K}\big(R_k^{\max} - R_k^{\min}\big) + R_k^{\min}. \tag{5.32}$$

With $\sum_{k=1}^{K} R_k = R^{\text{tot}}$, we can rearrange (5.32) to express $\hat{R}^{\text{tot}}$ as a function of R^{tot} which is given as

$$\hat{R}^{\text{tot}} = \frac{K\big(R^{\text{tot}} - \sum_{j=1}^{K} R_k^{\min}\big)}{\sum_{i=1}^{K}\big(R_k^{\max} - R_k^{\min}\big)}. \tag{5.33}$$

Substituting (5.33) back into (5.32) produces the closed-form solution of R_k^* as shown in (5.31). □

5.4.3 Pareto Boundary for NBS and RBS

It is shown in [72] that NBS lies on the Pareto boundary for $R^{\text{tot}} \geq \sum_{k=1}^{K} R_k^{\min}$. Intuituively, RBS also lies on the Pareto boundary for $\sum_{k=1}^{K} R_k^{\min} < R^{\text{tot}} < \sum_{k=1}^{K} R_k^{\max}$. A two-user illustrative example is presented in Figure 5.2 with parameters given as $\mathbf{R}^{\min} = [0.15, 0.25]$, $\mathbf{R}^{\max} = [0.7, 0.9]$ and $R^{\text{tot}} = 1$. The two-user bargaining solutions determined by (5.17) and (5.31) for Nash and Raiffa-Kalai-Smorodinsky models are given as $[0.45, 0.55]$ and $[0.425, 0.575]$, respectively.

From the geometrical interpretation as described in [7], NBS always lies on the tangent to the curve of $(R_1 - R_1^{\min})(R_2 - R_2^{\min}) = \textit{constant}$, while RBS always lies on the intersection of the Pareto optimal boundary (solid line) and the diagonal line (dashed line) that formed between $\mathbf{R}^{\min} = \left[R_1^{\min}, R_2^{\min}\right]$ and $\mathbf{R}^{\max} = [R_1^{\max}, R_2^{\max}]$, where these two lines can be expressed as

$$R_2 = -R_1 + R^{\text{tot}}, \tag{5.34}$$

$$R_2 = \frac{R_2^{\max} - R_2^{\min}}{R_1^{\max} - R_1^{\min}} R_1 + \frac{R_1^{\max} R_2^{\min} - R_1^{\min} R_2^{\max}}{R_1^{\max} - R_1^{\min}}, \tag{5.35}$$

respectively. Figure 5.2 verifies that the solutions obtained by the geometrical interpretation agree with the numerical values computed by the closed-form solutions derived in Sections 5.4.1 and 5.4.2.

5.4.4 Cooperative Resource Allocation Algorithm

The definition of a Nash bargaining point is highly dependent on a minimum requirement that a user wants to achieve, otherwise the user will not enter the game. In the context of resource allocation, the minimum requirement can be viewed as the guaranteed minimum transmission rate achieved by the user. By adopting the concept of Raiffa-Kalai-Smorodinsky bargaining model, the solution is also depending on a maximum requirement, which is perceived as the maximum transmission rate of the user.

For an OFDMA downlink system with K users and N sub-carriers, we consider the minimum and maximum rate requirements for all users as time-varying, $\mathbf{R}^{\min}(t)$ and $\mathbf{R}^{\max}(t)$, respectively. The total transmission rate, $R^{\text{tot}}(t)$, is determined from the theoretical achievable rate based on the channel condition at time t. With NBS and RBS, we obtain a set of Pareto optimal transmission rates, $\mathbf{R}^{*}(t)$. In order for all users to

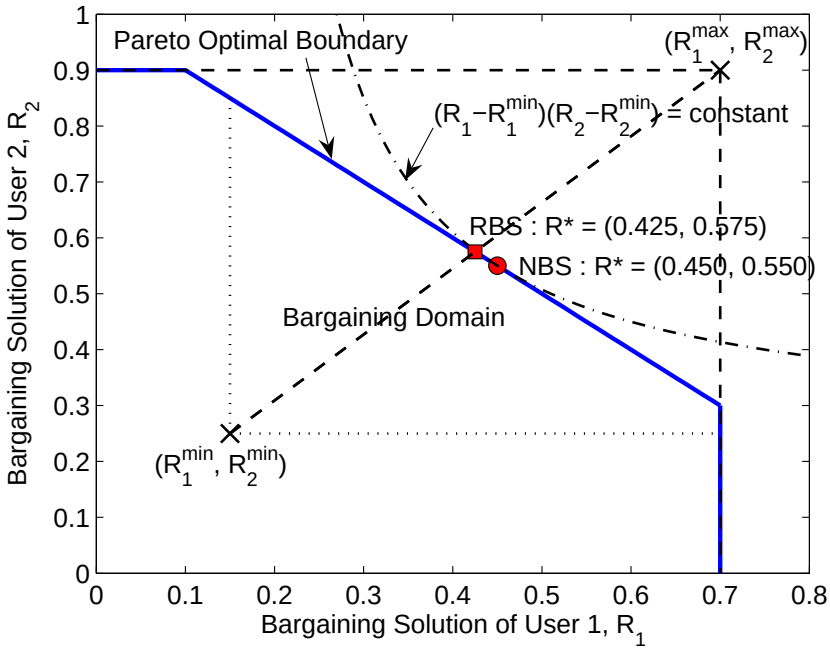

Figure 5.2. Illustrative example of bargaining solutions for two-user case.

achieve $\mathbf{R}^*(t)$, we apply sub-carrier and power allocations subject to the instantaneous channel conditions at time t. Without loss of generality, we can drop the term t since the allocations of sub-carrier and power are temporally independent.

The resource allocation problem is divided into two parts: sub-carrier allocation and power allocation. We model the sub-carrier allocation problem as problem (P4):

$$\begin{aligned} R_k^* \quad &\geq \quad \sum_{n=1}^{N} \frac{B}{N} \log_2 \left(1 + \beta_{k,n} P_{k,n} \gamma_{k,n}\right), \qquad (5.36) \\ \text{subject to} \quad &\sum_{k=1}^{K} \beta_{k,n} \leq 1, \end{aligned}$$

where the non-linear inequality function $R_k^* \in \mathbf{R}^*$ is the k^{th} user's assigned transmission rate, $\gamma_{k,n}$ is the SNR of user k at sub-carrier n, and $P_{k,n} = \bar{P} = P^{\max}/N$ is treated as a constant transmission power. Since $\beta_{k,n}$ only takes 0 or 1, problem (P4) is one form of integer-programming problem. Given that $R_k^*, \forall k$ can be computed from the closed-form expressions of the bargaining solutions, we can solve $\beta_{k,n}^*$ with a reduced complexity algorithm. The algorithm to achieve the transmission rate, R_k^*, is as follows:

Algorithm 5.2. *Consider a K-user OFDMA system with N sub-carriers. The outcome of this following algorithm is given by $\boldsymbol{\beta}_k^* = \{\beta_{k,n}\}, \forall k, n$. Note that the descending sort*

of $[\gamma_{k,1}, \ldots, \gamma_{k,N}]$ *is denoted as* $[\gamma_{k,(1)}, \ldots, \gamma_{k,(N)}]$ *where* $\gamma_{k,(1)}$ *is the largest and otherwise for* $\gamma_{k,(N)}$.

1. *Sort* $[\gamma_{k,1}, \ldots, \gamma_{k,N}]$ *in descending order, i.e.* $[\gamma_{k,(1)}, \ldots, \gamma_{k,(N)}]$ *for all* k *and initialise* $\beta^*_{k,n} = 0, \forall k, n$.

2. *In a round-robin fashion, user* k *takes turn to select one sub-carrier according to* $[\gamma_{k,(1)}, \ldots, \gamma_{k,(N)}]$. *If the selected sub-carrier is already occupied by another user, proceed to the next sub-carrier on the sorted list. An achievable rate,* R^{ach}_k *is computed for user* k. *If* $R^{\text{ach}}_k < R^*_k, \forall k$, *repeat step* ***2*** *for any user who has not met the desired rate; else if all sub-carriers are occupied, proceed to step* ***3***.

3. *Compute the efficiency ratio* $\eta_k = R^{\text{ach}}_k / R^*_k$ *and sort* η_k *in descending order such that* $\eta_{(k)} \geq \eta_{(k+1)}$.

3a. *If all* $\eta_{(k)}$ *is at least* 95% *or* $\eta_{(k)}$ *reaches convergence, exit program; else proceed to step* ***3b***.

3b. *Obtain the set of used sub-carriers for the user with the largest* $\eta_{(k)}$ *for* $k = 1$; *if only one sub-carrier is occupied, proceed to the next available* $\eta_{(k)}$ *for* $k = k+1$.

3c. *If* $k = K$, *repeat step* ***3a*** *by resetting* $k = 1$; *else obtain the best channel conditions among the same sub-carriers at user with the smallest* $\eta_{(K)}$ *and set* $\beta_{(K),(i)} = 1$ *while reset* $\beta_{(k),(i)} = 0$.

Remark 5.2. *This algorithm sparingly uses the concept of sorting to reduce its complexity. Initially, the instantaneous channel condition,* $\boldsymbol{\gamma}_k$, *is descending sorted among its sub-carriers. This algorithm consists of two iterative steps where step 2 assigns sub-carriers to users in order to achieve the target* R^*_k *while step 3 balances the efficiency ratio* $\eta_k, \forall k$. *At each iteration in step 2, the algorithm iteratively assigns the sub-carrier which exploits the best channel condition among the remaining available sub-carriers. The assigned sub-carrier is removed from the available set before the next iteration. This process is repeated until either all target* R^*_k *is achieved or the system runs out of sub-carriers. In the worst case scenario, step 2 requires to iterate* KN *times. The ratio of achievable rates to target rates for all users are computed in step 3 and sorted in descending order. As long as the user, say* x, *with the highest efficiency ratio occupies more than one sub-carrier, he will spare one sub-carrier to the user, say* y, *with the lowest efficiency ratio. This sub-carrier has to be the sub-carrier that user* y *exploits the best channel among all sub-carriers that*

occupied by user x. This process is repeated until efficiency ratio for all users either achieve at least 95% or establish a convergence. In the worst case scenario, step 3 has up to $\binom{K}{2}$ possible exchanges before convergence occurs. In any cases where majority users experience better channel quality, step 3 will not be required.

Based on the worst case scenario, the complexity of this algorithm is observed to be $O\big(KN + \frac{K(K-1)}{2}\big) \approx O(KN + K^2)$. For the case of $K \ll N$, we can approximate the complexity to be even lower. A similar problem was considered in [37] where the authors combined the sub-carrier allocation and fair bargaining problem as a single non-linear optimisation problem. However, no closed-form solution was deduced. They obtained the decision of sub-carrier assignment by comparing the optimality conditions of two users. The two-user case was extended to a multi-user case using coalitions and the Hungarian method in [37]. Their proposed algorithm has a complexity of $O(K^2 N \log_2 N + K^4)$ where K is the number of users and N is the number of sub-carriers. When $K = 10$ and $N = 256$, the complexity of the above-mentioned scheme is $K^2 N \log_2 N + K^4 = 2058000$ whereas the proposed scheme has the complexity of $KN + \frac{K}{2}(K-1) = 2605$. This huge improvement results from the simplicity of *Algorithm 5.2* due to the pre-determined Pareto-optimal rates, which are computed from (5.17) and (5.31) for NBS and RBS, respectively.

With the known outcome of adaptive sub-carrier allocation, $\boldsymbol{\beta}_k^*, \forall k$, we formulate the power allocation problem as problem (P5):

$$\begin{aligned} R_k^* \quad &\geq \quad \sum_{n=1}^{N} \frac{B}{N} \log_2 \big(1 + \beta_{k,n}^* P_{k,n} \gamma_{k,n}\big), \qquad (5.37) \\ \text{subject to} \quad & \sum_{k=1}^{K} \sum_{n=1}^{N} P_{k,n} \leq P^{\max}, \end{aligned}$$

where the non-linear inequality function $R_k^* \in \mathbf{R}^*$ is the k^{th} user's assigned transmission rate, $\gamma_{k,n}$ and $P_{k.n}$ are the SNR and transmission power of user k at sub-carrier n, respectively. Based on the assigned sub-channels, we use a similar power allocation scheme in (5.8) to distribute transmission power for each user. Therefore, we propose to compute the transmission power of any k^{th} user by considering the conditions of the l assigned sub-channels, where $l = \sum_{j=1}^{N} \beta_{k,j}^*$. The transmission power of user k at sub-channel n

can then be expressed as

$$P_{k,n} = \begin{cases} \dfrac{P_k^{\max} + \sum_{i=1}^{K}\sum_{j=1}^{N}\frac{\beta_{i,j}^*}{\gamma_{i,j}}}{\sum_{j=1}^{N}\beta_{k,j}^*} - \dfrac{1}{\beta_{k,n}^*\gamma_{k,n}}, & \text{for } \beta_{k,n}^* = 1; \\ 0, & \text{otherwise;} \end{cases} \tag{5.38}$$

where the pro rata power budget for each user is denoted as $P_k^{\max} = \frac{P^{\max}}{N}\sum_{j=1}^{N}\beta_{k,j}^*$. The algorithm to achieve the transmission rate, R_k^*, is as follows:

Algorithm 5.3. *Consider a K-user OFDMA system with N sub-carriers. The total power budget of this system is given as $P^{\max}$. The outcomes of this following algorithm are given by $\boldsymbol{\beta}_k^* = \{\beta_{k,n}^*\}$ and $\mathbf{P}_k^* = \{P_{k,n}^*\}, \forall k, n$.*

1. *Initialise $\beta_{k,n}^* = 0$ and $P_{k,n}^* = 0, \forall k, n$.*
2. *Run Algorithm 5.2 to perform sub-channel assignment, i.e. solve $\beta_{k,n}^*, \forall k, n$.*
3. *Compute transmission power for all users at the corresponding assigned sub-channels with (5.8).*

Remark 5.3. *This algorithm reuses Algorithm 5.2 to perform sub-carrier allocation. In addition, it also includes a water-filling-like power allocation scheme to distribute transmission power. The transmission power for each user at the assigned sub-channels is calculated with (5.8) based on the corresponding user's pro rata power budget. As there are N sub-channels for transmission, step 3 has at most N computations.*

The power allocation scheme has N computations, therefore the complexity of this algorithm is estimated to be $O\big(KN + \frac{K(K-1)}{2} + N\big) \approx O(KN + K^2)$. When $K = 10$ and $N = 256$, the proposed scheme has the complexity of $KN + \frac{K}{2}(K-1) + N = 2861$.

5.5 Simulation Results

We evaluate the performance of the cooperative and non-cooperative resource allocation games by three simulations. In the first simulation, we generate one sample channel model of the frequency-selective fading channel, which is based on the same model as described in Section 4.6.1, for a 10 users and 256 sub-carriers OFDMA system with an

average SNR of 10 dB. In Figures 5.3, 5.4 and 5.5, we illustrate the achievable bargaining outcomes of the cooperative games and the Nash equilibrium of the non-cooperative game, respectively, based on the corresponding feedback sub-channel condition, $\gamma_{k,n}, \forall k, n$, at the same time instant. Figure 5.3 illustrates the Nash bargaining model. It compares the outcomes of NBS, i.e. Pareto optimal rates which are computed by (5.17), to the achievable rates and the minimum rate requirements. It is observed that the achievable rates are a fraction lower than the Pareto optimal rates. In most practical situations, the Pareto optimal rates are not achievable due to the limited resources, i.e. sub-carrier and power. The only exception is when all sub-channel conditions are extremely good while all users have low minimum rate requirements. Similarly, Figure 5.4 illustrates the Raiffa-Kalai-Smorodinksy bargaining model where it compares the Pareto optimal rates of RBS, which are computed by (5.31), to the achievable rates and the minimum as well as maximum rate requirements. It is observed that some users may achieve Pareto optimal rates while others may only achieve a fraction lower than the Pareto optimal rates due to the introduction of maximum rate requirements. Figure 5.5 shows the comparison of achievable rates for five different schemes:

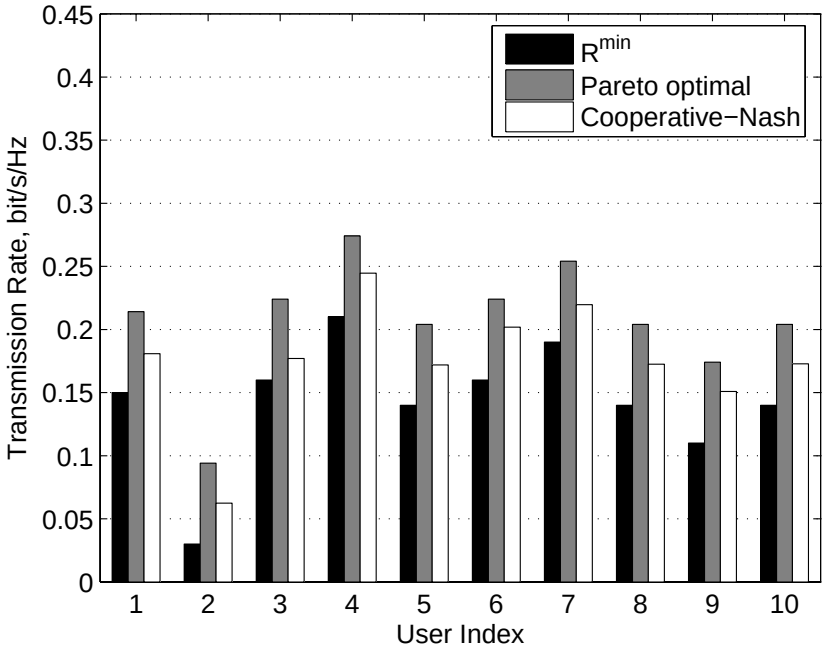

Figure 5.3. Achievable transmission rates of 10 users and 256 sub-carriers system based on Nash bargaining solutions.

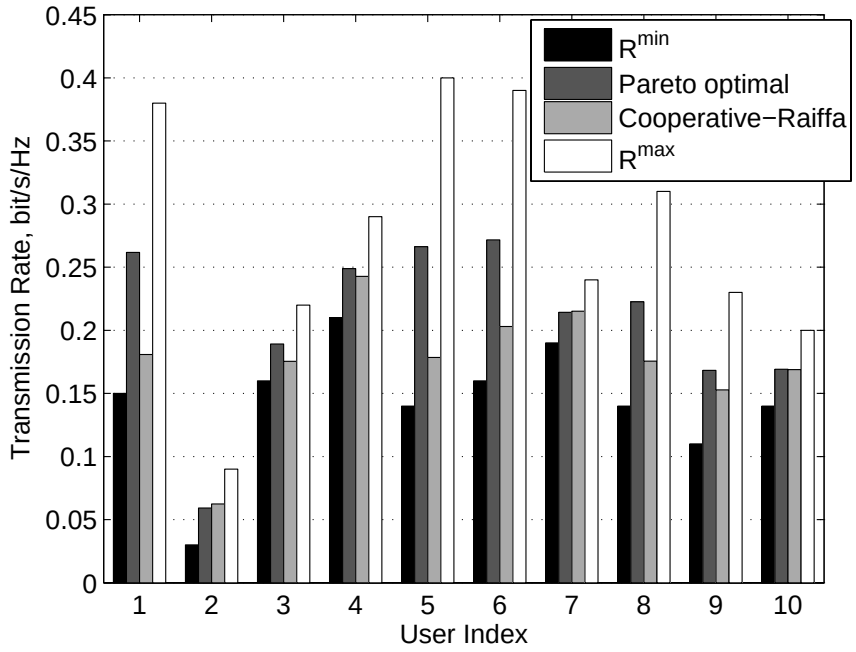

Figure 5.4. Achievable transmission rates of 10 users and 256 sub-carriers system based on Raiffa-Kalai-Smorodinsky bargaining solutions.

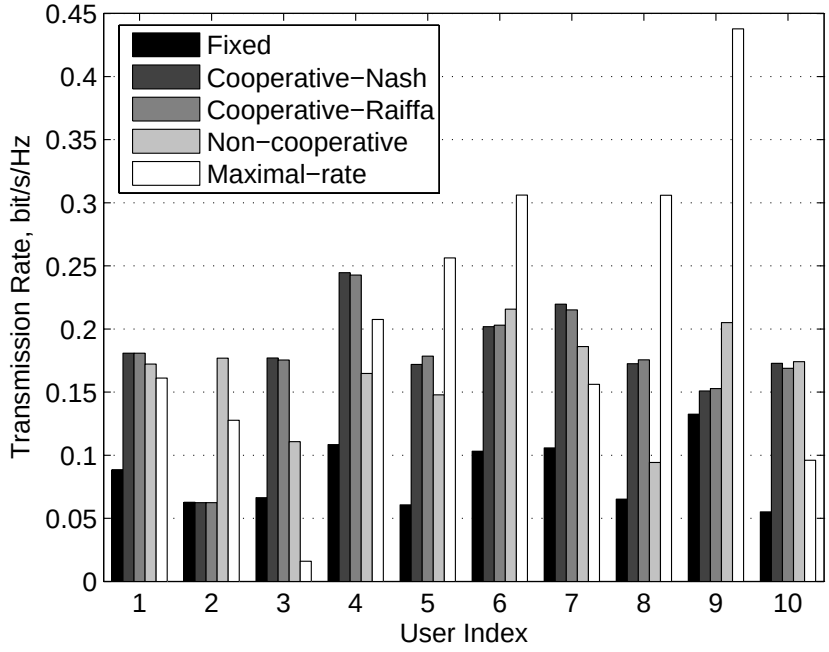

Figure 5.5. Comparison of achievable transmission rates by five different schemes, i.e. *Fixed*, *Cooperative-Nash*, *Cooperative-Raiffa*, *Non-cooperative* and *Maximal-rate*.

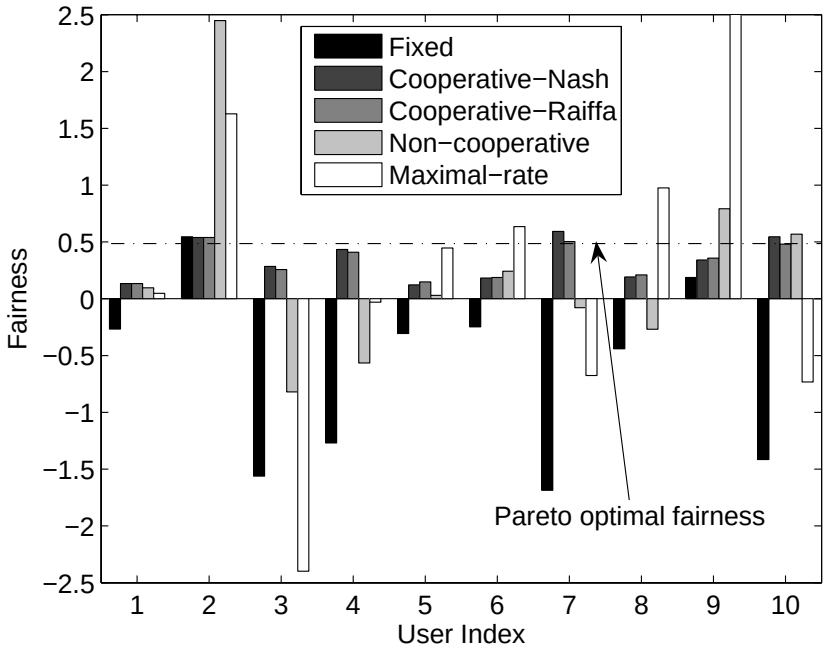

Figure 5.6. Fairness for five different schemes, i.e. *Fixed*, *Cooperative-Nash*, *Cooperative-Raiffa*, *Non-cooperative* and *Maximal-rate*.

1. *Fixed* - Each user occupies a fixed set of sub-carriers and transmits at an average power.

2. *Cooperative-Nash* - Based on the derived NBS in (5.17), each user relies on *Algorithm 5.3* to obtain a set of assigned sub-carriers and the corresponding transmission power.

3. *Cooperative-Raiffa* - Based on the derived RBS in (5.31), each user relies on *Algorithm 5.3* to obtain a set of assigned sub-carriers and the corresponding transmission power.

4. *Non-cooperative* - Based on a pre-specified order, each user takes turn to choose sub-carrier and eventually obtains the corresponding transmission power for the selected sub-carriers.

5. *Maximal-rate* - Overall system aggregate rate is maximised such that any sub-channel of better SNR is occupied and the corresponding transmission power is obtained.

In regard to fairness, it can be observed in Figure 5.5 that the maximal-rate scheme is unfairly allocating more resources to users with better channel quality and less resources to users with worse channel quality. Similarly, non-cooperative scheme also unfairly allocates resources based on a pre-specified order of users where each user is self-interested. On the contrary, both the cooperative schemes are allocating resources to all users in a fairer manner by considering all users' minimum and maximum requirements. These phenomena can be verified by the plot of fairness in Figure 5.6 with the quantification of fairness defined as

$$\mathcal{F}_k = \frac{R_k^{\text{achieve}} - R_k^{\min}}{R_k^{\max} - R_k^{\min}}, \tag{5.39}$$

where R_k^{achieve} is the achievable rate of user k under one of the five schemes. A positive $\mathcal{F}_k$ indicates that the achievable rate of user k meets his minimum rate requirement whereas a negative $\mathcal{F}_k$ indicates otherwise. A Pareto optimal fairness is defined as $\mathcal{F}^{\text{Pareto}} = \hat{R}^{\text{tot}}/K$, which is equivalent to the normalised RBS in (5.25) where $\hat{R}^{\text{tot}}$ is defined in (5.33). In the fairest scenario, $\mathcal{F}_k = \mathcal{F}^{\text{Pareto}}$, for $k \in \{1, \ldots, K\}$. Figure 5.6 shows that all achievable rates from both cooperative schemes are positive and yet half of them are attaining or approaching the Pareto optimal fairness. On the contrary, the other three schemes do not attain positive fairness for at least 1/3 of the users. From observation, this result also shows that the cooperative-Nash scheme can provide a slightly fairer outcome than the cooperative-Raiffa scheme if the gap between the maximum and minimum rate requirements is small; whereas the cooperative-Raiffa scheme outperforms the cooperative-Nash scheme if this gap is large.

We set up another simulation to investigate the overall system aggregate rate for a range of average SNR. We randomly generate 10^4 sets of frequency-selective fading channels for this simulation. The simulation result is shown in Figure 5.7. Since the main optimisation goal of the maximal-rate scheme is the system aggregate rate, we expect this scheme to act as an upper benchmark. By contrast, the fixed scheme that has no incentive of achieving any desired rate is observed to be the lower benchmark. The aggregate rates of both cooperative schemes overlap and lie between the aggregate rates of the maximal-rate scheme and the non-cooperative scheme. Due to the lack of cooperative decision in sharing resources, the cooperative schemes outperform the non-cooperative scheme. Figure 5.8 indicates the plot of price of anarchy, i.e. the quantified losses in efficiency, for the proposed schemes against the aggregate Pareto optimal rates. The cooperative

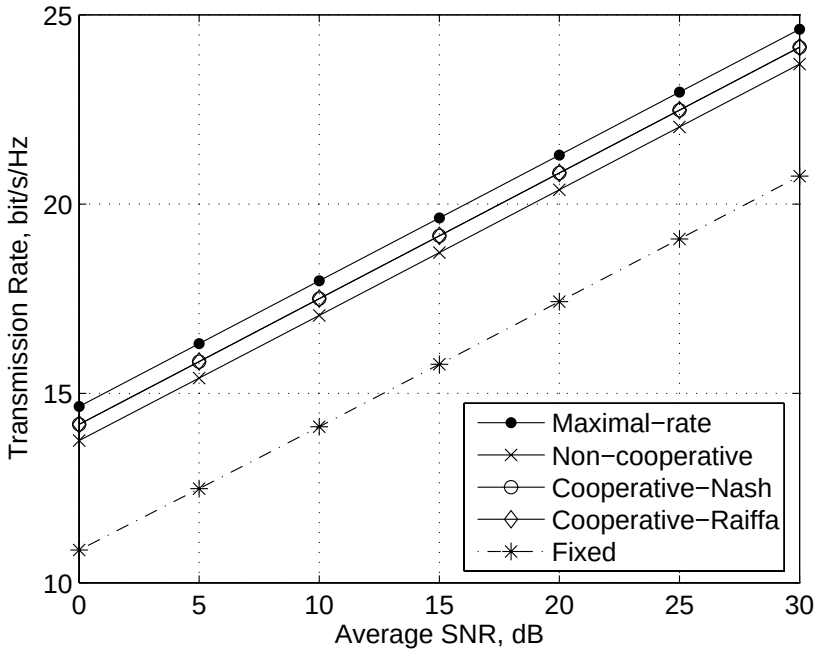

Figure 5.7. Average achievable transmission rates of 10 users and 256 sub-carriers system for an average SNR that ranges from 0dB to 30dB.

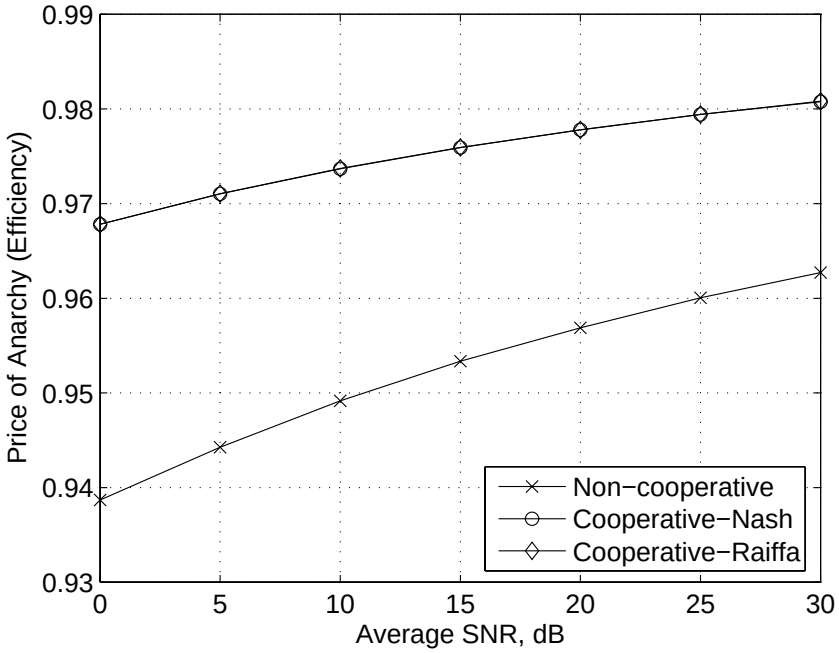

Figure 5.8. Price of anarchy of 10 users and 256 sub-carriers system for an average SNR that ranges from 0dB to 30dB.

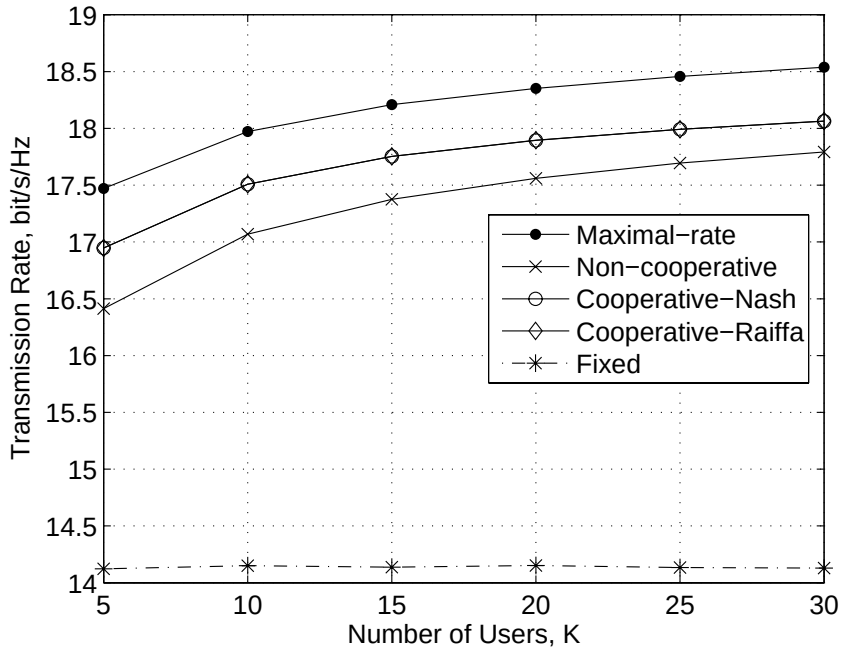

Figure 5.9. Average achievable transmission rates for system with K users and 256 sub-carriers where K ranges from 5 to 30, given an average SNR of 10dB.

schemes are experiencing $2\% \sim 3\%$ losses when compared with the $4\% \sim 6\%$ losses suffered by the non-cooperative scheme.

In the last simulation, we study the change in overall system aggregate rate for the proposed schemes by considering more users, given that the channel is experiencing an average SNR of 10 dB. The simulation result in Figure 5.9 is a plot of aggregate rates against the number of users in the system. The outcome of this simulation confirms that the cooperative schemes outperform the non-cooperative scheme. The plot of PoA in Figure 5.10 accentuates that the cooperative and the non-cooperative schemes are indeed experiencing $2\% \sim 3\%$ and $4\% \sim 6\%$ losses in the aggregate Pareto optimal rates, respectively.

5.6 Conclusion

In this chapter, we have addressed a downlink OFDMA resource allocation problem in the framework of cooperative and non-cooperative games. By non-cooperative game theory,

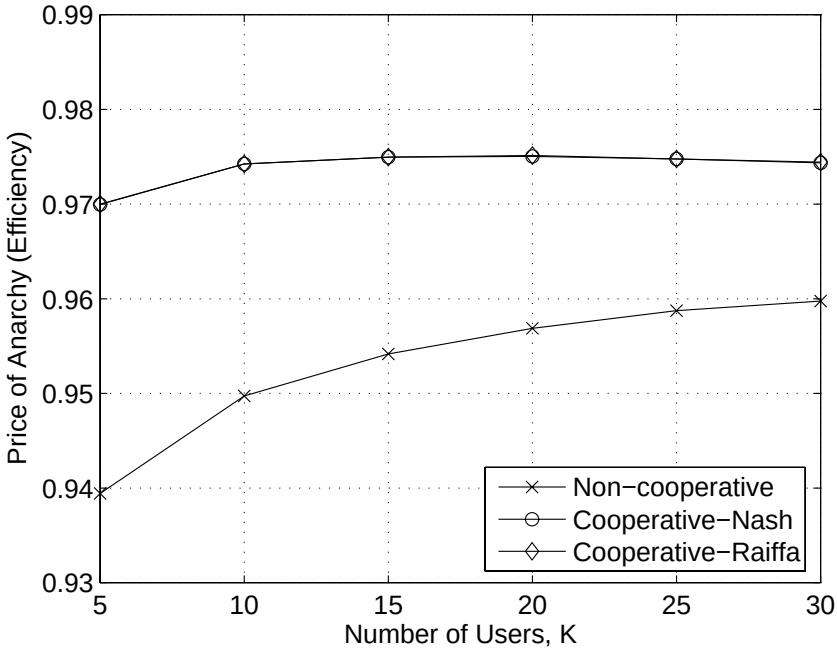

Figure 5.10. Price of anarchy for system with K users and 256 sub-carriers where K ranges from 5 to 30, given an average SNR of 10dB.

we have shown that it can achieve a unique Nash equilibrium for any pre-specified order of users in selecting a set of sub-carriers that maximises their own utilities in a self-interested manner. By cooperative game theory, we have derived a set of Pareto optimal rates via two branches, i.e. Nash bargaining and Raiffa-Kalai-Smorodinsky bargaining models. A reduced complexity algorithm is proposed to iteratively assign sub-carriers to users based on the outcome of the bargaining solutions. It has a complexity of $O(KN + K^2)$, which is much lower than the existing scheme of $O(K^2N \log_2 N + K^4)$, where K and N are the number of users and sub-carriers, respectively. A water-filling-like power allocation scheme is used to distribute transmission power among the assigned sub-carriers. Simulation results show that neither the proposed cooperative nor the proposed non-cooperative resource allocation scheme is capable of achieving the Pareto optimal rates. However, the cooperative schemes are more likely to achieve a fairer rate distribution among users than the self-interested non-cooperative scheme, the greedy maximal-rate scheme and the conventional fixed scheme. Furthermore, the proposed cooperative schemes suffered approximately $2\% \sim 3\%$ losses in aggregate Pareto optimal rates, which is half of the efficiency losses suffered by the non-cooperative scheme, i.e. $4\% \sim 6\%$. All in all, the significance of this work is to provide a comparison in fairness, achievable rates and

efficiency losses of the cooperative and non-cooperative resource allocation schemes under the same system with the same wireless resources for sharing.

Chapter 6

Conclusions and Future Research

6.1 Summary

This thesis presents a study of the performance of various resource allocation schemes in the context of an orthogonal frequency division multiple access (OFDMA) system. We have addressed several problems associated with the optimisation of the achievable spectral efficiency for a downlink OFDMA system with different resource allocation schemes. As described in Chapter 1, we have categorised our work into the divisions of resource allocation schemes with perfect feedback, limited feedback and fairness criteria among all users. We now summarise our key contributions:

In Chapter 3, we illustrated the optimisation process to obtain a sub-optimal closed-form water-filling solution to develop a multi-user power allocation algorithm in OFDMA systems. The objective is to achieve near-optimal capacity with minimal computation. Since all sub-carriers are allowed for sharing among all users, some may perceive this work to be idealistic but its results can provide us with a fair ground for comparison of computational complexity between existing water-filling algorithms and our proposed power allocation algorithms. Our results indeed show that the proposed sub-optimal and constant power allocation schemes can achieve near-optimal capacity with much lower computational complexities. The outcome of these schemes motivated us to develop a multi-user power allocation problem with uneven power budgets among users in order to meet different rate requirements.

Chapter 4 considered the power allocation problem with an extension to sub-carrier allocation. Sub-carriers are no longer available for sharing among users such that each sub-carrier cannot assign to more than one user in one transmission cycle. Using the concept of constrained optimisation with duality, we obtained the sub-optimal and optimal closed-form solutions to the sub-carrier and power allocation problems, respectively. From the observation of the resource allocation schemes in Chapters 3 and 4, it is clear that a perfect feedback of channel state information (CSI) is essential to ensure the effectiveness of these schemes. In a scenario where perfect feedback is not available, the impact of imperfect feedback can be quite severe as it degrades the performance of most, if not all, adaptive resource allocation schemes that strongly rely on accurate CSI. Chapter 4 presented a model channel prediction scheme based on a Markov model. We adopted the concept of a finite-state Markov channel to model the wireless fading channel of the multi-carrier OFDMA system. With the state transition probabilities and steady-state probabilities for the expanded Markov channel, the CSI is predicted at least one symbol duration in advance. The prediction outcome is very promising, especially in slow and moderate fading environments, as verified by simulation results. Moreover, the simplification process of the expanded Markov channel, which involved the formation of sub-band and lumpable states, enabled us to reduce the feedback overheads while maintaining a feasible amount of detail on channel quality.

In Chapter 5, we focused on using a game-theoretic framework to solve the downlink resource allocation problem. The game theory perspective has provided useful insights into a fair and optimal resource allocation in a multi-user environment. However, the complexity introduced by a multi-user multi-carrier system has posed obstacles for many to attempt a game-theoretic resource allocation framework in this system. This motivates us to model the resource allocation problem of an OFDMA system with game theory such that a reduced complexity algorithm is used to attain a feasible outcome. More specifically, we formulated the non-cooperative resource allocation game as a dynamic game by defining a sigmoid-like utility function. This approach ensures that the Nash equilibrium is achieved. As evidenced from the simulation results and the analysis of the price of anarchy (PoA), the outcome of the non-cooperative resource allocation game may not be fair or Pareto optimal. We also approached the same problem using a cooperative framework. We devised the cooperative resource allocation game with the Nash bargaining model and the Raiffa-Kalai-Smorodinsky bargaining model. The important finding of

this work is to derive the closed-form of the Nash bargaining solution (NBS) and the closed-form of the Raiffa-Kalai-Smorodinsky bargaining solution (RBS). These closed-form solutions are fair and Pareto optimal according to the users' maximum and minimum rate requirements. Simulation results showed that the NBS can provide a slightly fairer outcome than RBS if the gap between maximum and minimum rate requirements is small; whereas RBS outperforms NBS if this gap is large. We also showed that the cooperative schemes outperform the non-cooperative scheme under the same system with the same wireless resources for sharing.

6.2 Future Research Directions

As future generation wireless communication systems are focusing on broadband networks, the desired carrier frequency has to be in a higher range to induce a wider bandwidth. Since a higher carrier frequency often results in a larger Doppler shift, one option to negate the Doppler effect is to reduce the size of each cell in the wireless networks. It would be a matter of time before the wireless cellular networks are merged with the wireless mesh networks. Wireless mesh networking is currently a topic of keen research interest in the global wireless networking community. The application of wireless mesh networking approaches to the design of wireless local area networks (WLANs) has gained popularity recently [95]. The popularity of the wireless mesh networking research is enhanced by its potential application in networking homes and offices. Such networks are infrastructureless with distributed nodes that communicate via self-organising mechanisms. Each node may act as a repeater to deliver data packets to other nodes. Some nodes may carry high-rate data traffic while others carry low-rate data traffic. A suitable multiple access scheme is essential to support the dynamic range of data rates inherent in wireless mesh networks. Therefore, efficient radio resource management (RRM) is very important as it involves the allocation of a finite wireless resource among multiple concurrent nodes to satisfy certain traffic requirements.

Our studies in this dissertation lay the foundation for future work on optimising the radio resource allocation of the wireless mesh networks. The future research may take the following directions:

Optimal power allocation for wireless mesh networks

Optimal system throughput is critical for all wireless networks. Maintaining an optimal system throughput under a strict power budget is a common challenge for most wireless networks. In wireless mesh networks, not all the nodes have the same power budget, for example, nodes that are connected to the mains supply often have a larger power budget than those equipped with batteries. The study of power allocation with an uneven power budget in Chapter 3 can be modified and extended to consider the problem of power allocation among nodes with different power budget and data rate requirements. However, each node in the wireless mesh network may act as a repeater to deliver data packets to other nodes. This poses a different challenge to the power allocation scheme as compared to the downlink transmission of wireless cellular systems, which only comprise direct transmissions between mobile users and the base station.

Fair and efficient RRM based on a game theoretic framework

The design of an efficient channel-aware, traffic-aware self-organising RRM for the infrastructureless wireless mesh networks is a challenging task. Self-organising RRM based on game theory is a possible approach for achieving a fair and efficient resource allocation in infrastructureless networks. Game theory is used to resolve conflicts and maintain cooperation between intelligent rational decision-makers. The decision-makers are the wireless nodes that have to compete for a finite radio resource. Each node can be modelled as a player with the objective function for preferable adaptations, such as data rate and power. This game can be modelled as a cooperative or a non-cooperative game, depending on the situation being modelled. As suggested in Chapter 5, it is desirable to model the game as a cooperative game since it performs better than its non-cooperative counterpart under the same system with the same wireless resources for sharing.

Reduce network overheads with limited feedback information

Exchanging CSI among nodes is a critical issue in the implementation of optimal RRM schemes, as wireless utility is maximised and quality of service (QoS) requirements of the applications can be adapted. As cluster topology is commonly considered for wireless

mesh networks [95], it would be beneficial to consider a game between clusterheads for an overall RRM, while each clusterhead manages the distributed radio resource for the nodes within its cluster. Since cooperative game theory is suggested in the earlier part, the RRM can be solved as a bargaining problem. To realise the bargaining model, all clusterheads in a coalition must know the channel conditions of its members in order to cooperatively allocate radio resource to themselves and to other clusters. Since all clusters are possibly un-coordinated, this could place a prohibitively expensive burden on the network overhead. The work in Chapter 4 can be extended to model an expanded Markov channel for all nodes. By reducing the size of the expanded Markov channel, one can generate limited feedback information for a cooperative game between clusterheads to save overheads.

This page is blank

Appendix A

Proof of Theorem 4.1

For an arbitrary n^{th} sub-channel, with the property of $\sum_{i=0}^{M-1} \pi_i^{(n)} = 1$ and the steady-state probabilities of an M^N-state Markov chain in (4.43), we can show that

$$\begin{aligned}\sum_{i=0}^{M^N-1} \pi_{\mathbf{s}_i} &= \left[\pi_0^{(1)} \times \pi_0^{(2)} \times \cdots \times \pi_0^{(N)}\right] + \left[\pi_1^{(1)} \times \pi_0^{(2)} \times \cdots \times \pi_0^{(N)}\right] \\ &\quad + \left[\pi_0^{(1)} \times \pi_1^{(2)} \times \cdots \times \pi_0^{(N)}\right] + \ldots + \left[\pi_{M-1}^{(1)} \times \pi_{M-1}^{(2)} \times \cdots \times \pi_{M-1}^{(N)}\right].\end{aligned} \tag{A.1}$$

By collecting the steady-state probabilities that correspond to the same sub-channel in (A.1), it can be simplified as

$$\begin{aligned}\sum_{i=0}^{M^N-1} \pi_{\mathbf{s}_i} &= \left[\pi_0^{(1)} + \pi_1^{(1)} + \cdots + \pi_{M-1}^{(1)}\right] \times \left[\pi_0^{(2)} + \pi_1^{(2)} + \cdots + \pi_{M-1}^{(2)}\right] \\ &\quad \times \ldots \times \left[\pi_0^{(N)} + \pi_1^{(N)} + \cdots + \pi_{M-1}^{(N)}\right] \\ &= \prod_{n=1}^{N} \left(\sum_{j=1}^{M-1} \pi_j^{(n)}\right),\end{aligned} \tag{A.2}$$

where $\sum_{j=0}^{M-1} \pi_j^{(n)} = 1, \forall n$, as defined in Section 4.3.1. Therefore, we can show that

$$\sum_{i=0}^{M^N-1} \pi_{\mathbf{s}_i} = 1^N = 1. \tag{A.3}$$

This page is blank

Appendix B

Proof of Theorem 4.2

Given that the steady-state probabilities of the M-state Markov chain has the property of $\sum_{i=0}^{M-1} \pi_i = 1$, we need to prove that $\sum_{i=0}^{M^N-1} \pi_{\mathbf{s}_i} = 1$ where the steady-state probabilities of the M^N-state Markov chain are given in (4.48). The property of $\sum_{i=0}^{M-1} \pi_i = 1$ can be modelled as a multinomial function by enforcing power of N to both sides of the equation, such that

$$\begin{aligned} 1 &= \left(\sum_{i=0}^{M-1} \pi_i\right)^N \\ &= \left(\pi_0 + \pi_1 + \ldots + \pi_{M-1}\right)^N \\ &= \sum (N; n_0, n_1, \ldots, n_{M-1}) \pi_0^{n_0} \pi_1^{n_1} \ldots \pi_{M-1}^{n_{M-1}}, \end{aligned} \tag{B.1}$$

where $(N; n_0, n_1, \ldots, n_{M-1})$ is the number of ways of putting $N = n_0 + n_1 + \ldots + n_{M-1}$ different objects into M different boxes with n_m in the m^{th} box, for $m \in \{0, 1, \ldots, M-1\}$. In general, the coefficient term $(N; n_0, n_1, \ldots, n_{M-1})$, for any combination of $n_0, n_1, \ldots, n_{M-1}$ values, can be derived as

$$\begin{aligned} (N; n_0, n_1, \ldots, n_{M-1}) &= \binom{N}{n_0} \binom{N-n_0}{n_1} \cdots \binom{N-n_0-\ldots-n_{M-2}}{n_{M-1}} \\ &= \frac{N!}{n_0!(N-n_0)!} \times \frac{(N-n_0)!}{n_1!(N-n_0-n_1)!} \times \cdots \times \frac{n_{M-1}!}{n_{M-1}!0!} \\ &= \frac{N!}{n_0! n_1! \cdots n_{M-1}!}. \end{aligned} \tag{B.2}$$

Thus, by expanding the summation and collecting similar terms together, we can show that

$$\begin{aligned}
\sum_{i=0}^{M^N-1} \pi_{\mathbf{s}_i} &= (\pi_0)^N + N \cdot (\pi_0)^{N-1} \pi_1 + \ldots + N \cdot (\pi_{M-2})^{N-1} \pi_{M-1} + (\pi_{M-1})^N \\
&= \frac{N!}{N!0!\cdots 0!} (\pi_0)^N + \frac{N!}{(N-1)!1!0!\cdots 0!} (\pi_0)^{N-1} \pi_1 + \ldots \\
&\quad + \frac{N!}{0!\cdots 0!1!(N-1)!} (\pi_{M-2})^{N-1} \pi_{M-1} + \frac{N!}{N!} (\pi_{M-1})^N \\
&= \sum (N; n_0, n_1, \ldots, n_{M-1}) \pi_0^{n_0} \pi_1^{n_1} \ldots \pi_{M-1}^{n_{M-1}} \\
&= 1^N = 1. \qquad \text{(B.3)}
\end{aligned}$$

Bibliography

[1] F. Adachi, M. T. Feeney, and J. D. Parsons. Level crossing rate and average fade duration for time diversity reception in Rayleigh fading conditions. *IEE Proceedings*, 135 Pt. F no. 6:501–506, Dec 1988.

[2] H. Atarashi, S. Abeta, and M. Sawahashi. Performance evaluation of coherent high-speed TD-OFCDM broadband packet wireless access in forward link employing multi-level modulation and hybrid ARQ. *IEICE Trans. Commun.*, E84-A no. 7:1670–1680, Jul 2001.

[3] H. Atarashi, S. Abeta, and M. Sawahashi. Variable spreading factor-orthogonal frequency and code division multiplexing (VSF-OFCDM) for broadband packet wireless access. *IEICE Trans. Commun.*, E86-B no. 1:291–299, Jan 2003.

[4] F. Babich and G. Lombardi. A Markov model for the mobile propagation channel. *IEEE Trans. Veh. Technol.*, 49 no.1:63–73, Jan 2000.

[5] A. R. S. Bahai and B. R. Saltzberg. *Multicarrier Digital Communications: Theory and Applications of OFDM.* Kluwer Academic, 1999.

[6] S. Boyd and L. Vandenberghe. Convex optimization with engineering applications. Course Notes EE364, Stanford University, 2002.

[7] X. Cao. Preference functions and bargaining solutions. In *Proceedings of IEEE Conf. Decision and Control*, pages 164–171, 1982.

[8] X. Cao, H. Shen, R. Milito, and P. Wirth. Internet pricing with a game theoretical approach: Concepts and examples. *IEEE/ACM Trans. Networking*, 10 no.2:208–216, Apr 2002.

[9] S. Catreux, V. Erceg, D. Gesbert, and R.W. Heath. Adaptive modulation and MIMO for broadband wireless data networks. *IEEE Comm. Magazine*, 40 no. 6:108–115, June 2002.

[10] R. W. Chang. Synthesis of band-limited orthogonal signals for multichannel data transmission. *Bell System Technical Journal*, 45:1775–1796, 1966.

[11] K. Chawla and X. Qiu. Throughput performance of adaptive modulation in cellular systems. In *Proc. IEEE Int'l Conf. on Universal Personal Comm.*, volume 2, pages 945–950, Oct 1998.

[12] T. K. Chee, C.-C. Lim, and J. Choi. Adative power allocation with user prioritization for downlink OFDMA systems. In *Proc. IEEE 9th Int'l Conf. on Comm. Sys.*, pages 210–214, Sep 2004.

[13] T. K. Chee, C.-C. Lim, and J. Choi. Sub-optimal power allocation for downlink OFDMA systems. In *Proc. IEEE 60th VTC-Fall*, volume 3, pages 2015–2019, Sep 2004.

[14] T. K. Chee, C.-C. Lim, and J. Choi. A lumpable finite-state Markov model for channel prediction and resource allocation in OFDMA systems. In *Proc. IEEE 1st Int'l Conf. Wireless Broadband and Ultra Wideband Commun.*, Mar 2006.

[15] J. Chen and T. Berger. The capacity of finite-state Markov channels with feedback. *IEEE Trans. Inform. Theory*, 51 no.3:780–798, Jan 2005.

[16] R. Cheng and S. Verdu. Gaussian multiaccess channels with ISI: Capacity region and multiuser water-filling. *IEEE Trans. Inform. Theory*, 39 no.3:773–785, May 1993.

[17] H. Cheon, B. Park, C. Kang, and D. Hong. The performance impairment due to the imperfect channel information in OFDM-based WLAN. In *Proc. IEEE 55th VTC*, volume 2, pages 914–917, May 2002.

[18] S. Chung and J. M. Cioffi. Rate and power control in a two-user multicarrier channel with no coordination: The optimal scheme vs. suboptimal methods. In *Proc. IEEE 56th VTC*, volume 3, pages 1744–1748, Sep 2002.

[19] S. Chung and J. M. Cioffi. The capacity region of frequency-selective Gaussian interference channels under strong interference. In *Proc. IEEE Int'l Conf. on Comm.*, volume 4, pages 2753–2757, May 2003.

[20] S. Chung and A. Goldsmith. Adaptive multicarrier modulation for wireless systems. In *Conference Record of the 24th Asilomar Conf. on Sig., Sys. and Comp.*, volume 2, pages 1603–1607, Oct 2000.

[21] L. J. Cimini. Analysis and simulation of a digital mobile channel using orthogonal frequency division multiplexing. *IEEE Trans. Commun.*, COM-33 no. 7:665–675, Jul 1985.

[22] E. Costa, H. Haas, E. Schulz, and A. Filippi. Capacity optimization in MC-CDMA systems. *European Trans. on Tele-Communications*, 13 no.5:1–10, Oct 2002.

[23] T. M. Cover and J. A. Thomas. *Elements of Information Theory.* John Wiley and sons, New York, 1991.

[24] A. Duel-Hallen, S. Hu, and H. Hallen. Long range prediction of fading signals. *IEEE Sig. Processing Magazine*, 17 no.3:62–75, May 2000.

[25] E. O. Elliott. Estimates of error rates for codes on burst-noise channels. *Bell Syst. Tech. J.*, 42:1977–1997, Sep 1963.

[26] V. Erceg, L. J. Greenstein, S. Y. Tjandra, S. R. Parkoff, A. Gupta, B. Kulic, A. A. Julius, and R. Bianchi. An empirically based path loss model for wireless channels in suburban environments. *IEEE J. Select. Areas Commun.*, 17 no.7:1205–1211, Jul 1999.

[27] M. Ergen, S. Coleri, and P. Varaiya. QoS aware adaptive resource allocation technique for fair scheduling in OFDMA based broadband wireless access systems. *IEEE Trans. Broadcast.*, 49 no.4:362–370, Dec 2003.

[28] T. Eyceoz, S. Hu, and A. Duel-Hallen. Performance analysis of long range prediction for fast fading channels. In *Proc. 33rd Annual Conf. on Info. Sci. and Sys.*, volume II, pages 656–661, Mar 1999.

[29] S. Falahati, A. Svensson, T. Ekman, and M. Sternad. Adaptive modulation systems for predicted wireless channel. *IEEE Trans. Commun.*, 52 no.2:307–316, Feb 2004.

[30] E. N. Gilbert. Capacity of burst-noise channels. *Bell Syst. Tech. J.*, 39:1253–1265, Sep 1960.

[31] D. L. Goeckel. Adaptive coding for time-varying channels using outdated fading estimates. *IEEE Trans. Commun.*, 47 no.6:844–855, June 1999.

[32] A. Goldsmith. Adaptive modulation and coding for fading channel. In *Proc. IEEE Information Theory and Comm. Workshop*, pages 24–26, June 1999.

[33] A. Goldsmith and S. G. Chua. Variable-rate variable-power for fading channels. *IEEE Trans. Commun.*, 45 no. 10:1218–1230, Oct 1997.

[34] A. Goldsmith and S. G. Chua. Adaptive coded modulation for fading channels. *IEEE Trans. Commun.*, 46 no. 5:595–602, May 1998.

[35] A. Goldsmith and P. Varaiya. Capacity of fading channels with channel side information. *IEEE Trans. Inform. Theory*, 43 no.6:1986–1992, Nov 1997.

[36] D. Goodman and N. Mandayam. Network assisted power control for wireless data. *Mobile Networks and Applications*, 6:409–415, 2001.

[37] Z. Han, Z. Ji, and K. J. R. Liu. Fair multiuser channel allocation for OFDMA networks using nash bargaining solutions and coalitions. *IEEE Trans. Commun.*, 53 no.8:1306–1376, Aug 2005.

[38] Z. Han and K. J. R. Liu. Noncooperative power-control game and throughput game over wireless networks. *IEEE Trans. Commun.*, 53 no.10:1625–1629, Oct 2005.

[39] S. V. Hanly and D. N. Tse. Multiaccess fading channels - Part II: Delay- limited capacities. *IEEE Trans. Inform. Theory*, 44 no.7:2816–2831, Nov 1998.

[40] S. Hara and R. Prasad. Overview of multicarrier CDMA. *IEEE Comm. Magazine*, 35 no. 12:126–133, Dec 1997.

[41] S. Hara and R. Prasad. Design and performance of multicarrier CDMA system in frequency selective Rayleigh fading channels. *IEEE Trans. Veh. Technol.*, 48 no. 5:1584–1595, Sep 1999.

[42] M. Hassan, M. Krunz, and I. Matta. Markov-based channel characterization for tractable performance analysis in wireless packet networks. *IEEE Trans. Wireless Commun.*, 3 no.3:821–831, May 2004.

[43] J. Hayes. Adaptive feedback communications. *IEEE Trans. Commun.*, 16 no.1:29–34, Feb 1968.

[44] S. Hew and L. B. White. A game theoretical approach for resource bargaining in shared WCDMA networks: Symmetric and asymmetric models. In *Proc. IEEE 1st Int'l Conf. Wireless Broadband and Ultra Wideband Commun.*, Mar 2006.

[45] T. Holliday, A. Goldsmith, and P. Glynn. Wireless link adaptation policies: QoS for deadline constrained traffic with imperfect channel estimates. In *Proc. IEEE Int'l Conf. on Comm.*, volume 5, pages 3366–3371, 2002.

[46] S. Hu and A. Duel-Hallen. Combined adaptive modulation and transmitter diversity using long range prediction for flat fading mobile radio channels. In *IEEE GLOBECOM*, volume 2, pages 1256–1261, Nov 2001.

[47] W. C. Jakes. *Microwave Mobile Communications*. John Wiley and sons, 1974.

[48] R. Johari, S. Mannor, and J. Tsitsiklis. Efficiency loss in a network resource allocation game: The case of elastic supply. *IEEE Trans. Automat. Contr.*, 50 no.11:1712–1724, Sep 2005.

[49] R. Johari and J. Tsitsiklis. Efficiency loss in a network resource allocation game. *Mathematics of Operations Research*, 29 no.3:407–435, Aug 2004.

[50] S. Kaiser. OFDM code division multiplexing in fading channel. *IEEE Trans. Commun.*, 50 no. 8:1266–1273, Aug 2002.

[51] E. Kalai and M. Smorodinsky. Other solutions to Nash's bargaining problem. *Econometrica*, 4:513–518, 1975.

[52] F. P. Kelly. Charging and rate control for elastic traffic. *Eur. Trans. Telecommun. — Focus on Elastic Services Over ATM Networks*, 8 no.1:33–37, 1997.

[53] J. G. Kemeny and J. L. Snell. *Finite Markov Chains*. Princeton, NJ, 1960.

[54] D. Kivanc, G. Li, and H. Liu. Computationally efficient bandwidth allocation and power control for OFDMA. *IEEE Trans. Wireless Commun.*, 2 no.6:1150–1158, Nov 2003.

[55] L. Kleinrock. *Queueing Systems: Volume I - Theory.* Wiley Interscience, New York, 1975.

[56] R. Knopp and P. A. Humblet. Information capacity and power control in single-cell multiuser communications. In *Proc. IEEE Int'l Conf. on Commun.*, volume 1, pages 331–335, Jun 1995.

[57] H. Kong and E. Shwedyk. Sequence detection and channel state estimation over finite-state Markov channels. *IEEE Trans. Veh. Technol.*, 48 no.3:833–839, May 1999.

[58] J. Lee, R. Mazumdar, and N. B. Shroff. Downlink power allocation for multi-class wireless systems. *IEEE/ACM Trans. Networking*, 13 no.4:854–867, Aug 2005.

[59] J. Lee, R. V. Sonalkar, and J. M. Cioffi. A multi-user rate and power control algorithm for VDSL. In *Proc. IEEE Global Telecommunications Conf.*, volume 2, pages 1264–1268, 2002.

[60] A. Leke and J. M. Cioffi. Multicarrier systems with imperfect channel knowledge. In *Proc. IEEE 9th Int'l Symposium on PIMRC*, volume 2, pages 549–553, Sep 1998.

[61] Y. Li, L. J. Cimini, and N. R. Sollenberger. Robust channel estimation for OFDM systems with rapid dispersive fading channels. *IEEE Trans. Commun.*, 46 no.7:902–915, Jul 1998.

[62] Y. Li, N. Seshadri, and S. Ariyavisitakul. Channel estimation for OFDM systems with transmitter diversity in mobile wireless channels. *IEEE J. Select. Areas Commun.*, 17 no.3:461–471, Mar 1999.

[63] Y. Li and N. R. Sollenberger. Clustered OFDM with channel estimation for high rate wireless data. *IEEE Trans. Commun.*, 49 no.12:2071–2076, Dec 2001.

[64] X. Liu, E. Chong, and N. B. Shroff. A framework for opportunistic scheduling in wireless networks. *Computer Networks Journal (Elsevier)*, 41 no.4:451–474, 2003.

[65] N. Maeda, H. Atarashi, S. Abeta, and M. Sawahashi. Antenna diversity reception appropriate for MMSE combining in frequency domain for forward link OFCDM packet wireless access. *IEICE Trans. Commun.*, E85-B no. 10:1966–1977, Oct 2002.

[66] N. Maeda, H. Atarashi, S. Abeta, and M. Sawahashi. Pilot channel assisted MMSE combining in forward link for broadband OFCDM packet wireless access. *IEICE Trans. Commun.*, E85-A no. 7:1635–1646, Jul 2002.

[67] N. Maeda, H. Atarashi, S. Abeta, and M Sawahashi. Throughput comparison between VSF-OFCDM and OFDM considering effect of sectorization in forward link broadband packet wireless access. In *Proc. IEEE VTC 56th Fall*, volume 1, pages 47–51, 2002.

[68] N. Maeda, H. Atarashi, and M. Sawahashi. Performance comparison of channel interleaving methods in frequency domain for VSF-OFCDM broadband wireless access in forward link. *IEICE Trans. Commun.*, E86-B no. 1:300–313, Jan 2003.

[69] R. Mazumdar, L. Mason, and C. Douligeris. Fairness in network optimal flow control: Optimality of product forms. *IEEE Trans. Wireless Commun.*, 39 no.5:775–782, May 1991.

[70] A. C. McCormick and E. A. Al-Susa. Multicarrier CDMA for future generation mobile communication. *IEEE Electronics and Comm. Engineering Journal*, 14 no. 2:52–60, Apr 2002.

[71] F. Meshkati, H. V. Poor, S. Schwartz, and N. Mandayam. An energy-efficient approach to power control and receiver design in wireless data networks. *IEEE Trans. Commun.*, 53 no.11:1885–1894, Nov 2005.

[72] A. Muthoo. *Bargaining Theory with Applications*. Cambridge University Press, Cambridge, U.K., 1999.

[73] J. Nash. The bargaining problem. *Econometrica*, 18:155–162, Apr 1950.

[74] J. Neumann and O. Morgenstern. *Theory of Games and Economic Behavior*. Princeton University Press, 1944.

[75] C. H. Papadimitriou. Algorithms, games and the internet. In *Proceedings of 33rd Annual ACM Symposium on the Theory of Computing*, pages 749–753, 2001.

[76] A. Papoulis and S. U. Pillai. *Probability, Random Variables and Stochastic Processes*. McGraw Hill, fourth edition, 2002.

[77] H. Raiffa. *Contributions to the Theory of Game II*. Princeton University Press, Princeton, NJ, 1953.

[78] T. S. Rappaport. *Wireless Communications: Principles and Practice*. Prentice Hall PTR, Englewood Cliffs, NJ, second edition, 2002.

[79] T. S. Rappaport, A. Annamalai, R. M. Beuhrer, and W. H. Tranter. Wireless communications: Past events and a future perspective. *IEEE Comm. Mag.*, 40 no.5:148–161, May 2002.

[80] W. Rhee and J. M. Cioffi. Increase in capacity of multiuser OFDM system using dynamic subchannel allocation. In *Proc. IEEE 51st VTC*, volume 2, pages 1085–1089, May 2000.

[81] C. Saraydar, N. Mandayam, and D. Goodman. Pareto efficiency of pricing based power control in wireless data networks. In *Proc. IEEE WCNC*, volume 1, pages 231–235, Sep 1999.

[82] C. E. Shannon. A mathematical theory of communication. *Bell Syst. Tech. J.*, 27:379–423, 1948.

[83] Z. Shen, J. G. Andrews, and B. L. Evans. Short range wireless channel prediction using local information. In *Proc. IEEE 37th Asilomar Conf. on Sig., Sys. and Comp.*, volume 1, pages 1147–1151, Nov 2003.

[84] Z. Shen, J. G. Andrews, and B. L. Evans. Adaptive resource allocation in multiuser OFDM systems with proportional rate constraints. *IEEE Trans. Wireless Commun.*, 4 no.6:2726–2737, Nov 2005.

[85] N. R. Sollenberger and L. J. Cimini. Receiver structures for multiple access OFDM. In *Proc. IEEE VTC 49th*, volume 1, pages 468–472, Jul 1999.

[86] G. Song and Y. Li. Cross-layer optimization for OFDM wireless networks — Part I: Theoretical framework. *IEEE Trans. Wireless Commun.*, 4 no.2:614–624, Mar 2003.

[87] G. Song and Y. Li. Cross-layer optimization for OFDM wireless networks — Part II: Algorithm development. *IEEE Trans. Wireless Commun.*, 4 no.2:625–634, Mar 2003.

[88] H. Song, S. Kang, M. Kim, and Y. You. Error performance analysis of STBC-OFDM systems with parameter imbalances. *IEEE Trans. Broadcast.*, 50 no.1:76–82, Mar 2004.

[89] M. R. Souryal and R. L. Pickholtz. Adaptive modulation with imperfect channl information in OFDM. In *Proc. IEEE Int'l Conf. on Comm.*, volume 6, pages 1861–1865, June 2001.

[90] M. Sternad and D. Aronsson. Channel estimation and prediction for adaptive OFDM downlinks. In *Proc. IEEE 58th VTC-fall*, volume 2, pages 1283–1287, Oct 2003.

[91] C. Sung and W. Wong. A noncooperative power control game for multirate CDMA data networks. *IEEE Trans. Wireless Commun.*, 2 no.1:186–194, Jan 2003.

[92] P. Svedman, S. K. Wilson, and B. Ottersten. A QoS-aware proportional fair scheduler for opportunistic OFDM. In *Proc. IEEE 60th VTC-Fall*, Sep 2004.

[93] C. Tan and N. Beaulieu. On first-order Markov modeling for Rayleigh fading channel. *IEEE Trans. Commun.*, 48 no.12:2032–2040, Dec 2000.

[94] Y. Teng, T. Nagaosa, K. Mori, and H. Kobayashi. Proposal of grouping adaptive modulation method for burst mode OFDM transmission system. *IEICE Trans. Commun.*, E86-B no. 1:257–265, Jan 2003.

[95] C. K. Toh. *Ad Hoc Mobile Wireless Networks: Protocols and Systems*. Prentice-Hall, Eaglewood Cliffs, NJ, 2001.

[96] D. N. Tse and S. V. Hanly. Multiaccess fading channels - Part I: Polymatroid structure, optimal resource allocation and throughput capacities. *IEEE Trans. Inform. Theory*, 44 no.7:2796–2815, Nov 1998.

[97] T. Tung, K. Yao, and R. E. Hudson. Channel estimation and adaptive power allocation for performance and capacity improvement of multiple-antenna OFDM

systems. In *Proc. IEEE 3rd Workshop on Sig. Processing Advances in Wireless Comm.*, pages 82–85, Mar 2001.

[98] T. L. Turocy and B. Stengel. *Encyclopedia of Information Systems - Game Theory.* Academic Press, 2002.

[99] M. Umehira and T. Sugiyama. OFDM/CDMA technologies for future broadband mobile communication systems. *IEICE Trans. Commun.*, E85-A no. 12:2804–2812, Dec 2002.

[100] P. Viswanath, D. N. Tse, and V. Anantharam. Asymptotically optimal water-filling in vector multiple access channels. *IEEE Trans. Inform. Theory*, 47 no.1:241–267, Jan 2001.

[101] H. Wang and P. Chang. On verifying the first-order Markovian assumption for a Rayleigh fading channel model. *IEEE Trans. Veh. Technol.*, 45 no.2:353–357, May 1996.

[102] H. S. Wang and N. Moayeri. Finite-state Markov channel - a useful model for radio communication channels. *IEEE Trans. Veh. Technol.*, 44 no.1:163–171, Feb 1995.

[103] L. White, R. Mahony, and G. Brushe. Lumpable hidden Markov models-model reduction and reduced complexity filtering. *IEEE Trans. Automat. Contr.*, 45 no.12:2297–2306, Dec 2000.

[104] C. Wong, R. Cheng, K. Letaief, and R. Murch. Multiuser subcarrier allocation for OFDM transmission using adaptive modulation. In *Proc. IEEE 49th VTC*, volume 1, pages 479–483, Jul 1999.

[105] C. Wong, R. Cheng, K. Letaief, and R. Murch. Multiuser OFDM with adaptive subcarrier, bit and power allocation. *IEEE J. Select. Areas Commun.*, 17 no.10:1747–1758, Oct 1999.

[106] C. Wong, C.Y. Tsui, R. S. Cheng, and K. Letaief. A real-time subcarrier allocation scheme for multiple access downlink OFDM transmission. In *Proc. IEEE 50th VTC Fall*, volume 2, pages 1124–1128, Sep 1999.

[107] M. Xiao, N. B. Shroff, and E. Chong. A utility-based power-control scheme in wireless cellular systems. *IEEE/ACM Trans. Networking*, 11 no.2:210–221, Apr 2003.

[108] H. Yaiche, R. Mazumdar, and C. Rosenberg. A game theoretic framework for bandwidth allocation and pricing in broadband networks. *IEEE/ACM Trans. Networking*, 8 no.5:667–678, Oct 2000.

[109] T. Yang and A. Duel-Hallen. Adaptive modulation using outdated samples of another faing channels. In *Proc. IEEE WCNC*, volume 1, pages 477–481, Mar 2002.

[110] T. Yang, A. Duel-Hallen, and H. Hallen. Reliable adaptive modulation aided by observations of another fading channel. *IEEE Trans. Commun.*, 52 no.4:605–611, Apr 2004.

[111] S. Ye, R. S. Blum, and L. J. Cimini. Adaptive modulation for variable-rate OFDM systems with imperfect channel information. In *Proc. IEEE VTC 55th Spring*, volume 2, pages 767–771, 2002.

[112] H. Yin and H. Liu. An efficient multiuser loading algorithm for OFDM broadband wireless system. In *Proc. IEEE Global Telecommunications Conf.*, pages 103–107, Nov 2000.

[113] S. Yoon, C. Suh, Y. Cho, and D. S. Park. Orthogonal frequency division multiple access with an aggregated sub-channel structure and statistical channel quality measurement. In *Proc. IEEE 60th VTC-Fall*, volume 2, pages 1023–1027, Sep 2004.

[114] W. Yu and J. M. Cioffi. On constant power water-filling. In *Proc. IEEE Int'l Conf. on Comm.*, volume 6, pages 1665–1669, June 2001.

[115] W. Yu, G. Ginis, and J. M. Cioffi. Distributed multiuser power control for digital subscriber lines. *IEEE J. Select. Areas Commun.*, 20 no.5:1105–1115, June 2002.

[116] W. Yu, W. Rhee, S. Boyd, and J. M. Cioffi. Iterative water-filling for Gaussian vector multiple access channels. *IEEE Trans. Inform. Theory*, 50 no.1:145–152, Jan 2004.

[117] C. Zeng, L. Hoo, and J. M. Cioffi. Efficient water-filling algorithms for a Gaussian multiaccess channel with ISI. In *Proc. IEEE 52nd VTC*, volume 3, pages 1072–1077, Sep 2000.

[118] Q. Zhang and S. Kassam. Finite-state Markov model for Rayleigh fading channels. *IEEE Trans. Commun.*, 11 no.47:1688–1692, Nov 1999.

[119] Y. Zhang and K. Letaief. Multiuser subcarrier and bit allocation along with adaptive cell selection for OFDM transmission. In *Proc. IEEE Int'l Conf. on Comm.*, volume 2, pages 861–865, 2002.

[120] Y. Zhang and K. Letaief. An efficient resource-allocation scheme for spatial multiuser access in MIMO/OFDM systems. *IEEE Trans. Commun.*, 53 no.1:107–116, Jan 2005.

[121] R. E. Ziemer and W. H. Tranter. *Principles of Communications: Systems Modulation and Noise*. John Wiley and sons, fifth edition, 2002.